Investigations of Near and Mid Infrared Pyrotechnics

Detonation Velocities of New Secondary Explosives

SUSANNE SCHEUTZOW

PhD Thesis

Dissertation zur Erlangung des Doktorgrades
der Fakultät für Chemie und Pharmazie der
Ludwig-Maximilians-Universität München

Investigations of Near and Mid Infrared Pyrotechnics

Detonation Velocities of New Secondary Explosives

SUSANNE SCHEUTZOW

aus

München

2012

Erklärung

Diese Dissertation wurde im Sinne von §7 der Promotionsordnung vom 28. November 2011 von Herrn Prof. Dr. T. M. Klapötke betreut.

Eidesstattliche Versicherung

Diese Dissertation wurde eigenständig und ohne unerlaubte Hilfe erarbeitet.

München, den 13. November 2012

(Susanne Scheutzow)

Dissertation eingereicht am	16. November 2012
1. Gutachter	Prof. Dr. T. M. Klapötke
2. Gutachter	Prof. Dr. K. Karaghiosoff
Mündliche Prüfung am	13. Dezember 2012

Für meine Eltern

Tue es oder tue es nicht. Es gibt kein Versuchen.
Yoda. Episode V. Kapitel 28

Danksagung

Mein herzlichster Dank gilt meinem Doktorvater Prof. T. M. Klapötke. Danke für die freundliche Aufnahme in Ihrem Arbeitskreis, für das interessante und anspruchsvolle Thema, Ihre Geduld, Ihr Vertrauen und die hilfreichen sowie lustigen Gespräche wissenschaftlicher und privater Natur (…vielleicht doch irgendwann mal ein BMW).

Lieber Conni (Prof. Karaghiosoff), dir danke ich für die Übernahme des Zweitgutachtens, dafür dass du immer ein offenes Ohr hattest, sei es für Chemie oder alles andere und für die schöne Zeit in Brüssel.

Dr. B. Krumm danke ich für sämtliche Sicherheits- und Syntheseratschläge, für viele amüsante Gespräche, USA Reisetipps und DVD Austausche.

Der Firma Diehl BGT Defence, speziell Dr. A. Hahma, Dipl. Chem. O. Pham und J. Licha danke ich für die stets gute Zusammenarbeit und Durchführung vieler Messungen.
Dr. E.- C. Koch danke ich für die freundliche Aufnahme in seiner Gruppe in Brüssel und für viele gute wissenschaftliche Ratschläge.

Liebe Karin, dir danke ich für eine tolle gemeinsame Zeit seit ich in diesem Arbeitskreis bin, deine Freundschaft, deine unerschöpfliche Geduld mir das mit den Kristallstrukturen beizubringen (um sie dann doch wieder selber lösen zu müssen) und dass du immer für mich da warst. Lieber Jörg, dir danke ich für viele hilfreiche Diskussionen, anstrengende Bergtouren und dafür dass du meine liebe Karin glücklich machst. Liebe Vroni, dir danke ich für eine schöne gemeinsame Zeit im Studium und eine Freundschaft die hoffentlich nicht nur bis Innsbruck reicht.

Mein lieber Michael: mein größter Dank gilt dir (diese Seite würde nicht reichen), dafür dass du alle meine Matlab Fehler korrigiert hast, für deine unerschöpfliche Geduld und dass du mich länger wie eine Woche ausgehalten hast (und dabei hab ich nicht einmal titriert…).

Lieber Niko, dir danke ich für eine tolle Zeit im Labor und auf dem Berg, eine gute Zusammenarbeit und jetzt schon mal für eine tolle gemeinsame Doktorfeier (jetzt brauch ich einen neuen Squashpartner). Dear Davin, thanks, see you somewhere. Liebe Chrissi und lieber Stefan, danke für eure Unterstützung, Freundschaft und den Stressabbau (gute Drinks und viele blaue Flecke).

Danke auch an meine Laborkollegen Steffi, Andi, Andy, Caro und selbstverständlich Stefan (The Walking Dead) Huber für eine tolle Atmosphäre, hilfreiche Diskussionen und Gespräche. Danke an meine Praktikanten/Diplomanden Lukas, Chrissi K., Annette und vor allem nochmal Andy, die viel zu dieser Arbeit beigetragen haben. Dr. Markus Kowalewski danke ich für die ersten Matlab Schritte.

Vielen Dank an meinen gesamten Arbeitskreis, vor allem aber an die Computerspezialisten Norbert, Richard und Camilla ohne die mein Rechner vermutlich noch öfter abgestürzt wäre. Selbstverständlich danke ich Frau Scheckenbach für sämtliche Ratschläge, dem AK Kornath für die Adoption, der gesamten Werkstatt der LMU München für immer sehr schnelle Reparaturen und der Wache der LMU München für das ständige Abschalten des Brandmelders.

Danke an meine Familie, dass sie dieses lange Studium mit mir durchgehalten haben ebenso wie meine Freundin Sandra mit Bäda. Zuletzt danke ich den drei??? dafür dass ich wenigstens ab und zu mal nicht an Chemie gedacht habe.

List of Figures, Tables, Schemata

List of Figures, Tables, Schemata

Table of Contents

Energetic Materials

Based on the toxicity of commercially used explosives like RDX or HMX the research focus on the synthesis of new less toxic ('green') explosives raises exponentially since the early 1990´s.[1] Because of the variety of work in this area the new commonly used term 'high energy material' (HEM) or 'energetic material' (EM) were introduced and comprises the three main branches: Explosives, Pyrotechnics, and Propellants (Figure 1). Hence, HEM or EM is another description for explosives, pyrotechnics or propellants depending on their formulation and their intended use.[2]

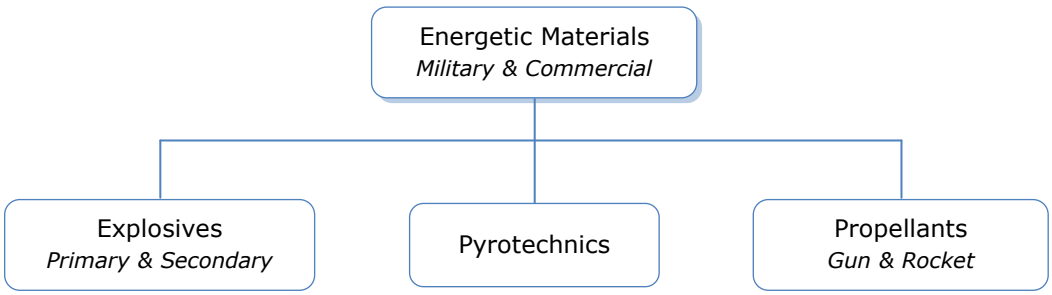

Figure 1 Classification of Energetic Materials (EMs).

Another frequently used term is the so called 'insensitive high explosive' (IHE) which is based on the use of inherently insensitive (chemically stable) molecules like TATB (1,3,5-triamino-2,4,6-trinitrobenzene), FOX-7 (1,1-diamino-2,2-dinitroethane) or DADNP (2,6-diamino-3,5-dinitropyridine)(Figure 2). IHEs are characterized by very high decomposition temperatures and high sensitivity data (>350 N friction, >40 J impact). They withstand accidentally shock, fire or impact e. g. by shrapnels or bullets and only burn instead of detonate. But they detonate if desired.

[1] J. Agrawal, High Energy Materials: Propellants, Explosives and Pyrotechnics, Wiley-VCH, **2010**.
[2] J. Akhavan, The Chemistry of Explosives, 3rd Edition, The Royal Society of Chemistry, **2011**.

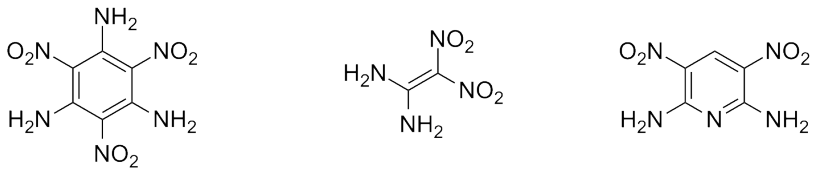

1 **2** **3**

Figure 2 Chemical structures of IHEs: TATB (**1**), FOX-7 (**2**) and DADNP (**3**).

An explosive material consists either of solids (e. g. TNT), liquids (e. g. nitroglycerin) or gaseous (H_2/O_2) components. It can be a single chemical compound (RDX), or a combination of two (pentolite) or more compositions (gunpowder). Energetic materials are in most cases metastable compounds. Any impulse (heat, friction, shock, electric spark) can lead to a very fast reaction accompanied by the release of a great amount of energy and gaseous (and/or solid) products at high temperature and pressure.[3] The energy can be emitted in form of shock waves, propulsion of debris, or by thermal and ionizing radiation.[2] The American Society for Testing and Materials (ASTM) defines an energetic material as a composition, containing fuel and oxidizer at once and which react under the release of energy and gas. Thus the exothermic decomposition of energetic compounds needs no atmospheric oxygen to sustain the reaction. Explosives are further subdivided in primary and secondary explosives. Common secondary explosives consist mostly of the elements carbon (C), hydrogen (H), nitrogen (N), and oxygen (O) and are so called 'CHNO' explosives. Main research interests on new (secondary) explosives are in high power, less sensitivity, and less toxicity of the material and their detonation products. Some characteristics which refer to the 'power of explosives' are the [4]

- heat of formation Q (kJ kg^{-1})
- detonation velocity D (m s^{-1})
- detonation pressure p (kbar)
- released gaseous volume V (L kg^{-1})

Novel HEs should reach high heat of formations (>5000 kJ kg^{-1}), detonation velocities around 10.000 m s^{-1}, detonation pressures of >>400 kbar, and densities of 2 g cm^{-3} or higher.

[3] E.-C. Koch, S. Scheutzow, Review: On the Relation Between Sensitivity Parameters and Molecular Structure of Energetic Materials, NATO-MSIAC, Belgium, **2009**.
[4] T. M. Klapötke, Chemie der Hochenergetischen Materialien, Walter de Gruyter, 2nd Edition, Berlin, **2012**.

Explosives are used in civil and military applications. Commercial use comprises for instance quarry operations, mining industry and tunneling. Typical explosives in this area are ANFO, dynamite, emulsion or slurry explosives. Civil pyrotechnics are used for special effects like illumination or sound effects and civil propellants for acceleration in rockets and other vehicles.

Primary Explosives such as lead azide ($Pb(N_3)_2$), lead styphnate (2,4,6-trinitroresorcinate) or mercury fulminate ($C_2HgN_2O_2$) are very sensitive towards heat, shock or friction (Figure 3). They are normally initiated by burning. The transition from burning (deflagration) to detonation (DDT) occurs within very short time (ms) but with less energy content compared to secondary explosives. Detonation velocities are in the range of 3500–5500 m s^{-1}. This behavior leads to the use for initiating devices such as detonators or priming caps.

Mainly used secondary explosives are for instance RDX (1,3,5-trinitro-1,3,5-triazacyclohexane), HMX (1,3,5,7-tetranitro-1,3,5,7-tetraazacyclooctane) or HNS (1,2-bis(2,4,6-trinitrophenyl)ethylene) (Figure 3). They are stable up to 200–350°C, less or moderate sensitive towards friction, impact or electric discharge and are normally initiated by the shock wave of a primary explosive. Detonation velocities of secondary explosives are in the range of 5500–10000 m s^{-1}.[2] The released energy and the power of the shock wave is much higher compared to primaries.

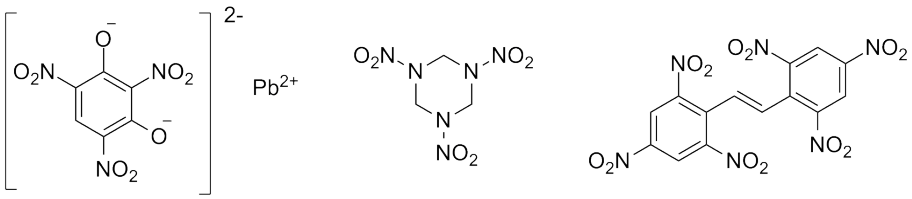

Figure 3 Chemical structures of lead styphnate (**1**), RDX (**2**) and HNS (**3**).

Propellants (low explosives) are divided in gun propellants (e. g. black powder, nitrocellulose) or rocket propellants (e. g. LOX/liq.H_2, monomethyl hydrazine/dinitrogen tetroxide). They can consist either of solids, liquids or gaseous compounds or depending on their use as single or multiple propellants (fuel and oxidizer). They are characterized by deflagration (produces large amounts of gaseous products) instead of detonation which is described by the burn rate given in m s^{-1} or g s^{-1}. The parameter to describe the efficiency of rockets and engines is the specific Impulse I_{sp} (in m s^{-1} or N s kg^{-1}), which gives the force with respect to the amount of propellant used per unit time.[4]

Pyrotechnics

The word 'pyrotechnic' is derived from the Greek and means the 'art of fire' ('pyr' for fire and 'techne' for art). A more popular regarded synonym for pyrotechnic is the word 'firework', although this correlation is imprecise.[5] As stated under chapter 1, pyrotechnics are differentiated in military or civilian pyrotechnics.

Pyrotechnic compositions are capable of self-containing and self-sustaining exothermic chemical reactions of solid mixtures and with or without the formation of gaseous products. Reaction rates of pyrotechnics lay between explosives (high reaction rates) and propellants (low reaction rates). In contrast to HEs, they consist of an oxidizer and a reducing agent and produce mainly solid and liquid reaction products.[1,4,5] According to the varieties of applications several additives are blended to the formulations. Because pyrotechnic compositions exist of multiple compounds the manufacturing considers several variables like humidity, temperature, confinement, grain size, or sensitivity data (e. g. for (per)chlorates).

Corresponding to their favored effect and civil or military use, pyrotechnics are separated in heat, sound, (colored) smoke, (colored) light, flame, delay or gas producing pyrotechnics (Figure 4). Compared to military pyrotechnics, commercially used fireworks are further categorized in ground-based, aerial, aquatic, and additionally used fireworks for theater and special effects in motion pictures, as well as 'toy' fireworks like snakes, sparklers, toy caps or party poppers.[5]

[5] A. Hardt, Pyrotechnics, Pyrotechnica Publications, **2001**.

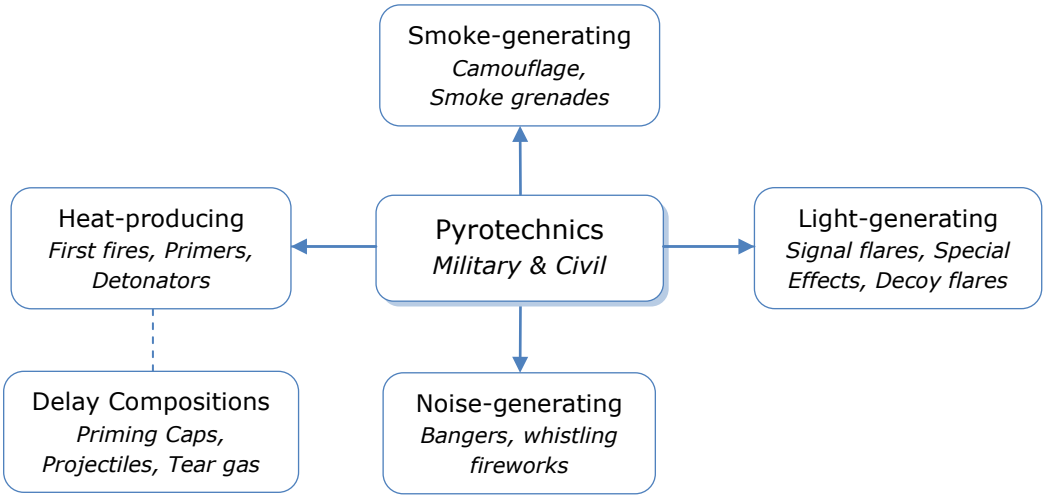

Figure 4 Classifications of Pyrotechnics.

Heat-producing pyrotechnics

Heat-producing pyrotechnics are used for instance as primers, 'first fires', as propellants in rocket motors, or in incendiary devices. Primers are ignited mechanically by a small metal pin or electrically by bridge wire and are able to generate heat or shock. They are used in detonator caps to ignite a primary explosive or for the ignition of gun propellants. In detonators the primer emits a small flame and ignites a primary explosive, which in turn produces a shock wave to initiate the main charge (e. g. secondary explosive).

First fires are used to ignite other (less sensitive) materials and are ignited itself by a primer or igniter charge. In fireworks the first fire consists normally of a combination of black powder, dextrin and water. A typical first fire which is used for *Black Knight* composition (chapter 3) is denoted in Table 1.

Compositions used in primers or first fires are normally very easy to initiate and are therefore hazardous materials, whereas heat-generating devices in contrast are less sensitive. The sensitivity of these formulations can be monitored by using less sensitive oxidizing compounds or by reducing the amount of oxidizer.[2]

Exclusively heat-generating pyrotechnics are used in sealed units, e. g. heating canned food or water and they produce heat without flames, sparks or gases. To avoid an increase of pressure they only produce solid or liquid reaction products and low amounts of energy or gas. Heat-generating compositions can be initiated by impact or friction.[4]

Table 1 Examples for pyrotechnic formulations used as heat-producing agents.

Pyrotechnic composition	Uses
Potassium chlorate, lead peroxide, antimony sulfide, trinitrotoluene	Percussion Primer
Potassium perchlorate, lead thiocyanate, antimony sulfide	Stab Primer
Barium nitrate, tetranitrocarbazole, silicon, zirconium hydride, binder	First Fire
Zinc, zirconium or barium chromate, manganese	Heat-generator

Delay pyrotechnics

Delay pyrotechnics are divided in gassy and gasless compositions. They provide a requested time delay in ms or s from ignition to the favored effect of the pyrotechnic charge. Some examples for delay formulations are listed below.[2]

Table 2 Examples for pyrotechnic formulations used as ignition delays.

Pyrotechnic composition	Effect
Blackpowder	Gassy
Tetranitrocarbazole, potassium nitrate	Gassy
Boron, silicon, potassium dichromate	Gasless
Tungsten, barium chromate, potassium perchlorate	Gasless
Lead chromate, barium chromate, manganese	Gasless
Chromium, barium chromate, potassium perchlorate	Gasless

Gasless delays are used in confined settings or at high altitudes without variations of normal ambient pressures, whereas gas-producing delays are used in low altitudes and under air conditions. Blackpowder (sulfur, potassium nitrate, charcoal) is a typical gas producing formulation. Mixtures of metal oxides or metal chromates and elemental fuels like silicon or manganese are typical gasless formulations.

Delays used in projectiles or bombs and which detonate on impact having very fast burn rates of greater than 1 mm ms^{-1}. Delays with slow burn rates (1–6 mm s^{-1}) are used in smoke pots, tear gas or smoke and hand grenades. Civil use includes quarry operations, mining, and tunneling.[2]

Basically, the difference of standard and delay detonators is the delay composition, which can vary in length, reliant on the preferred lagging (ms or s). A schematic construction is illustrated in Figure 5.

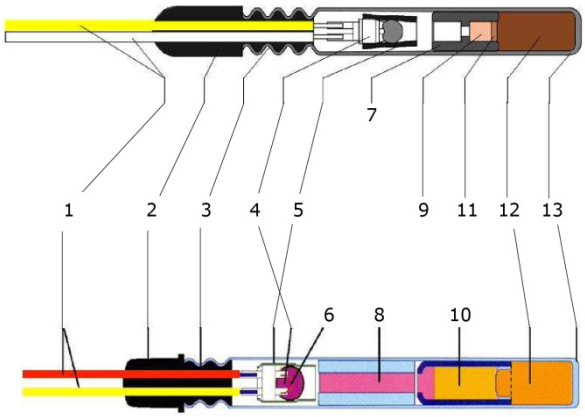

Figure 5 Example for standard and delay detonators.[6] **1** Wires, **2** Plug, **3** Fixing, **4** Primer, **5** Isolation, **6** Bridge wire, **7** Matter for primary, **8** Delay composition (different lengths), **9** Primary explosive, **10** Firing element, **11** Cover, **12** Secondary explosive, **13** Cartridge.

[6] Orica Mining Services, Technical data sheet, Dynadet Detonators.

Smoke-generating pyrotechnics

Depending on their ingredients, smoke-generating formulations produce varieties of colors and large amounts of gas to increase the colored surface. To avoid decomposition of the powdered pigment they burn at low temperatures. Examples of smoke formulations are presented below.

Table 3 Examples for pyrotechnic formulations used as smoke generators.

Pyrotechnic composition	Color of Smoke
Zinc dust, hexachloroethane, aluminium	white
Potassium chlorate, naphthalene, charcoal	black
Silicon tetrachloride, ammonia vapour	grey
Auramine, lactose, potassium chlorate, chrysoidine	yellow
Rhodamine red, potassium chlorate, baking soda, sulfur	red
Malachite green, potassium chlorate, antimony sulfide	green
Indigo, potassium chlorate, antimony sulfide	blue

The colored smoke is produced by an organic dye which first sublimes and then condenses in air to form small particles. They are strong absorbers of visible light and reflect discrete wavelengths of light depending on the used colored ingredient. Smoke pyrotechnics are used in camouflaging, wind direction indicators or in special effects (theatre, films) (Figure 6).[2,4]

Figure 6 Colored smoke grenade.[7]

Noise-producing pyrotechnics

The typical noise that a pyrotechnic composition produces is a loud 'bang' or a 'whistle'. The 'bang' is produced by a gas-generating formulation, for instance black powder, which is placed inside a paperboard tube and which is ignited by a fuse. This principle is known for bangers or aerial bomb shells. Flash powders react faster and at higher temperatures, releasing more high pressure gas then black powder. The noise of flash powder compositions are much louder then black powder compositions.

'Whistles' are produced by mixtures which are placed into an open-ended tube. Such compositions are very sensitive and hazardous to handle. Compounds which are added to whistlers are aromatic acids and their derivatives, potassium derivatives of benzoic acid or 2,4-dinitrophenol, picric acid and sodium salicylate. The noise is generated after ignition by the formation of a resonation standing wave. The length of the standing wave is influenced by the length of the pyrotechnic mixture and therefore the whistle can be controlled in lower or higher frequencies.[2]

[7] http://2.bp.blogspot.com/_Ku0lA8wyASE/S-zwWoK9zHI/AAAAAAAAEbU/LHPJha-rw9M/s1600/mk13smokeflare.jpg [Stand: 1.11.2012]

Light-producing pyrotechnics

Light–producing pyrotechnics emit light in the narrow spectral range of the visible light (400−780 nm). The intensity of the emitted light depends on the individual constituent parts of the composition and the produced heat after ignition. They consists mostly of an oxidizer (typical nitrates, perchlorates), a fuel (elemental metal powders) and additives (binders, etc.). Flame temperatures can vary from 2000–3000°C, dependent on the fuel (Mg, shellac, rosin). Pyrotechnics which emit light at a favored characteristic frequency (e. g. infrared) are discussed in detail within chapter 3 and 9.

The standard colors (red, green, yellow, blue) are generated by salts of the elements strontium, barium or boron, sodium, and copper (Table 4). Ideally, a compound bearing chlorine in its molecular structure is added to these formulations, e. g. perchlorates. At high temperatures the dye compound decomposes and reacts with the chlorine of the oxidizer to form molecules like $SrCl^+$ or SrOH. The ion emits light in the red region (600–690 nm) for strontium compounds, in the green region (505–535 nm, $BrCl^+$, BaOH, BaO) for barium or boron (BO_2) compounds and in the blue for $CuCl^+$ (420–460 nm).[1,2]

Table 4 Examples for pyrotechnic formulations used as white and colored emitters.

Pyrotechnic composition	Light effect
Magnesium, barium nitrate, potassium nitrate	white
Potassium perchlorate, barium nitrate, binder	green
Potassium perchlorate, strontium oxalate, binder	red
Potassium perchlorate, sodium oxalate, binder	yellow
Potassium perchlorate, copper carbonate , PVC	blue

To obtain white light the pyrotechnic formulation must burn at very high temperatures. The formed solid and liquid particles emit then light in a broad range in the visible electromagnetic spectrum. Because the oxidation of the metal fuels is a highly exothermic process high temperatures can be achieved. High temperatures form large amounts of atoms and molecules which are excited, resulting in higher intensity emissions. Elements which are preferred for very hot flames are magnesium or aluminum. Low temperatures are obtained by fuels like silicon or zinc.

Near Infrared Pyrotechnics

Abstract: *Alkaline metal salts are widely used in pyrotechnic formulations. For NIR pyrotechnics, e. g.* BLACK KNIGHT *compositions, potassium and cesium nitrate are mainly used as oxidizers and infrared emitters between 700–900 nm. Herein, new hand-held near infrared signal flare compositions were tested using several potassium and cesium salts of high nitrogen compounds such as tetrazole and triazole derivatives. The research of new formulations comprises the evaluation of sensitivity data and radiometric measurements of new formulations. Furthermore it was investigated if the IR emission can be improved using different nitrogen releasing agents like 5-aminotetrazole or diethylen triamino trinitrate (DETT) as hexamine replacements.*

Introduction

A typical human eye responds to wavelengths between 390–700 nm. A light-adapted eye has its maximum sensitivity in the green region of the visible spectrum at around 555 nm (Figure 7). The near infrared region starts from 700 nm and ending at about 2000 nm. Since the development of night vision devices (NVD or NOD) new pyrotechnic formulations emitting in the NIR region are of research interest. The mainly used spectral region for night vision detection is from 700–1000 nm, which can be explained by the spectral limit of night vision goggle detectors (Figure 8, red and orange graph).[8]

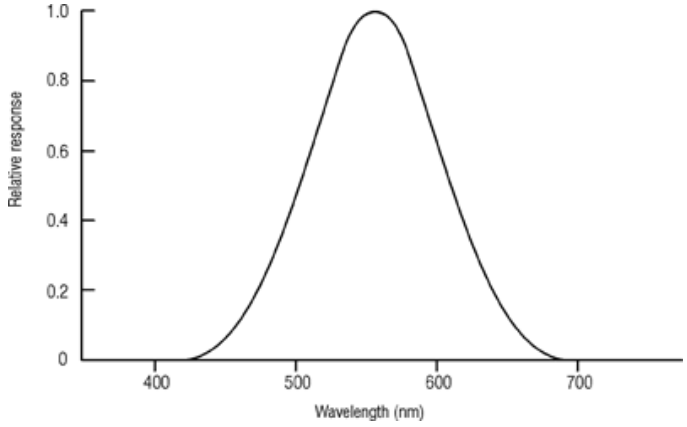

Figure 7 Spectral response of the human eye.[9]

[8] E.-C. Koch, Survey on State-of-the-art Near-Infrared Emitting Compositions for Flares and Tracers, NATO-MSIAC, Belgium, **2009**, and literature therein.
[9] http://utopia.cord.org/step_online/st1-6/images/Fig06-17.gif

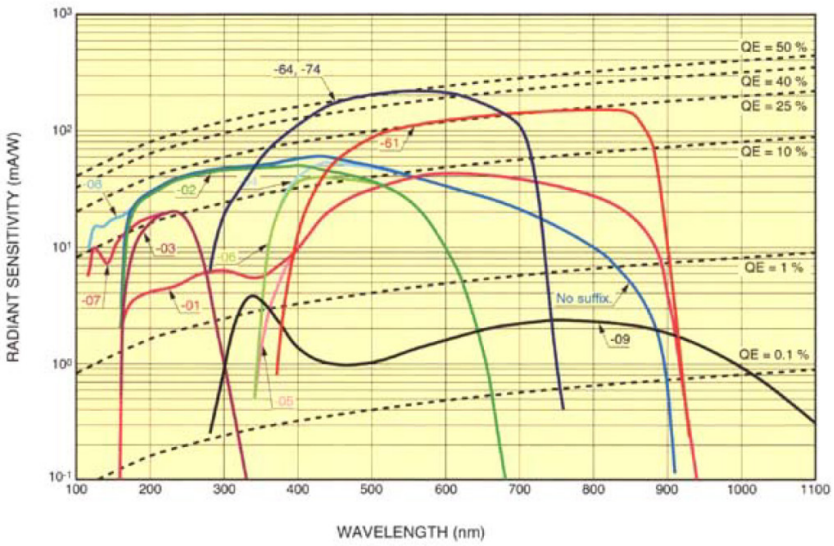

Figure 8 Radiant sensitivity of various detector types (UV, VIS–NIR).[8]

First attempts on infrared converter tubes were carried out in 1928 in the Netherlands (G. Holst and H. de Boer) but a first success was obtained from G. Holst in 1934 when he was working for Philips. The first device on the market was for civilian use and developed by D. Zworykin (Generation 0). NVDs in military use were introduced by the Germans in 1939 and first used of both sides during World War II (Generation 1) and then regularly in the Vietnam War. The intensifier tube uses an anode and an S-1 photocathode which consist of silver, cesium, and oxygen (Ag-O-Cs).[10] The sensitivity of the S-1 was from 300–1200 nm. Since the inception of image intensifier tubes the development of new night vision devices increases extensively. The latest generation (GEN III+) is the so called 'Omnibus-VII' (OMNI-VII). The new generations of high tech devices are able to adapt to changing light conditions, they produce less image noise, and operate with a luminous sensitivity of 700, instead of 1800 of GEN III devices.[11] NVD photocathode's of the III and III+ Generation are made of gallium arsenide which improves the image resolution. Another new feature is the auto-gating function (ATG) which leads to the best resolution and contrast at dynamic light conditions. They are useful for Aviator night vision goggles, operations in urban area or during sudden illumination of dark rooms or areas. The optical instrument includes an image intensifier tube, a water-resisting housing and a mounting system. Most of them include furthermore sacrificial lenses, IR illuminators, and telescopic lenses (Figure 9).

[10] a) Guo, H., Feng, L., Research on an extended blue GaAs photocathode, Proceedings of the International Society for Optical Engineering **2005**, 579. b) K. Stahl, Infrarottechnik, Hühtig Verlag, Heidelberg **1980**.
[11] Saldana, M., Night vision device having improved automatic brightness control, PCT Int. Appl. **1999**, WO9905697 A1.

NIR pyrotechnics find therefore their applications in (military) clandestine night operations and are used for instance as hand-held signal flares (ground) or parachute flares (ground to air) to illuminate large (combat) areas or aiding in emergency landings of aircrafts. Hence, they have two purposes: illumination and recognition.[5]

Figure 9 Night vision device in military application.[12,13]

Radiometric principles

IR pyrotechnics vary in their characterization in those who produce standard colored light. Therefore, every pyrotechnic composition can be characterized by different kinds of measurements. Colored-light or pyrotechnics which emit in the visible range of the spectrum are described by *photometric* measurements. Important parameters are the 'luminous intensity', given in candela [Cd] or lumen per steradians [lm sr^{-1}] and the 'dominant wavelength' [nm]. IR illuminants are specified by *radiometric* measurements. Important radiometric parameters within this thesis are the 'radiant intensity' and the introduced 'concealment index'. Hence, to discuss NIR illuminants several relevant radiometric terms are defined first.

The **Illumination**, given in units of W m^{-2}, can be expressed with equation 1 by:

$$Illumination = (I4\pi)/(4\pi R^2) \qquad (1)$$

where I is the Intensity in W sr^{-1} and R is the distance in feet (flare to illuminated object).[14]

[12] http://www.pvs4.com/AV-Night-vision-goggles.jpg [Stand: 1.11.2012]
[13] http://www.longwarjournal.org/photos/i/Afgh-Khost-NV.jpg[Stand: 1.11.2012]
[14] D. B. Nielson, Castable Infrared Illuminant Compositions, US Patent, WO94/02435, **1994**.

The **Irradiance E_e**, also given in W m^{-2}, is the power incident on a surface. They can be also called radiant flux density. Irradiance is often confusingly described as Intensity (Figure 10a).

The **Radiant Intensity I_e** is described as the power per unit solid angle and is given in units of Watts per steradian [W sr^{-1}].

The **Visible Radiant Intensity I_v** is given in Candela [Cd], because the visible intensity (or luminous intensity) is a photometric unit. For calculations of the dimensionless concealment index it is converted to W sr^{-1}. 1 W sr^{-1} is 12.566 watts or 683 Cd at 555 nm (Figure 10b).

a

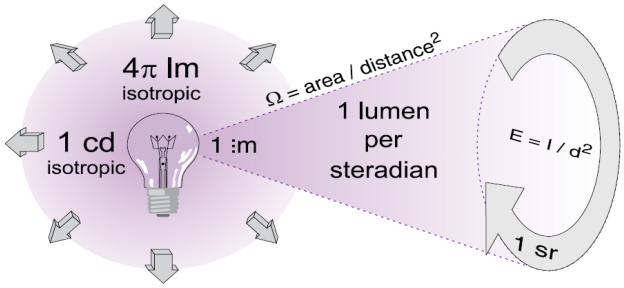

b

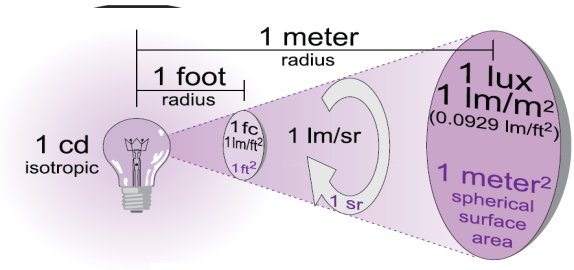

Figure 10 Irradiance (**a**) *vs*. Radiant Intensity (**b**).[15]

[15] A. Ryer, Light Measurement Handbook, International Light Technologies Inc. **1997**.

The **solid angle Ω** (A r^{-2}) is the two-dimensional angle in three dimensional space that an object subtends at a point. The SI unit is steradian [sr]. From mathematical or physical point of view the solid angle is dimensionless [m^2 m^{-2}] (Figure 11).

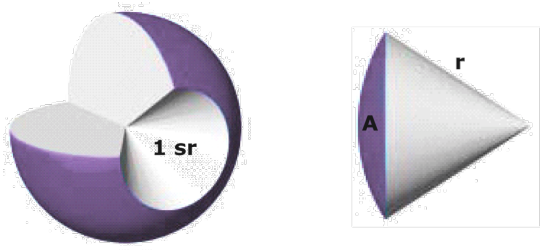

Figure 11 Illustration of the solid angle Ω, where A is the surface and r the radius.[15]

The **concealment index** χ gives the ratio of the emitted NIR radiation to the emitted visible light (equation 2).

$$\chi = \frac{I_{NIR}}{I_{Vis}} \qquad (2)$$

with λ_{NIR} = 700–1000 nm and λ_{Vis} = 400–700 nm. Both values can be calculated from radiometric intensity measurements. Typical values for concealment indices of parachute formulations are given in section 'Ammunition'.

Challenges of NIR pyrotechnics

Although NIR flares are in the field since a long period of time, several problems were found during the use of inserted illuminants.

As mentioned above the radiant intensity can be measured with special sensing devices, which respond to the invisible emission. It is favored to obtain a high concealment index χ, high NIR emission, and low in the visible area (equation 2). A commonly known disadvantage of many conventional compositions is the high emission of visible light which leads by mischance to a low concealment index.

A further problem of many known compositions is their burn rate. The burn rate describes the measurement of the linear combustion rate of a compound and is given in length over time. Burning rates normally increases with pressure and time (exceptions e. g. black powder). Formulations having low burn rates emit less IR radiation, hence high burn rates are required.

It is desired that the IR emission has its maximum at high altitudes. An undesired characteristic is therefore regarded to the burning time of the flare composition. Requested burning times of parachute flares are in the range of 20 seconds to several minutes. Parachute illuminants are ignited on ground and subsequent launched into the air. It is described that the burning surface area of flares increases over time. This means that a large amount of IR radiation is emitted near the surface and less radiation is emitted in higher altitudes. Additionally to avoid detection or fire of the area which is illuminated, parachute flares should not burn after they hit the ground.

A problem which is observed by emitting pyrotechnics is chunking. Large pieces of the flare material break away from the main charge or the propellant and fall to the ground. This leads to less illumination of the area, shorter burning times and large burning pieces can cause fire on the surface.

As pyrotechnic compositions are normally blended with several additives like binders, it is difficult to avoid the formation of soot. Most commonly used binders contain large carbon backbones which leads to the formation of solid carbon and carbon oxides. Depending on the binder and fuel, the formation of carbon and carbon oxides raises the amount of emitted visible light or causes black body radiation at high temperatures.

Due to temperature, pressure, or humidity variations while stored at different locations, pyrotechnics can undergo an aging process which is as well undesired.[8,14]

'Black Knight' compositions

Material

Main focuses of new NIR illuminants are on high burn rates, a clean burning behavior, high NIR emission and low emission in the visible. Non visible diffuse flames which disseminate condensed reaction products would be favored. Solid reaction products which are close to the flame can alter or dim the radiant characteristics. Therefore compounds which release large amounts of nitrogen are desirable. Nitrogen-rich compounds produce non-luminous flames and leads to a clear burning behavior. The main charge of presently used NIR formulations and which avoid most of the problems discussed above is the '*Black Knight*' (BK) composition. BK formulations consist of the compounds:[8,14,16,17,18]

- Silicon powder
- Potassium nitrate
- Cesium nitrate
- Hexamine
- Epoxy binder

As stated at the beginning, pyrotechnic compositions consist of an oxidizer and a fuel. For NIR illuminants the fuel is silicon powder, due to its non-luminous emission and nearly exclusively solid state combustion. It is important to avoid as much visible light as possible therefore fuels are used with low specific energy and burning temperature. Compared to other metal fuels, the specific energy of silicon is 250 [Cd s g^{-1}]. In contrast, magnesium has a specific energy of 18.200 [Cd s g^{-1}] and is therefore used in pyrotechnics where black body radiation is preferred (chapter 9).
Another possible fuel with similar characteristics is boron (900 [Cd s g^{-1}]). Both Si and B act as good heat sources and combustion rate catalysts.[8,16]

The alkaline metals potassium, cesium, and rubidium have intense emission lines in the infrared. The most intense transitions are at 766–769 nm for K, 780–794 nm for Rb and 852 & 894 nm for Cs. Their corresponding nitrates fulfill two functions: they are oxidizers and IR emitters.

[16] B. E. Douda, Visible Radiation from Illuminating-Flare flames: Strong Emission Features, *Journal of the Optical Society of America* **1970**, *60*, 1116.
[17] Lohkamp, Near Infrared Illuminating Composition, US Patent 3733223, **1973**.
[18] L. L. Jones, B. B. Nielson, Infrared Illuminant and Pressing Method, US Patent, 5056435, **1991**.

Standard NIR pyrotechnic formulations contain potassium nitrate or better a combination of potassium and cesium nitrate. Although high values for χ are obtained for rubidium it is not commonly used in IR pyrotechnics due to financial reasons. It was observed from intensity measurements that a combination of both nitrates lead to better infrared emission and to a high concealment index. Cesium nitrate is favored because it increases performance, accelerates the burn rates, broadens the infrared output, and reduces at the same time the visible output.[8]

Hexamine is added to the formulation to release nitrogen and enlarge the surface of the luminous area. Condensed products near the flame which can dim the IR emission are disseminated. However, it is mentioned in literature that hexamine support chunking of the flare charge.[14]

Several different types of binders (e. g. Laminac/Lupersol, Witco premix, VAAR, Epon 813/Versamid 140) are available for commercially used IR flares. A regularly used binder for *BK* compositions is a two component epoxy binder which consists of an epoxy resin and a curing agent.

Requirements on NIRs

The performance and radiometric requirements for new near infrared hand-held signal flares, based on *Black Knight* compositions are:

- 600–900 nm > 25 W sr^{-1}
- 695–1050 nm > 30 W sr^{-1}
- Visible light < 350 Cd
- Burn time ~ 45 seconds

The intensity values above 25 and 30 Watts per steradian, as well as the amount of visible light and burn time relates to the complete parachute illuminant with an igniter charge, a first fire and the main NIR flare and comprises in most cases a charge size of 20 g and larger.

Ammunition

NIR illuminants compared to visible flares provide a larger illuminated area after ignition (Figure 12a). They are supplied in different sizes for instance as 60, 80, 120 mm caliber. An example of IR candles is the aerial flare for target illumination LUU-19 Infrared Illuminant Rocket (Figure 12b). The size of this parachute flare is 12.4 cm and the burning time > 7 minutes. At 1500 m height this flare illuminates an area of 5.1 km^2 (radius 1.277 km) and provides an irradiance of 2.33 x 10^{-4} W m^{-2}. A 26.5 mm parachute flare with a payload mass of 20 g is provided by Rheinmetall. The burning time is 15 s, the radiant intensity is 20 W sr^{-1} (NIR) and 250 Cd (VIS), the concealment index χ is 54. The 40 mm hand-held parachute rocket (Rheinmetall) burns 28 s with a NIR emission of 25 W sr^{-1}, 250 Cd, and a χ of 68. A further example and profile of an artillery IR projectile is shown in Figure 13.[8]

a

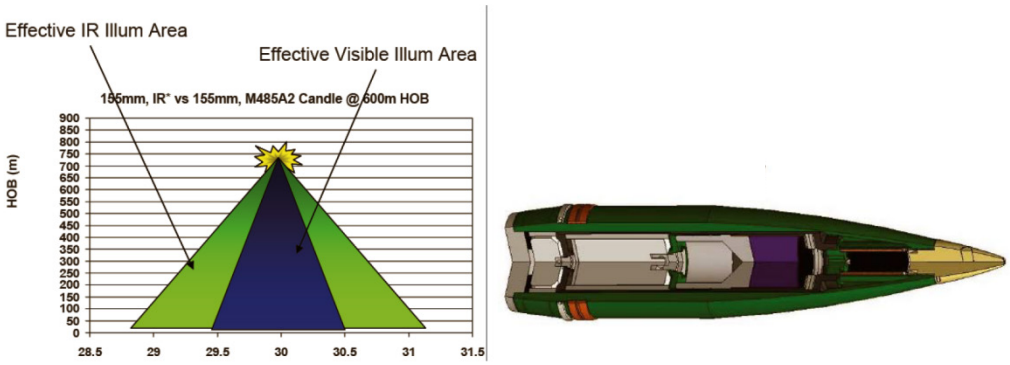

b

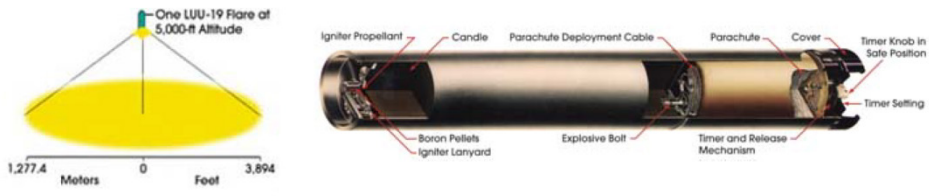

Figure 12 Illumination performance of XM 1064/6 155 MM Artillery IR Illuminant (**a**) and LUU-19 IR illuminant rocket (**b**).[8]

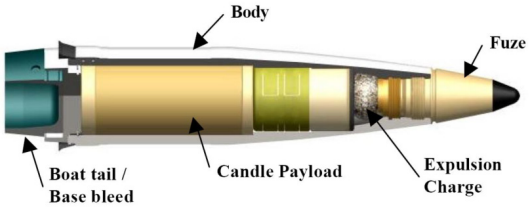

Figure 13 M0235 105 MM Infrared Illuminant cartridge.[8]

Research objective

Although common NIR formulations are already in use, it is favored to improve some characteristics like the performance data. Values of more than 25 and 30 W sr^{-1}, respectively, low visible emission and burn times of at least 45 seconds are desired. To discuss new NIR formulations it is nowhere near enough to synthesize new compounds. Important tools for analyzing modifications of pyrotechnic compositions are radiometric measurements.

Until now no radiometric measurements were carried out in our research group, therefore the major intention within this thesis is the establishment of a set up for radiometric near infrared measurements with the new OCEAN OPTICS spectrometer and further to write a MATLAB code for evaluating the radiometric results.

It is assumed that certain potassium and cesium compounds possess enough energy to achieve both exothermal decomposition and thermal excitation but generate sufficient nitrogen gas to remain dim in the visible range. Therefore a further challenge is the synthesis of several high nitrogen energetic materials, to analyze the energy content, safety and NIR emission behavior of cesium and potassium salts of these HEs and to find potential candidates for new molecular pyrotechnic NIR flare formulations. The synthesis of new formulations comprises the addition of cesium and potassium salts in a defined ratio, to raise the emission between 600 and 1000 nm, and to avoid visible emission. Radiometric results of standard main charges of *Black Knight* compositions were compared with the results obtained from new formulations. Possible candidates for NIR emitting compounds are potassium and cesium salts of 3-nitro-1,2,4-triazol-5-(1*H*,4*H*)-one (NTO), 4,4´,5,5´-tetranitro-2,2´-bisimidazole (TNBI), 5,5´-bistetrazolyl amine (BTA), 3-nitro-1,2,4-triazole, etc. (Figure 14).

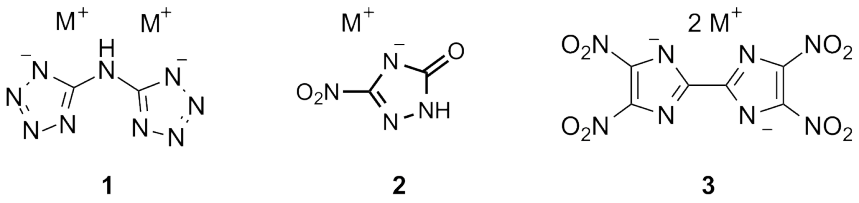

Figure 14 Chemical structures of BTA (**1**), NTO (**2**), and TNBI (**3**) salts (M = K, Cs).

Due to chunking of formulations containing hexamine it was further tested whether similar constituted compounds like lactose or 5-amino-1,2,4-triazole avoid this negative effect and additionally remain dim in the visible range by nitrogen or carbon dioxide release.

Discussion – Synthesis of NIR Additives

Remarkable classes of new energetic materials are high nitrogen compounds (HNC) such as tetrazoles or triazoles. They are not only interesting as primary or secondary explosives and RDX replacements also as additives in pyrotechnics or propellants. The benefit of high nitrogen compounds derive from their very high heats of formation, due to the large amount of N-N and C-N bonds within their chemical structure and of the formation of large amounts of nitrogen. The heat of formation of 1,2,3-triazole and 1,2,4-triazole for example are 272 kJ mol^{-1} and 109 kJ mol^{-1}, respectively and 237 kJ mol^{-1} for 1*H*-tetrazole. Compared to their carbon equivalents nitrogen rich heterocyclic ring systems are further favorable because of their higher heats of formation, densities, oxygen balance, and thermal stability. Together with substituents like nitro, amino or azide groups they are multiple insertable.[19] For additives in pyrotechnic compositions there are worth considering because of the formation of non luminous flames and the absence of soot or smoke. New approaches in the synthesis of pyrotechnic formulations comprise the use of already known energetic materials such as TNT.[20] Hence, for new *Black Knight* compositions studied in this work it is worthwhile to test common nitrogen rich explosives e. g. NTO and compounds with similar chemical structure like triazoles, tetrazoles and bistetrazoles and to investigate their radiometric properties. In the following the synthesis, physical behavior or crystal structure of several HNCs are discussed, whereas not all of these compounds are possible additives in pyrotechnic formulations, due to their sensitivity data, low yield or high costs.

[19] T. M. Klapötke, Structure and Bonding, High Energy Density Materials, Springer Verlag, p. 36-79, **2007**.
[20] E.-C. Koch, 2,4,6-Trinitrotoluene: A Surprisingly Insensitive Energetic Fuel and Binder in Melt-Cast Decoy Flare Compositions, *Angewandte Chemie* **2012**, *51*, 1.

Potassium and cesium 3-nitro-1,2,4-triazolate (1a & 1b)

Based on the patent DE 4115365 A1 3-nitro-1,2,4-triazole[21], potassium, and cesium 3-nitro-1,2,4-triazolate were synthesized using the following procedure:

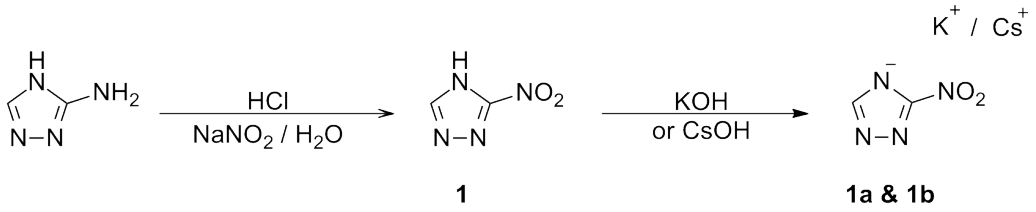

Schema 1 Synthesis of potassium and cesium 3-nitro-1,2,4-triazolate (**1a** & **1b**).

3-Amino-1,2,4-triazole was nitrated under acidic conditions to form 3-nitro-1,2,4-triazole (**1**). The driving force of the diazotization mechanism is the nitrogen release of the intermediate formed diazonium cation. The reaction can be accelerated by heating the solution to 55°C. At the end of the reaction the excess of nitrite was quenched using concentrated hydrochloric acid und urea.

The best yield of 57% was obtained using 10 g (119 mmol) of 3-amino-1,2,4-triazole. Potassium and cesium 3-nitro-1,2,4-triazolate was received after isolation and purifying **1** and adding the corresponding alkaline base as hydroxides or carbonates (**1a**, **1b**). Both salts could be recrystallized from ethanol/water. **1a** (yellow powder) was obtained water free, whereas **1b** (orange crystals) was found to be the monohydrate.

Analytic and physical-chemical data

The analytical data (^{1}H, ^{13}C NMR, IR, Raman, elemental analysis) of **1**, **1a**, and **1b** conforms to the data given in literature.[21] The chemical shift of the nitro group in the ^{14}N NMR is at -27 ppm. The symmetric valence mode in the IR spectra for the nitro group of **1a** is observed at 1362 and 1549 cm^{-1}, for **1b** at 1356 and 1521 cm^{-1}. The melting point of around 212°C for **1** conforms to the literature value of 210–214°C.

1, **1a**, and **1b** are insensitive against friction (FS), impact (IS), and electric discharge (ESD). Their sensitivity data are given in Table 5.

[21] M. Heschel, Preparation of 3-nitro-1,2,4-triazole, DE 4115365 A1, **1992**.

Table 5 Sensitivity data of 3-nitrotriazol (**1**), potassium (**1a**) and cesium salt (**1b**).

	1	**1a**	**1b · H_2O**
IS / J	40	40	40
FS / N	240	288	240
ESD / J	0.5	0.5	0.4

Potassium and cesium 3,5-dinitro-1,2,4-triazolate (DNT) (2a & 2b)

The synthesis of both, potassium and cesium DNT, starting from 3,5-diamino-1,2,4-triazole were carried out according to BAGAL *et al*.[22]

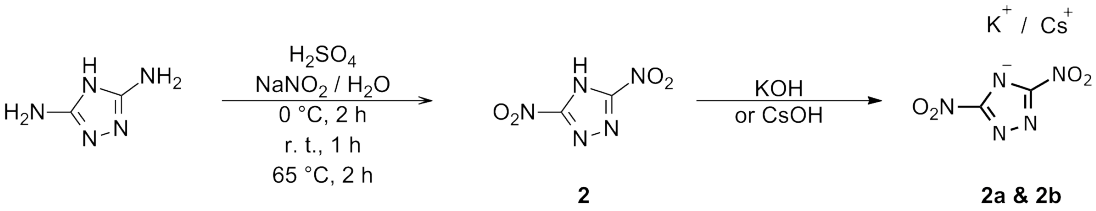

Schema 2 Synthesis of potassium and cesium 3,5-dinitro-1,2,4-triazolate (**2a** & **2b**).

Under ice-cooling 3,5-diamino-1,2,4-triazole in water was added to sodium nitrite in sulfuric acid. In contrast to the diazotation described above, a large excess of nitrite was used to avoid unrequested side reactions. The mixture was heated to 65°C and stirred at this temperature until a clear red solution was obtained. The excess of nitrite was quenched under ice-cooling with 30% sulfuric acid and urea. The solution was extracted with ether and then treated with acetone. **2a** and **2b** were obtained in moderate yields of 50% after adjusting the pH to 7 with the corresponding alkaline base (1 M). The purification steps described in the patent[23] were not successful. Therefore, the crude product was recrystallized from isopropyl alcohol and water. **2a** was obtained as a dihydrate. **2b** was obtained as a monohydrate using cesium carbonate, whereas the water free compound was obtained using cesium hydroxide.

[22] L. I. Bagal, M. S. Pevzner, Heterocyclic nitro compounds. I. Synthesis of nitro derivatives of 1,2,4-triazole, 1,3,4-thiadiazole, tetrazole, 1,3,4-oxadiazole and pyrazole by the noncatalytic substitution of a diazo group for a nitro group, *Chemistry of Heterocyclic Compounds* **1970**, *6*, 259.
[23] T. K. Highsmith, J. M. Hanks, Process for the synthesis and recovery of nitramines, WO 02060881 A1, **2002**.

Analytic and physical-chemical data

Elemental analysis, NMR shifts, and vibrational spectra are comparable to the data given in literature.[22] The chemical shifts in the ^{14}N NMR for the nitro group is located at -22 ppm for **2a** and -24 ppm for **2b**. The RAMAN symmetric valence mode of the nitro group is around 1404 cm^{-1} (**2a**) and 1397 cm^{-1} (**2b**), whereas the deformation mode is at 525 (**2a**) and 517 cm^{-1} (**2b**). Neither NH_2 or NH-modes (RAMAN, IR spectra) nor proton signals (^1H NMR) are obtained. Both salts are insensitive against impact, friction, and electric discharge.

Table 6 Sensitivity data of potassium and cesium 3,5-dinitro-1,2,4-triazolate (**2a** & **2b**).

	2a · 2 H_2O	**2b · H_2O**
IS / J	40	40
FS / N	240	144
ESD / J	0.3	0.15

Crystal structure of cesium 3,5-dinitro-1,2,4-triazolate (2b)

Single crystals of cesium 3,5-dinitro-1,2,4-triazolate with 0.75 water molecules were obtained after recrystallization from ethanol/water. Compound **2b** crystallizes in the orthorhombic space group *Pbca* with 8 molecules in the unit cell and a size of a = 9.6332(5) Å, b = 11.7893(5) Å, c = 13.6302(5) Å, $\alpha = \beta = \gamma = 90°$. The volume of the cell is 1547.8(1) $Å^3$ and the crystal density 2.613 g cm^{-3} (T = 25 °C). Figure 15 displays the molecular unit of **2b**. Bond lengths and bond angles of the unit cell are given in Table 7.

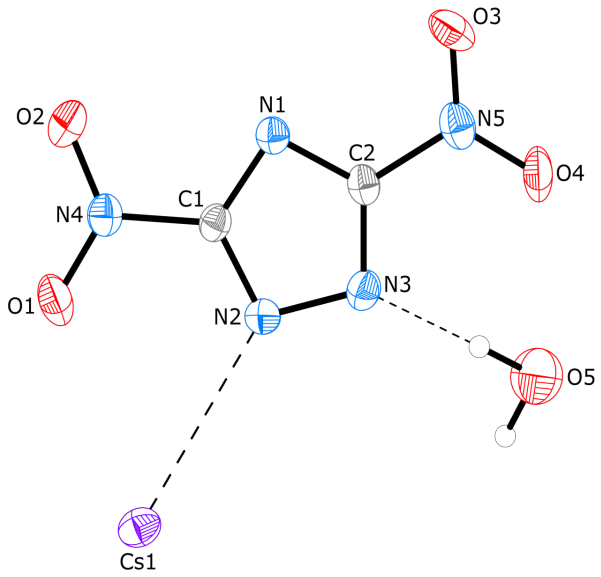

Figure 15 Crystal structure of cesium 3,5-dinitro-1,2,4-triazolate · 0.75 H_2O; Thermal ellipsoids in figures of crystal structures were drawn to 50% probability.

The C-N bond distances of 1.325(4)–1.442(4) Å are between a formal C-N single (1.47 Å) and C-N double bond (1.22 Å) and the N-N bond distance of 1.363(4) Å is between a formal N-N single (1.45 Å) and N-N double bond (1.25 Å).[24] Both are in good agreement with the literature known tetraammine copper salt of DNT.[25]

The Cs-O distances (3.123–3.617 Å) and Cs-N distances (3.227–3.505 Å) in **2b** are longer than in cesium structures described in literature.[26] Coordination of the NO_2-nitrogen atom is neglected, due to a positive partial charge of the nitrogen and therefore less electron density. Mainly eight oxygen atoms, six of the nitro groups and two from water molecules, saturate the coordination sphere of the cesium ion. Four nitrogen atoms of different anions coordinate with a distance of 3.23-3.51 Å.

The view along the c-axis displays a wave structure of the anion and water molecules located between the layers (Figure 16). A view along b-axis shows that two alternate molecular units are orthogonal to each other and one water molecule is located on every bend of the wave.

[24] A. Holleman, E. Wiberg, N. Wieberg, Lehrbuch der Anorganischen Chemie 102nd Edition, Walter de Gruyter, **2007**.
[25] M. H. V. Huynh, M. A. Hiskey, Preparation and explosive properties of tetraamminebis(3,5-dinitro-1,2,4-triazolato-N1)copper(II), Journal of Energetic Materials **2005**, 23, 27.
[26] H. Radies, T. M. Klapötke, Alkali Salts of 1-Methyl-5-nitriminotetrazole, *Zeitschrift für Naturforschung* **2007**, *62*, 1343.

The crystal lattice is stabilized through moderate hydrogen bonds which lead in a helical structure, consisting of Cs-H_2O-units, and from H-bonds formed from N1 as acceptor and a water molecule as donor. The O-H distance is 0.951(37) Å and the N···H distance 1.989(37) Å. Therefore, the resulting donor-acceptor distance is 2.938(37) Å with an O-H-N angle of 175.73(28)°.

Table 7 Bond lengths and bond angles of **2b**.

	Bond length [Å]		**Bond angle [°]**
O1-N4	1.224(4)	O2-N4-O1	124.4(3)
N4-O2	1.224(3)	O2-N4-C1	117.5(3)
N4-C1	1.442(4)	O1-N4-C1	118.1(3)
C1-N2	1.326(4)	N2-C1-N1	117.6(3)
C1-N1	1.331(4)	N2-C1-N4	121.3(3)
C1-C2	2.004(41)	N1-C1-N4	121.1(3)
N1-C2	1.335(2)	N2-C1-C2	76.2(2)
N3-C2	1.325(4)	N1-C1-C2	41.35(17)
N3-N2	1.363(4)	N4-C1-C2	162.4(3)
O4-N5	1.219(4)	C2-N3-N2	104.4(3)
O3-N5	1.230(4)	C1-N2-N3	103.6(3)
		N3-C2-N1	117.0(3)
		N3-C2-N5	121.5(3)
		N1-C2-N5	121.6(3)
		N3-C2-C1	75.8(2)
		N1-C2-C1	41.19(17)
		N5-C2-C1	162.7(3)
		O4-N5-O3	124.2(3)
		O4-N5-C2	117.8(3)
		O3-N5-C2	118.0(3)

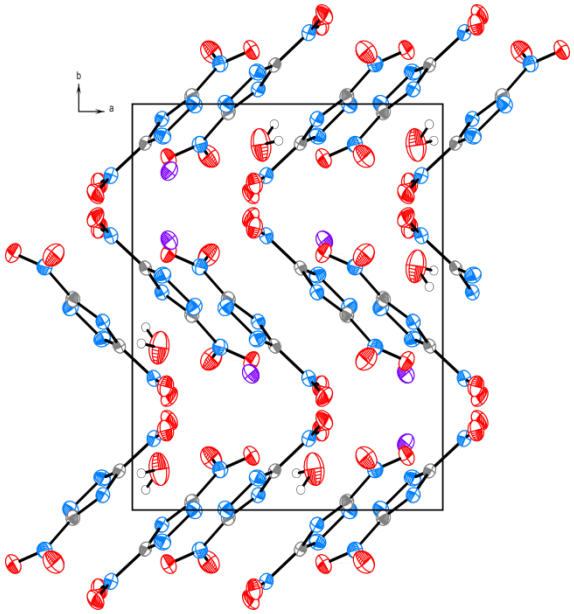

Figure 16 View along c-axis of cesium 3,5-dinitro-1,2,4-triazolate · 0.75 H_2O; Thermal ellipsoids in figures of crystal structures were drawn to 50% probability.

Synthesis of potassium and cesium 3,3'-bis(1,2,4-oxadiazol-5-one) (5a & 5b)[27]

Synthesis of diaminoglyoxim (3)

The synthesis of diaminoglyoxime was carried out according to ZELENIN and TRUDELL.[28] To a solution of sodium hydroxide and hydroxylammonium chloride was added glyoxal (40% solution). After 12 h reflux and 36 h crystallization at 4°C the product was obtained in 56% yield.

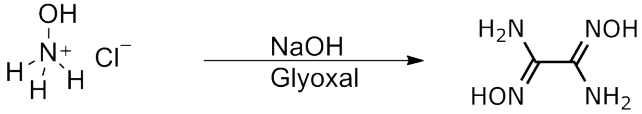

3

Schema 3 Synthesis of diaminoglyoxim (**3**).

[27] N. Mayr, PhD thesis, Ludwig-Maximilians-University, Munich **2012**, and literature therein.
[28] A. K. Zelenin, A. K. Trudell, A two-step synthesis of diaminofurazan and synthesis of N-monoarylmethyl and N,N'-diarylmethyl derivatives, *Journal of Heterocyclic Chemistry* **1997**, *34*, 1057.

Synthesis of oxamiddioxime dicarboxylic acid diphenylester (4)

4 was synthesized by treating **3** in THF with phenyl chloroformate and adding slowly triethyl amine under ice-cooling. After 4 h triethylamine hydrochloride was filtered off and the yellow solution was added to water. The product precipitated immediately, was filtered off and washed with diethyl ether.

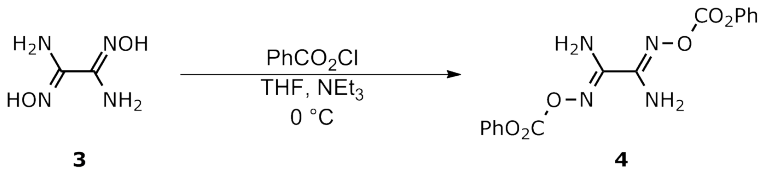

3 **4**

Schema 4 Synthesis of oxamiddioxim dicarboxylic acid diphenylester (**4**).

The obtained yield of 89% for the second reaction step using 84.7 mmol of **3** could not be improved by using the double amount of **3** (169.4 mmol). The analytical data of **4** agree with the data given in literature.[27]

Synthesis of 3,3'-bis(1,2,4-oxadiazol-5-one) (5) (BOX)

The second last reaction step comprises a base induced ester cleavage followed by an acid catalyzed ring closure leading to compound **5**.

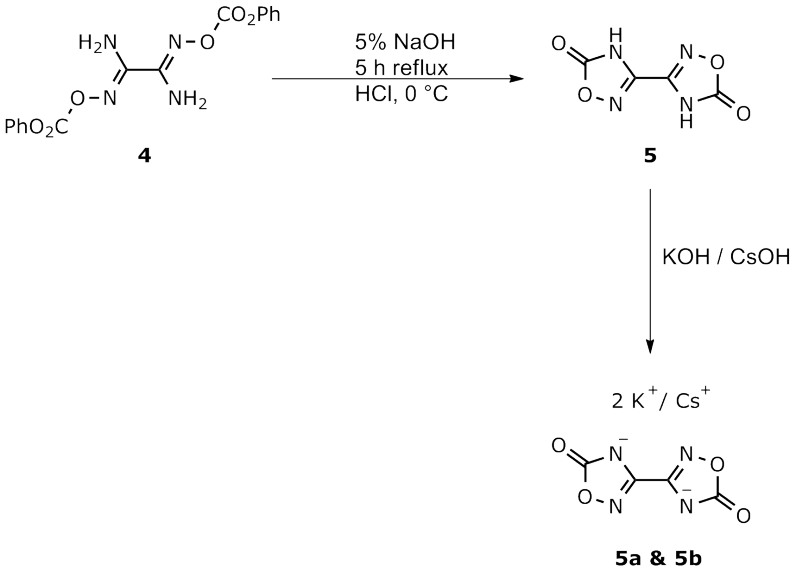

4 **5**

5a & 5b

Schema 5 Synthesis of 3,3'-bis(1,2,4-oxadiazol-5-one) (**5**).

To improve the moderate yield of 60%, **5** was treated with 10% sodium hydroxide solution instead of 5% NaOH which results in an amount of only 45%. It is expected that the concentration of sodium hydroxide influenced the ring closure; $PhCO_2^-$ separates too fast and therefore the ring closure does not occur.

5a and **5b** were synthesized with two equivalents KOH or CsOH in water. Analytical data and crystal structures of **5**, **5a** and **5b** are discussed in detail within the PhD thesis of N. Mayr.[27] The sensitivity data of both salts are given in Table 8.

Table 8 Sensitivity data of potassium and cesium 3,3'-bis(1,2,4-oxadiazol)-5-one.

	5a	**5b**
IS / J	40	40
FS / N	360	360
ESD / J	1.0	1.0

Synthesis of potassium and cesium 3-nitro-1,2,4-triazole-5(4*H*)-one (NTO) (7a & 7b)

An already known and commercially available secondary explosive is 3-nitro-1,2,4-triazole-5(1*H*,4*H*)-one (NTO) (**7**). NTO is discussed as RDX (1,3,5-trinitro-1,2,5-triazacyclohexane) or HMX (1,3,5,7-tetranitro-1,3,5,7,tetraazacyclooctane) replacement in military applications due to comparable performance, less sensitivity and high density of 1.93 g cm^{-3}. NTO is used in automobile airbags as alternative to the toxic primary explosive lead azide.[29] Therefore it is an interesting candidate as additive in other pyrotechnic formulations. Because pyrotechnic compositions require compounds with high friction data cesium and potassium NTO were synthesized and tested as possible ingredients for *Black Knight* formulations.

The synthesis of potassium and cesium 3-nitro-1,2,4-triazole-5(1*H*,4*H*)-one is described in Schema 6.[29,30]

[29] H. S. Jadhav, M. B. Talawar, Synthesis, characterization and thermolysis of 2,4-dihydro -2,4,5-trinitro-3*H*-1,2,4-triazol-3-one (DTNTO): a new derivative of 3-nitro-1,2,4-triazol-5-one (NTO), *Indian Journal of Engineering & Material Sciences* **2005**, *12*, 467.

[30] D. Izsák, unpublished results, Ludwig-Maximilians-University Munich, **2012**.

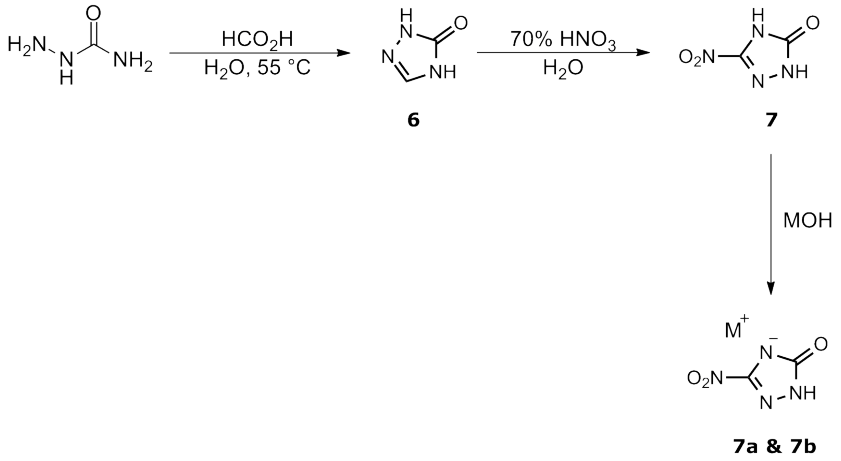

Schema 6 Synthesis of 3-nitro-1,2,4-triazole-5(1*H*,4*H*)-one (**7**), **7a** and **7b** with M = K or Cs.

To a hot solution of 85% acetic acid was added semicarbazide. After refluxing the solution for 7 h the acid was evaporated. The solid was treated with water and the solvent was again evaporated. This procedure was repeated two more times. Afterwards the solid was recrystallized from hot water. TO (**6**) was obtained in moderate yields of 61%. **7** was obtained after adding **6** to an excess of 100% nitric acid under ice-cooling. After 2 h the cooling was removed and the mixture was stirred at room temperature over night. The solid was isolated and washed with water. NTO was obtained as a colorless powder with a yield of 23%. Crystalline NTO was obtained from the cooled solution (4°C) after four days.
1 equivalent of potassium and cesium hydroxide, respectively were used for synthesizing the salts of NTO **7a** and **7b.** Both were recrystallized from ethanol/water. Potassium NTO (**7a**) was obtained as a dihydrate and cesium NTO (**7b**) as a monohydrate.

Analytic and physical-chemical data

The standard analytical data (NMR, EA, mass) for NTO is comparable with the data given in literature.[29] Symmetric valence modes of the nitro group in the RAMAN spectra are at 1376 cm^{-1} (**7a**) and 1377 cm^{-1} (**7b**). The bend mode of the NO_2-group is at 484 (**7a**) and at 488 cm^{-1} (**7b**), respectively. The antisymmetric stretch mode for the nitro group in the IR is located at 1587 cm^{-1} for **7a** and 1591 cm^{-1} for **7b**. NH modes in the IR spectra are at 3342 cm^{-1} for **7a** and 3349 cm^{-1} for **7b**. The FAB^- mass spectra indicate a single deprotonation at the ring system. Sensitivity data of both salts are given in Table 9.

Table 9 Sensitivity data of potassium and cesium 3-nitro-1,2,4-triazol-5(*4H*)-one.

	7a	**7b**
IS / J	40	40
FS / N	288	288
ESD / J	0.3	0.3

Synthesis of potassium and cesium bis(1-methyl-tetrazole-5-yl)-triazene monohydrate (8a & 8b) (BMTT)

The formation of bis(1-methyl-tetrazole-5-yl)-triazene (**8**) is illustrated in Schema 7. The compound was obtained as a monohydrate.[31]

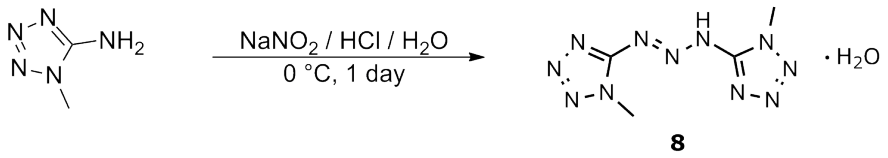

8

Schema 7 Synthesis of bis(1-methyl-tetrazol-5-yl)-triazene · H_2O (**8**).

Using a half equivalent of sodium nitrite **8** was obtained under acidic conditions by diazotation of 2-methyl-5-aminotetrazole. After stirring the mixture for 24 h under ice-cooling the product was isolated with a yield of 32%. Because of an intense reaction (large amount of fume) and nitrogen release a large reaction flask was used to avoid flooding. Both salts were obtained by solving **8** in ethanol and adding one equivalent of the corresponding base. **8a** and **8b** were recrystallized from ethanol/water and dried at 50°C. Both were obtained as very fine yellow-greenish powders.

Analytic and physical-chemical data

Standard analytic was carried out for the potassium and the cesium salt of **8**. The methyl group in the ^{1}H NMR is detected as a singlet at 3.87 (**8a**) and 3.84 (**8b**) ppm. Both ring carbons are located at 162 and both methyl groups at 33 ppm in the ^{13}C NMR spectra. Raman and IR spectra are also comparable with the data given in literature.[31]

[31] T. M. Klapötke, J. Stierstorfer, Investigations of bis(methyltetrazolyl)triazenes as nitrogen-rich ingredients in solid rocket propellants - Synthesis, characterization and properties, *Polyhedron* **2009**, *28*, 13.

Although **8** was obtained as a monohydrate the impact sensitivity is very low in contrast to a friction sensitive greater than 360 N (Table 10). Compared to the neutral compound the impact sensitivity was improved by the formation of salts. **8a** and **8b** are suitable as possible NIR ingredients but due to very low electrostatic discharge values and very low yields, both compounds are only second quality for pyrotechnic composition studied in this work.

Table 10 Sensitivity data of **8a** & **8b.**

	8	**8a**	**8b**
IS / J	3	40	35
FS / N	360	360	288
ESD / J	n.d.	0.03	0.03

Synthesis of 3,6-bis-nitroguanidyl-1,2,4,5-tetrazine, bis-potassium and bis-cesium BNGT (12a & 12b)

Potassium and cesium BNGT were synthesized *via* multiple step synthesis (Schema 8).

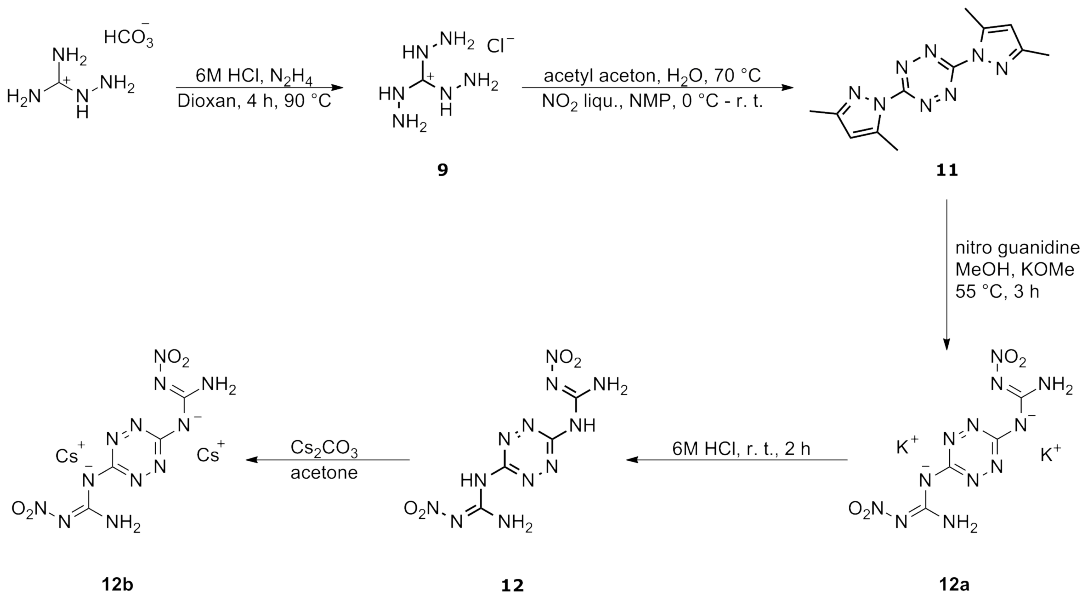

Schema 8 Synthesis of **12a** & **12b**.

Starting from TAG·HCl (**9**), which is obtained in good yields of 79%, the ring closure and the followed oxidation with NO_2 synthesizing **11**, were carried out according to M. D. COBURN and M. A. HISKEY.[32,33,34] The oxidizing agent could be added either gaseous by a medium nitrogen flow using a washing flask between the NO_2 and the reaction flask or adding liquid NO_2. Choosing the latest, the loss in NO_2 is higher and therefore an excess of 30 % should be used to balance the stoichiometry. Unfortunately NMP is not the solvent of first choice, due to its high boiling point and the solubility of **11** to some extent, but no superior solvent was found within this work. For the synthesis of **12a** all used chemicals must be water free, concerning the hydrolysis of potassium methanolate. The *in situ* formed bis potassium salt was obtained as a dark red powder which could be recrystallized from water.
The next step comprises the formation of the neutral compound **12** with HCl. An adequate solvent to recrystallize **12** was not found.
It is known that tetrazines could be dissociated by a nucleophilic attack of the hydroxide anion to the carbon atoms leading to semicarbazide, hence the addition of cesium hydroxide for the formation of the cesium salt must be stoichometric.[34] Because the deprotonation is faster than the nucleophilic attack, an accurate amount of the hydroxide leads to a reaction without any difficulties. Pure **12b**, as well as pure **12a**, were obtained in very low yields and therefore only one pyrotechnic formulation of each compound was prepared.

Analytic and physical-chemical data

In some cases the methyl group of the pyrazole leaving group was still detected in the ^{1}H and ^{13}C NMR. Crystals for x-ray measurements of both were not obtained. RAMAN and IR data conform to the data given in literature.[33,34]

Table 11 Sensitivity data of **12**, **12a** and **12b**.

	12	**12a**	**12b**
IS / J	8.5	40	40
FS / N	240	240	288
ESD / J	0.1	0.6	0.6

[32] K. Y. Lee, M. D. Corburn, 3-nitro-1,2,4-triazol-5-one: a less sensitive explosive, US 4733610 **1988**.
[33] M. C. Corburn, G. A. Buntain, An improved synthesis of 3,6-diamino-1,2,4,5-tetrazine. II. From triaminoguanidine and 2,4-pentanedione, *Journal of Heterocyclic Chemistry* **1991**, *28*, 2049.
[34] D. E. Chavez, M. A. Hiskey, Novel high-nitrogen materials based on nitroguanyl-substituted tetrazines, *Organic Letters* **2004**, *6*, 2889.

Synthesis of 3,6-bis (1*H*-1,2,3,4-tetrazol-5-yl-amino)-1,2,4,5-tetrazine (15)

Compound **13** was synthesized in good yields of 85% *via* nucleophilic substitution of the pyrazole ring of **11** by hydrazine at 50°C and acetonitrile as solvent. To remove the hydrazine from the ring system **13** was treated with chlorine at room temperature, obtaining **14** in quantitative yield. **14** should not be dried under high vacuum due to sublimation of the product (Schema 9).

The literature known synthesis of **15** was carried out with sodium 5-amino-tetrazolate.[35,36] To avoid as much sodium as possible, the respective potassium and cesium salts were used instead. But the exchange of chlorine with potassium or cesium 5-amino-tetrazolate to form compound **15** was not successful yet. ^{1}H and ^{13}C NMR signals are only detected for both amino tetrazolate salts.

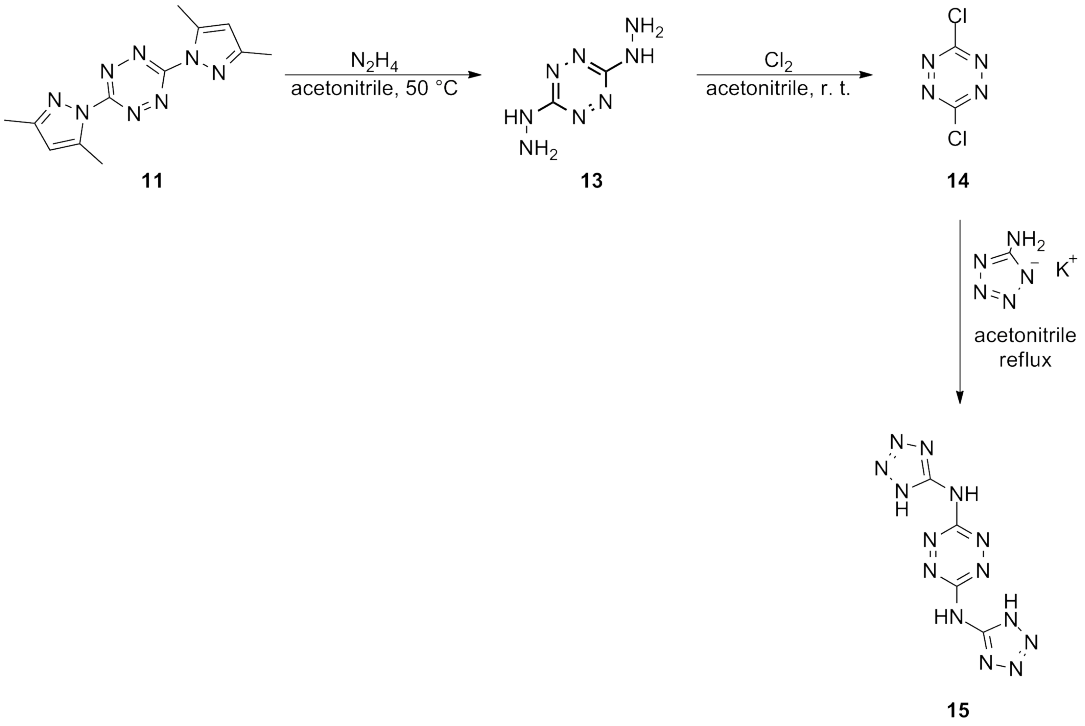

Schema 9 Attempted synthesis of **15**.

[35] M. Hang, M. A. Hiskey, 3,6-Di(azido)-1,2,4,5-tetrazine: a precursor for the preparation of carbon nanospheres and nitrogen-rich carbon nitrides, *Angewandte Chemie* **2004**, *43*, 5658.
[36] D. E. Chavez, M. A. Hiskey, 1,2,4,5-Tetrazine-based energetic materials, *Journal of Energetic Materials* **1999**, *17*, 357.

Following the procedure described by A. SAIKIA *et al.*, compound **11** was treated directly with 5-aminotetrazole in sulfolane at 135°C.[37] The crude product was purified in DMF for 4 h at 120°C and afterwards refluxed in ethanol. Weak ^{1}H and ^{13}C NMR signals are detected for 5-aminotetrazole. Variations on scale and temperature led to no reaction. Therefore no further attempts were carried out synthesizing compound **15**.

Synthesis of 3,6-diamino-1,2,4,5-tetrazine (16)

Schema 10 describes the synthesis of 3,6-diamino-1,2,4,5-tetrazine with ammonia.[38]

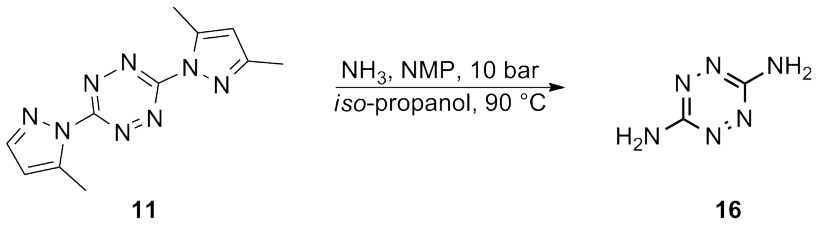

Schema 10 Synthesis of 3,6-diamino-1,2,4,5-tetrazine (DAT) (**16**).

DAT is a favorite precursor for synthesizing several secondary explosives. Presently, tetrazine based explosives are synthesized *via* 1,3-diaminoguanidine and are therefore expensive and extensive.[39] The synthesis of compound **16** and e. g. salts of nitramino aminotetrazine (**17**) in a steel autoclave is favorable because of low costs and provides yields up to 90%.

11 and NMP were added in a steel autoclave and cooled with liquid nitrogen. After 20 min the autoclave was evacuated and ammonia condensed into the container. The mixture was allowed to come to room temperature and was then heated to 90°C for several hours. Afterwards the mixture was treated with isopropanole and cooled in a fridge over night and the solid was filtered off on the next day. The purity of the bright red compound **16** was checked by elemental analysis and NMR. The signal for both amine groups is located at 6.70 (4 H) in the proton spectra and the signal of both carbon atoms of the tetrazine ring are located at 162.3 ppm (2 C) in the ^{13}C NMR.

[37] A. Saika, Synthesis and characterization of 3,6-bis(1*H*-1,2,3,4-tetrazol-5-ylamino)-1,2,4,5-tetrazine (BTATz): Novel high-nitrogen content insensitive high energy material, *Journal of Hazardous Materials* **2009**, *170*, 306.
[38] M. D. Coburn, D. G. Ott, Synthesis of 3,6-diamino-1,2,4,5-tetrazine, US 5281760, **1994**.
[39] M. Göbel, PhD thesis, Ludwig-Maximilians-University Munich, **2010**.

Synthesis of 3-amino-6-nitramino-1,2,4,5-tetrazine (17) and the potassium and cesium salts (17a & b) (ANAT)

Compound **17a** und **17b** were synthesized according to the procedure illustrated below.

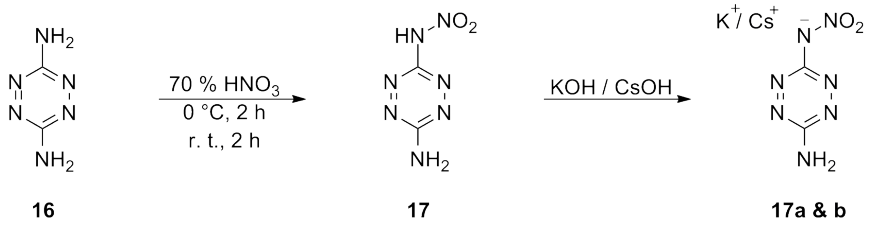

Schema 11 Synthesis of K and Cs 3-amino-6-nitramino-1,2,4,5-tetrazine (**17a** & **b**).

DAT was solved in 70% nitric acid and stirred for several hours, forming **17**. 3-Amino-6-nitramino-1,2,4,5-tetrazine was added to potassium or cesium hydroxide to form the salts **17a** and **17b** in a yield of 88% for potassium and 77% for the cesium salt. It was observed that both salts decompose after several days and therefore there were not further investigated as additives in NIR formulations.

Analytic and physical-chemical data

The purity of compound **17** was proven by NMR an IR spectroscopy. The melting point of **17** is 167°C. Because of the zwitter ionical structure the amino group is located as a broad signal at 8.67 ppm in the proton NMR. Two carbon signals in the ^{13}C spectrum are located at around 164 and 162 ppm. The nitro group of the NNO_2 group is found at -13 ppm in the ^{14}N NMR for **17a** and **b**. The symmetric and antisymmetric valence modes for the nitro and amino group are detected at around 1651 and 1634 cm^{-1} and 1400 and 1415 cm^{-1}, respectively. Elemental analysis complains with the values given in literature.[36] Sensitivity data for compound **17** and its salts are given in Table 13.

Table 12 Sensitivity data of **17**, **17a** and **17b**.

	17	**17a**	**17b**
IS / J	12	23	2
FS / N	288	252	160
ESD / J	0.6	0.5	0.3

Synthesis of 2,4,5-trinitroimidazole (21)

Referred to literature, 2,4,5-trinitroimidazole was attempted to synthesize *via* 2,4,5-triiodoimidazole.[40,41]

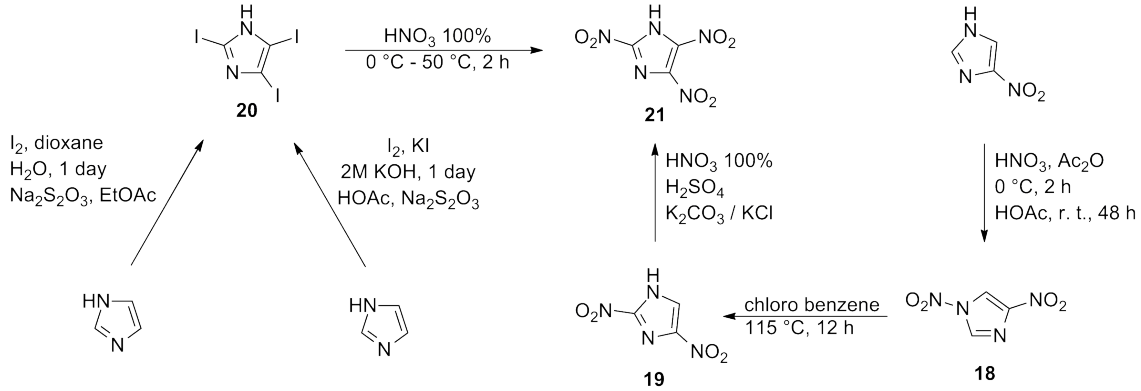

Schema 12 Synthesis of 2,4,5-trinitroimidazole (**27**).

The nitration of 4-nitroimidazole, obtaining **18**, is proceeded with the *in situ* formation of acetyl nitrate. The authors solving 4-nitroimidazole in glacial acetic acid, afterwards the mixture is treated with nitric acid and acetic anhydrate. This order is only suitable for small scales (about 1 g) and leads to yields of only 30%.[40] To obtain higher yields then described, several attempts were carried out to improve this reaction sequence. Two parameters which were modified are the order of the added compounds and the temperature. It was also found that acetic acid is not necessary for the nitration step, but the product was obtained in low yields.

The best conditions for this reaction were as follows: acetic acid and acetic anhydrate was added in a flask and stirred for 30 minutes at -5°C. Afterwards nitric acid was added and the mixture was stirred for further 2 h at this temperature. 4-Nitroimidazole was added in small portions to the cooled solution and the flask was allowed to warm to room temperature and stirred for further 48 h. The solution was poured onto ice water, whereas **18** precipitated. The yield after purification was 69%. **18** decompose at 50°C to 4-nitroimidazole and should therefore not dried in an oven.

2,4-Dinitroimidazole (**19**) was formed by isomerization of 1,4-dinitroimidazole in dry chloro benzene. Impurities of water lead to hydrolysis of **18**.

NMR spectra indicate signals for 4-nitroimidazole, as well as signals for compound **18** and **19**. The mixture could not be separated by column chromatography.

[40] H. Aissaoui, C. Boss, 5,6,7,8-Tetrahydro-Imidazo[1,5-A]Pyrazine Derivatives, WO 2008/078291 **2008**.
[41] A. R. Katritzky, D. J. Cundy, Polyiodoimidazoles and their nitration products, *Journal of Energetic Materials* **1993**, *11*, 345.

The iodation of imidazole to obtain **20** was carried out using two different syntheses strategies (Schema 12). No product was obtained synthesizing **20** without the use of potassium iodine.[40] A proper way was the use of iodine/potassium iodine. After recrystallization from ethanol **20** was obtained in low yields (13%). Therefore the precipitate of the aqueous layer was again treated with iodine, assuming the precipitate was iodine imidazole. Because of moderate yields of **20** the nitration step to synthesize **21** was not conducted and no further attempts were carried out obtaining 2,4,5-trinitroimidazole yet.

Synthesis of 4,4',5,5'-tetranitro-2,2'-bisimidazole (23)

Schema 13 describes the synthesis of 2,2'-bisimidazol (BI) (**22**) and 4,4',5,5'-tetranitro-2,2'-bisimidazole (TNBI) (**23**).

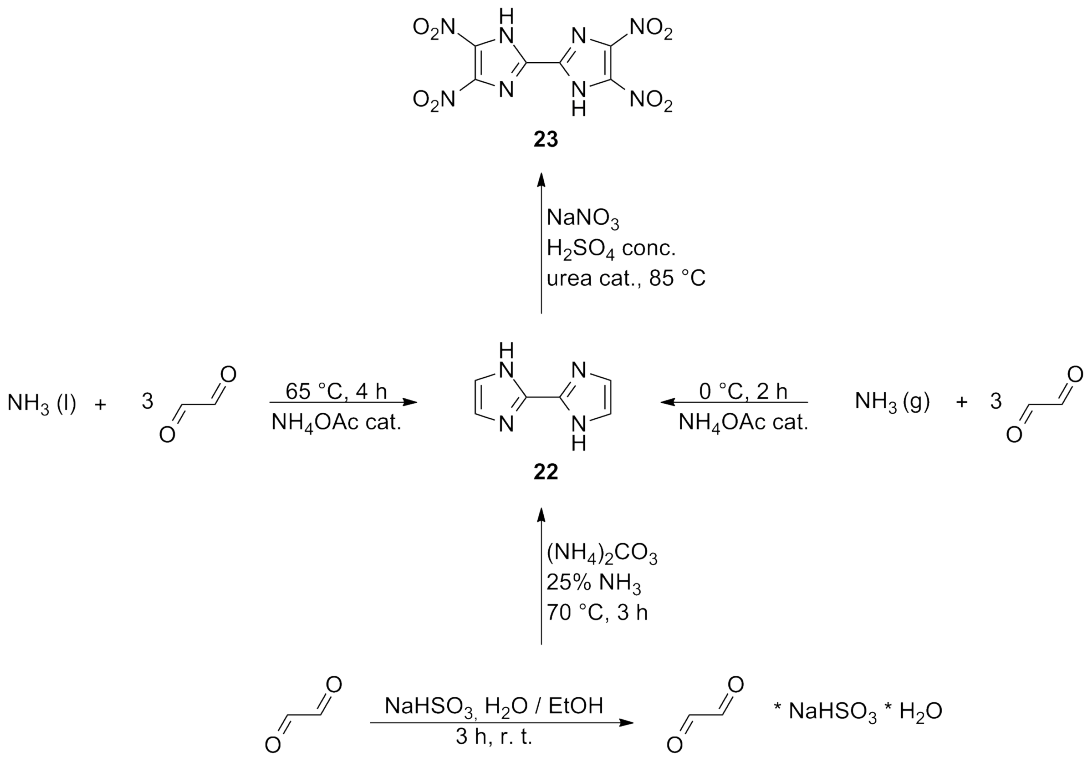

Schema 13 Synthesis of BI (**22**) und TNBI (**23**).

The first synthesis step to 4,4',5,5'-tetranitro-2,2'-bisimidazole is the formation of the precursor 2,2'-bisimidazole. Several methods are known in literature, leading to moderate results. Procedures, using 20–40% glyoxal, 25% ammonia, and a catalytically amount of

ammonium acetate or 20% glyoxal and gaseous ammonia, led to no product or in some cases with very low yields to TNBI.[42,43,44]

The best method obtaining **22** is the synthesis *via* bis-sodiumbisulfite monohydrate. The reaction in 25% ammonia and ammonium carbonate led to the pure compound.

Due to imprecise details for the nitration of **22** to **23** within literature, the best formation was found to be as follows: a mixture of sodium nitrite in sulfuric acid and a catalytically amount of urea was stirred under ice-cooling. **22** was added and the temperature was kept at 0 °C for half an hour. Then the mixture was allowed to warm to r. t., and afterwards heated to 85°C over night. After cooling to room temperature the solution was poured onto ice and **23** precipitated. The product was recrystallized from ethanol/water, obtaining good yields of 70%. Both salts were synthesized using potassium or cesium hydroxide, potassium hydroxide in ethanol or cesium carbonate (**23a**, **23b**).

Analytic and physical-chemical data

Potassium and cesium TNBI were fully characterized by multinuclear NMR (^{1}H, ^{13}C, ^{14}N), elemental analysis, different scanning calorimetry, IR, and Raman spectroscopy. Additionally sensitivity data are given in Table 13.
As excepted for complete deprotonation, no hydrogen signal is observed for compound **23a** and **b**. The ^{13}C NMR detects one signal for C4/C4´, C5/C5´, and one signal for C3/C3´. The carbon bearing the nitro group is shifted 3 ppm to lower field (144.9 ppm) compared to the quartary ring carbon at 141.0 ppm. The ring nitrogen's of the imidazole ring are not detected in the ^{14}N NMR, whereas the NO_2 nitrogen's are at -25 ppm for the potassium salt and for the cesium salt at -34 ppm.

[42] E. E. Bernarducci, K. P. Bharadwaj, Molecular structures, electronic spectra, and ESR spectra of bis(4,4',5,5'-tetramethyl-2,2'-biimidazole) copper(II) dinitrate and bis (4,4',5,5'-tetramethyl-2,2' biimidazole) zinc(II) 0.90copper(II)0.10 dinitrate, *Inorganic Chemistry* **1983**, *22*, 3911.
[43] D. T. Cromer, C. B. Storm, Structure of 4,4´,5,5´-tetranitro-2,2´-biimidazole dihydrate, *Acta Crystallographica (C)* **1990**, *46*, 1957.
[44] S. G. Cho, J. R. Cho, Synthesis and Characterization of 4,4´,5,5´-tetranitro-2,2´-bi-1*H*-imidazole (TNBI), *Propellants, Explosives, Pyrotechnics* **2005**, *30*, 445.

The typically nitro group modes in IR and RAMAN spectra are located at 1562, 1390, and 754–704 for both salts and the C-N valence modes at 940 cm^{-1}.
Both compounds are stable up to 312°C, what makes them suitable for pyrotechnic formulations. Regarding to sensitivity data it is shown that the cesium salt is much more sensitive against friction and impact compared to the potassium salt or the neutral compound.

Table 13 Sensitivity data of **23**, **23a** and **23b**.

	23 · H_2O	**23a**	**23b**
IS / J	40	40	9
FS / N	240	216	192
ESD / J	1.0	0.2	0.1

Crystal structure of cesium 3,3',5,5'- tetranitro-2,2'-bisimidazole (23b)

Compound **23b** crystallizes water free in the monoclinic space group *C*2/*m* with 2 molecules in the unit cell. The size is *a* = 10.0357(4) Å, *b* = 12.7869(4) Å, *c* = 5.4750(2) Å, *α* = 90°, *β* = 109.233(4)°, *γ* = 90°, with a volume of 663.37(4) $Å^3$. The calculated density is 2.893 g cm^{-3} at room temperature. Figure 17 highlights the molecular unit of **23b**.

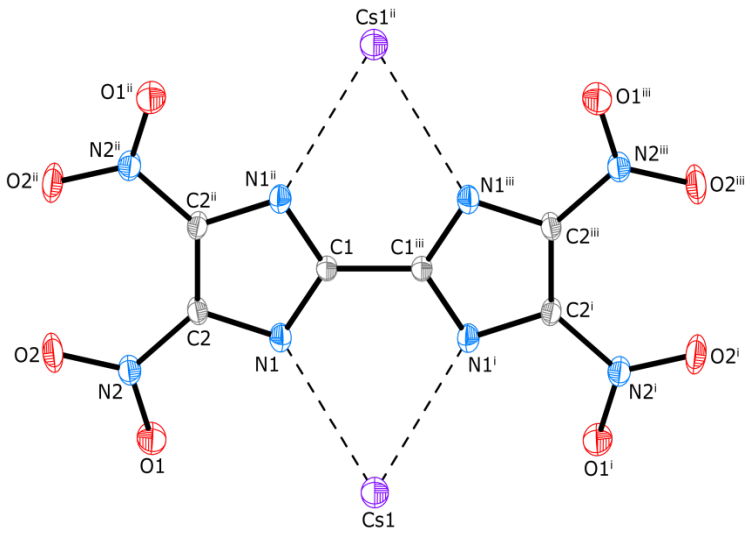

Figure 17 Molecular unit of Cs_2TNBI, symmetry codes: (i) x, -y, z; (ii) 1-x, y, 1-z; (iii) 1-x, -y, 1-z; Thermal ellipsoids in figures of crystal structures were drawn to 50% probability.

The C-N bond distances of **23b** are in the range of 1.346(3)–1.435(3) Å which is between a formal C-N single (1.47 Å) and C-N double bond (1.22 Å).[24] The bond lengths are comparable with values obtained for potassium TNBI.[45]

The torsion angles of the nitro groups to the ring layer are 174.8(2)° and -4.6(3)°, respectively. Therefore the molecule is not completely planar.

The Cs-O distances (3.2121–3.5564 Å) and Cs-N distances (3.2093–3.728 Å) in **23b** are longer than in cesium structures described in literature.[26] Bond lengths and angles for the cesium salt are given in Table 14.

Table 14 Bond lengths and bond angles within **23b**.

	Bond length [Å]		**Bond angles [°]**
O1-N2	1.236(3)	C2-N1-C1	102.70(19)
O2-N2	1.233(3)	N1-C2-C2^{ii}	109.23(13)
N1-C2	1.346(3)	N1-C2-N2	117.44(19)
N1-C1	1.351(2)	C2-C2i-N2^{ii}	133.32(12)
C2-C2^{ii}	1.406(4)	O2-N2-O1	122.3(2)
C2-N2	1.435(3)	O2-N2-C2	120.21(19)
C1-N1^{ii}	1.351(2)	O1-N2-C2	117.51(19)
C1-C1^{iii}	1.459(6)	N1-C1-N1^{ii}	116.1(3)
		N1-C1-C1^{iii}	121.93(14)

Figure 18 displays the layer structure of TNBI in b direction with cesium ions lying in the same plane between two molecules. The framework is stabilized by Cs-O contacts of 3.447 Å to NO1 and 3.556 Å to N2 between the formed layers. Compared to **23b** the crystal structure of the potassium salt consists of a layer structure with two different orientations A and B of the anions. Within one direction the anions are congruent and anions laying in A and B direction are orthogonal. It can be assumed that the difference of the impact sensitivity of both salts is due to their variant crystal structure.

[45] A. Preimesser, T. M. Klapötke, Energetic Derivatives of 4,4´5,5´-Tetranitro-2,2´-bisimidazole (TNBI), *Zeitschrift für Anorganische und Allgemeine Chemie* **2012**, *638*, 9.

The neutral compound crystallizes as a dihydrate and the bis-ammonium salt water free.[43] Because of hydrogen bonds to the distorted NO_2 oxygen's (27.56° according to the ring layer) the ammonium cation lays between two orthogonal and congruent layers similar as for potassium TNBI.

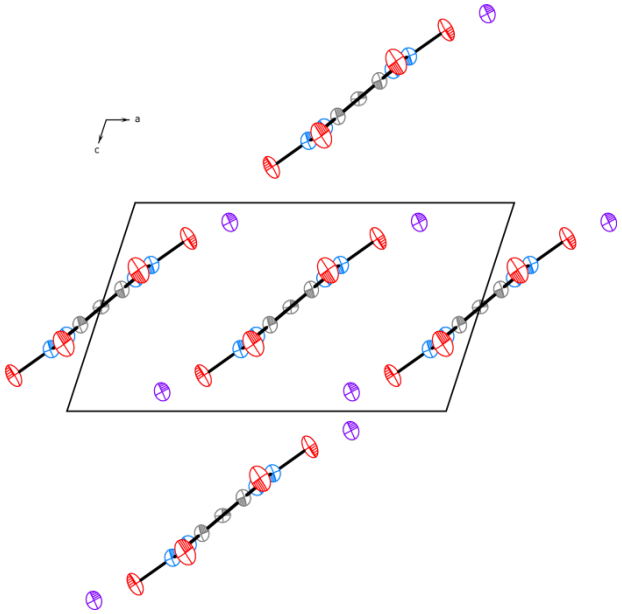

Figure 18 Layer structure of **23b**; Thermal ellipsoids in figures of crystal structures were drawn to 50% probability.

Additional compounds

Several additional compounds were synthesized within our research group and tested as possible additives and/or hexamine replacements. Their syntheses are discussed in literature[46] (**26**, **27**, **33, 34, 35**), literature[47] (**28**), literature[48] (**29**), and respectively. **30** and **31** were synthesized according to literature[49] and compounds **32**, **36**, **37** were used as received from Sigma-Aldrich (Figure 19 and 20).

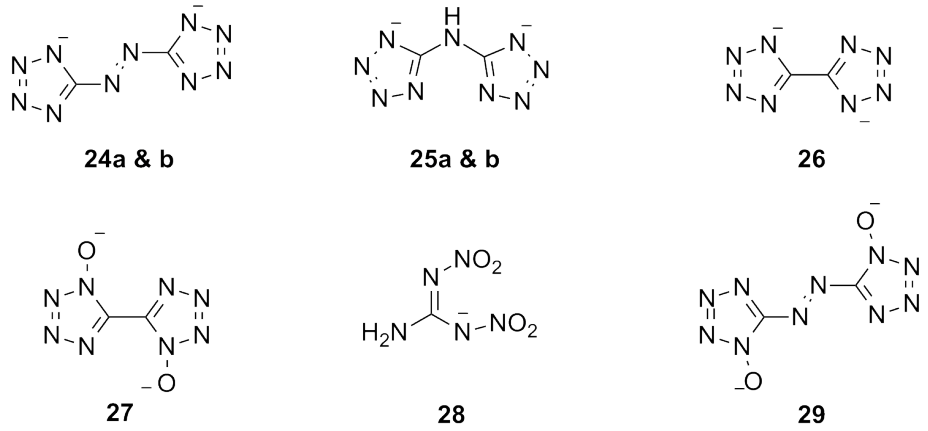

Figure 19 5,5´Azt (**24**), BTA (**25**), 5,5´-BT (**26**), 5,5´-1-BTO (**27**), DNQ (**28**), and 5,5´-AzOT (**29**).

[46] N. Fischer, PhD thesis, Ludwig-Maximilians University Munich, **2012**.
[47] A. Penger, PhD thesis, Ludwig-Maximilians University Munich, **2011**.
[48] D. Fischer, unpublished results, Ludwig-Maximilians University Munich, **2012**.
[49] a) W. E. Bachmann, *Journal of the American Chemical Society* **1994**, *71*, 1842 b) W. E. Bachmann, *Journal of the American Chemical Society* **1951**, *73*, 2769.

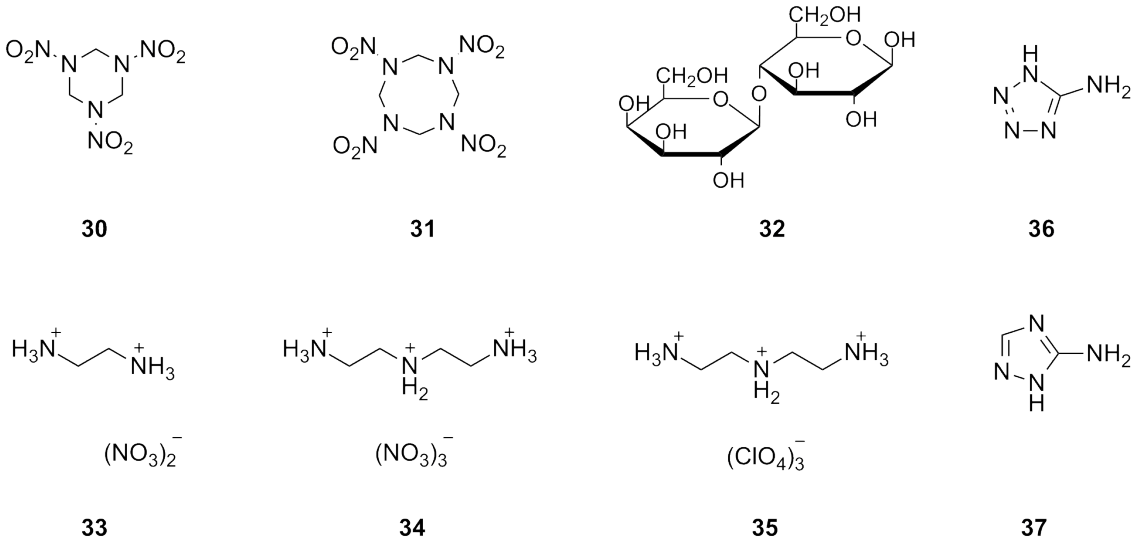

Figure 20 RDX (**30**), HMX (**31**), lactose (**32**), EDD (**33**), DETT (**34**), DETP (**35**), 5-aminotetrazole (**36**), and 3-amino-1*H*-1,2,4-triazole (**37**).

'Black Knight' Compositions – Preparation

Caution! *Although no problems occurred during the preparation and handling of pyrotechnic compositions prepared in this work, some potassium or cesium salts are sensitive to shock and/or friction and all compositions are flammable. The materials when alight yield high temperatures and can cause severe skin burns. Safety equipment such as Kevlar® gloves, leather coat, wrist protection, face shield, ear protection, grounded equipment, and shoes are mandatory.*

For the syntheses of pyrotechnic formulations several important parameters must be considered in advance by selecting fuels, oxidizers and further additives: purity of the compound, particle size, particle shape, particle surface, crystal structure, and water content. Because the pyrotechnic effect can be influenced by these properties, an absolute homogeneity of the mixture is obligatory; fuel and oxidizer must be in close contact to each other.[50]

NIR compositions were prepared as stated from the Armament Research, Development and Engineering Center (ARDEC).

Epon 828, Epicure 3140 (binder system) and silicon MIL-S-250 (grade 2, class C) were obtained from ARDEC. The epoxy system was used as 70 % Epon and 30 % Epicure with a total amount of 4 %. Hexamine, potassium nitrate p. a., cesium nitrate p. a. and rubidium nitrate p. a. were received from Sigma-Aldrich, pulverized separately in a ball mill from HARBOR FREIGHT TOOLS for several hours, sieved and dried at 60 °C for at least 12 h before use. *Black Knight* compositions were prepared as 50 g (5 x 10 g) batches according to their respective weight percentages in the formulations (Table 16-19). 10 g of the composition was pressed with 2–3 t in a 54PM250 hydraulic press and corresponding 20 mm die set from MAASSEN GmbH. The average weight of five 10 g pellets and their average densities are stated in chapter 6, Table 22 and 23.

Notations for reference and new *BK* formulations listed in Table 16-19 refer to the contained oxidizer(s), high nitrogen compounds (HNC) or hexamine (H) replacements, respectively.

Reference 1 contained potassium nitrate, reference 2 cesium nitrate and reference 3 rubidium nitrate as oxidizer. Reference 4 contained cesium and potassium nitrate and reference 5 cesium and rubidium nitrate. The acronym _r, _m, and _f stand for the different mixing grade of the ingredients and means rough, medium, and fine. The rough composition was mixed for 5 min, the medium composition 10 min, and the fine for at least 20 min in a

[50] B. Berger, Parameters Influencing the Pyrotechnic Reaction, *Propellants, Explosives, Pyrotechnics* **2005**, *30*, 27.

mortar. In addition oxidizer(s) and hexamine were pulverized in advance in a ball mill (Figure 21). BK_L contained lactose (L) instead of hexamine, BK_LH lactose and hexamine, BK_5AT contained 5-aminotetrazole and BK_ATR 3-amino-1,2,4-triazole, BK_EDD ethylendiamine dinitrate, BK_DETT diethylentriamine trinitrate, and BK_DETP diethylentriamine triperchlorate instead of hexamine. BTA compositions contained the corresponding potassium and/or cesium salt of 5,5´-bis(1*H*-tetrazolyl)amine, NTO compositions the salts of 3-nitro-1,2,4-triazole-5-one, DNT compositions the salts of 3,5-dinitro-1,2,4-triazole, BK_BOX K and Cs 3,3'-bis(1,2,4-oxadiazol)-5-one, TNBI compositions the salts of 4,4´,5,5´-tetranitro-2,2´- bisimidazole, BK_BT K and Cs 5,5´-bistetrazolate, BK_BTO K and Cs 5,5´-bis(tetrazol-1-oxide), BK_BMTT K and Cs bis(1-methyl-tetrazole-5-yl)-triazene, BK_3NT potassium 3-nitro-1,2,4-triazolate, BK_DNQ both salts of *N*,*N*´-dinitroguanidine, BK_BNGT salts of 3,6-bis-nitroguanidyl-1,2,4,5-tetrazine, and BK_CsAzOT the cesium salt of 5,5´-azo-bis-(1-oxido)-tetrazolate.

Although the secondary explosives RDX and HMX are environmental harmful both were synthesized from hexamine therefore tests were performed using both to compare their radiometric results with the reference compositions.

Black Knight compositions were prepared using the following procedure:

1. Weight amount of epoxy resin (Epon 828) into a plastic cup
2. Weight amount of Epicure into the same plastic cup
3. Mix for 1 minute with a plastic / wood spatula
4. Add fuel (Si) to the binder system
5. Mix for 1 minute
6. Add hexamine and HNC to the binder system
7. Mix for 5 minutes
8. Mix oxidizer(s) in a mortar for 5 minutes (in advance)
9. Add oxidizer(s) to the fuel/binder system and mix everything in a mortar for at least 10 – 20 minutes. Notice: The curing time for the epoxy binder starts from mixing the oxidizer with the fuel/binder system
10. If a homogenous mixture is obtained spread mix out onto metal trays
11. Allow mixture to cure for 3–4 h
12. Press 5 x 10 g pellets (2 t)
13. Place flares into the oven (60 °C) to cure for two days
14. Remove flares from the oven and after cooling to r. t. place them into desiccators with drying agent
15. For NIR measurements light pellets with a sparkler
16. Alternative: use a cover or a primer charge and light pellet with a sparkler (Table 15)

Figure 21 Pressed (2 t) NIR pellets with different mixing grain size (_f, _m, _r) and ball mill.

Table 15 Primer Charge for a 20 g batch; Total: 106% (Nitrocellulose in addition to other ingredients).

	w%	**Amount (g)**
Potassium nitrate	35	6.92
Silicon	26	5.14
Iron Oxide, black	22	4.35
Aluminum, powder	13	2.57
Charcoal	4	0.79
Nitrocellulose	6	0.24
Acetone	94	3.72

Mix dry and sieved potassium nitrate (12 h, 60°C) and silicon (8 h, 60°C) into a plastic cup. Weight out the ingredients listed above. Blend Al, Si, Fe_2O_3, C, and potassium nitrate together. Mix nitrocellulose and acetone (Binder). Mix ingredients with binder solution to form homogenous slurry. Due to evaporation of the solvent the amount of acetone is not considered.

Black powder (BP) cover for NIR-flares

2.52 g potassium nitrate, 0.48 g carbon, 0.32 sulfur, and 0.07 g dextrin were mixed with a plastic spatula. The first layer contained 85 % of BP and 15 % (0.5 g) Al powder. The flares were less moisturized with water from an aerosol can and then pored over the BP-Al mixture. After 20 min a second layer of BP without Al was applied using a small sieve (Figure 22).

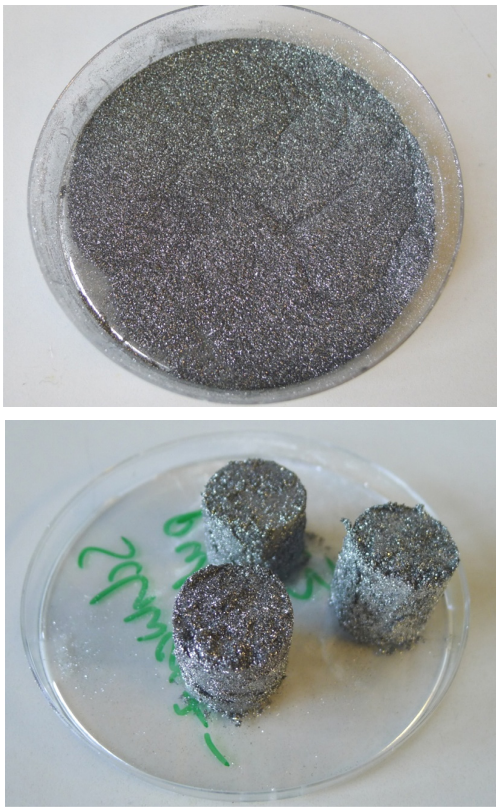

Figure 22 NIR pellets with BP/Al-coating.

Table 16 Weight percentages of *BK* formulations.

Formulation	Si	DETT	EDD	DETP	L	5AT	ATR	H	Epon	Epicure	KNO_3	$CsNO_3$	$RbNO_3$
reference1_r	10							16	2.8	1.2	70		
reference1_m	10							16	2.8	1.2	70		
reference1_f	10							16	2.8	1.2	70		
reference2	10							16	2.8	1.2		70	
reference3	10							16	2.8	1.2			70
reference4	10							16	2.8	1.2	30	40	
reference5	10							16	2.8	1.2		40	30
BK_L	10				16				2.8	1.2	70		
BK_5AT	10					16			2.8	1.2	70		
BK_ATR	10						16		2.8	1.2	70		
BK_LH1	10				8			8	2.8	1.2	70		
BK_DETT	10	8						8	2.8	1.2	70		
BK_DETT1	10	16							2.8	1.2	70		
BK_EDD	10		8					8	2.8	1.2	70		
BK_DETP	10			8				8	2.8	1.2	70		

Table 17 Weight percentages of *BK* formulations (continued).

Formulation	HNC_K	HNC_Cs	Si	L	H	Epon	Epicure	KNO_3	$CsNO_3$	$RbNO_3$
BK_BTA1	10		10		16	2.8	1.2	60		
BK_BTA2	8		10		8	2.8	1.2	70		
BK_BTA3	10		10	8	8	2.8	1.2	60		
BK_BTA4	5	5	10	8	8	2.8	1.2	60		
BK_BTA5	5	5	10		16	2.8	1.2		35	25
BK_BTA6	5	5	10	8	8	2.8	1.2		35	25
BK_BTA7		10	10		16	2.8	1.2	20	40	
BK_NTO1	10		10	8	8	2.8	1.2	20	40	
BK_NTO2	5	5	10	8	8	2.8	1.2	20	40	
BK_NTO3	5		10		16	2.8	1.2	65		
BK_NTO4		10	10		16	2.8	1.2	60		
BK_NTO5	3		10		16	2.8	1.2	30	37	
BK_NTO6		15	10		16	2.8	1.2	25	30	
BK_NTO7	10		10		16	2.8	1.2	60		

Table 18 Weight percentages of *BK* formulations (continued).

Formulation	HNC_K	HNC_Cs	Si	L	H	Epon	Epicure	KNO_3	$CsNO_3$	$RbNO_3$
BK_TNBI1	10		10		16	2.8	1.2	60		
BK_TNBI2		10	10		16	2.8	1.2	60		
BK_TNBI3	5	5	10	8	8	2.8	1.2	25	35	
BK_TNBI4		5	10		16	2.8	1.2		40	25
BK_TNBI5	3		10	8	8	2.8	1.2	67		
BK_TNBI6		3	10	8	8	2.8	1.2	30	37	
BK_DNT1	2		10	6	8	2.8	1.2	70		
BK_DNT2	2	2	10		12	2.8	1.2	30	40	
BK_DNT3		5	10	5	6	2.8	1.2	70		
BK_BOX1	8		10		8	2.8	1.2	30	40	
BK_BOX2		8	10	8		2.8	1.2	30	40	
BK_BOX3	4	4	10		8	2.8	1.2	70		

Table 19 Weight percentages of *BK* formulations (continued).

Formulation	HNC_K	HNC_Cs	Si	RDX	HMX	L	H	Epon	Epicure	KNO_3	$CsNO_3$
BK_BT1		10	10				6	2.8	1.2	70	
BK_BT2	3		10			7	6	2.8	1.2	30	40
BK_BTO1	5		10				11	2.8	1.2	70	
BK_BTO2		1	10				15	2.8	1.2	30	40
BK_RDX			10	16				2.8	1.2	70	
BK_RDX1			10	8			8	2.8	1.2	70	
BK_HMX			10		3.5		12.5	2.8	1.2	70	
BK_BMTT1	2.5		10				13.5	2.8	1.2	70	
BK_BMTT2		1.5	10				14.5	2.8	1.2	70	
BK_3NT	5		10				11	2.8	1.2	70	
BK_DNQ	1.4	2.6	10				12	2.8	1.2	70	
BK_BNGT	2.6	1.4	10				12	2.8	1.2	70	
BK_CsAzOT		2.5	10				13.5	2.8	1.2	30	40

Sensitivity data

Pyrotechnic formulations are thermodynamically metastable and therefore they can decompose unexpected.[51] An important aspect which is linked with the safety of fireworks is the sensitivity data of the formulation. Because pyrotechnics are manufactured in large quantities it is important to know their properties against impact, friction and electric discharge. The sensitivities of all new formulations were determined by BAM (Bundesanstalt für Materialforschung- und prüfung) methods[52,53] and are presented in Table 20 and 21. To investigate their thermal behavior DSC measurements were performed.

BAM sensitivity

Exclusively all *Black Knight* formulations are insensitive against friction and electric discharge (350 N, 1.5 J). Only several compositions are less sensitive (35–25 J) e. g. reference 1, 4, 5, ATR, LH, NTO2, NTO5, HMX, DETP or sensitive (25–7 J) against impact e. g. BK_L, 5AT, BTA2, BT1, BT2, RDX, RDX1, and CsATzO. Usually compounds blended with a binder show less sensitivity compared to the pure compound. For compositions with RDX and CsAzOT this property could not be confirmed. Both mixtures show the same impact sensitivity then the real substance (RDX: 7 J, CsAzOT: 20 J). Because of the very hygroscopic behavior of formulations containing DETT and EDD their sensitivity data were not determined (Table 20 and 21). Concerning the safety it is important to mention that all formulations are highly flammable and can cause severe skin burns.

[51] G. Steinhauser, T. M. Klapötke, 'Green' Pyrotechnics: A Chemists' Challenge, *Angewande Chemie Int. Ed.* **2008**, *47*, 3330–3347.

[52] a) NATO standardization agreement (STANAG) on explosives, *impact sensitivity tests*, no. 4489, Ed. 1, Sept. 17, **1999**. b) WIWEB-Standardarbeitsanweisung 4-5.1.02, Ermittlung der Explosionsgefährlichkeit, hier der Schlagempfindlichkeit mit dem Fallhammer, Nov. 8, **2002**. c) http://www.bam.de d) http://www.reichel-partner.de e) NATO standardization agreement (STANAG) on explosive, *friction sensitivity tests*, no. 4487, Ed. 1, Aug. 22, **2002**. f) WIWEB-Standardarbeitsanweisung 4-5.1.03, Ermittlung der Explosionsgefährlichkeit oder der Reibeempfindlichkeit mit dem Reibeapparat, Nov. 8, **2002**. g) WIWEB-Standardarbeitsanweisung 4-5.1.03, Ermittlung der Explosionsgefährlichkeit oder der Reibeempfindlichkeit mit dem Reibeapparat, Nov. 8, **2002**. h) Impact: Insensitive > 40 J, less sensitive ≥ 35 J, sensitive ≥ 4, very sensitive ≤ 3 J; friction: Insensitive > 360 N, less sensitive = 360 N, sensitive < 360 N a. > 80 N, very sensitive ≤ 80 N, extreme sensitive ≤ 10 N; According to the UN Recommendations on the Transport of Dangerous Goods.

[53] a) http://www.ozm.cz/testing-instruments/small-scale-electrostatic-discharge-tester.html; b) S. Zeman, V. Pelikan, J. Majzlik, *Central European Journal of Energetic Materials* **2006**, *3*, 45; c) D. Skinner, D. Olson, A. Block-Bolten, *Propellants, Pyrotechnics, Explosives* **1997**, *23*, 34.

Differential Scanning Calorimetry (DSC) measurements

To investigate the thermal behavior DSC measurements were carried out. Mostly the same endothermic signals beginning at 128°C and ending close to 393°C were observed (Table 20 and 21). In addition to melting points or phase transitions, exothermic signals for several formulations were observed between 160 and 390°C. Melting points obtained at 310 and 330°C correlates with the melting point of rubidium (lit.[24] 310°C) and potassium nitrate (lit.[24] 334°C). The signal achieved between 128–131°C conforms to the crystal state change of potassium nitrate (lit.[24] 129°C). Because DSC measurements were carried out until 400°C, the melting point of cesium nitrate with 410°C and exothermic redox reactions of the combustion process of the formulation were not detected. Hence, other characteristics like the influence of the amount of oxidizer were not investigated but were of particular interest. Further measurements above 500°C should be performed. Experiments described in literature demonstrate that the amount of oxidizer influences the decomposition temperature. Reducing the amount of oxidizer within a formulation containing boron as fuel and potassium nitrate as oxidizer, a decrease of the decomposition temperature from 570°C (20:80) to 510°C (30:70) was observed.[50]

Formulation DETT, DETT1 and EDD were not characterized because of their strong hygroscopic behavior and/or incompatibility with hexamine. All 15 pellets show strong hexamine exhalations and dampish surfaces which were also difficult to light by a sparkler for NIR emission experiments. Because of the poor burning characteristics and moreover because of their intolerance with other ingredients DETT, DETP and EDD are unfortunately not suitable as hexamine replacements, although they are cheap and easy to synthesize.

Table 20 Sensitivity data of Black Knight formulations.

Formulation	FS [N]	IS [J]	ESD [J]	DSC [°C]
Reference1	360	35	1.5	128, 265, 330
Reference2	360	40	1.5	152, 237
Reference3	360	40	1.5	164, 205, 282, 310
Reference4	360	35	1.5	128, 152, 224, 350.2
Reference5	360	25	1.5	152
BK_L	360	15	1.5	128, 329
BK_5AT	360	10	1.5	128, 175, 330.7
BK_ATR	360	30	1.5	128, 326, 393
BK_LH	360	35	1.5	n.d.
BK_BTA1	360	40	1.5	128
BK_BTA2	360	15	1.5	128, 290, 319, 340.2
BK_BTA3	360	40	1.5	131
BK_BTA4	360	40	1.5	128, 331.4
BK_BTA5	360	40	1.5	128, 320.4, 383.9
BK_BTA6	360	40	1.5	363.3
BK_BTA7	360	40	1.5	n.d.
BK_NTO1	360	40	1.5	120
BK_NTO2	360	35	1.5	129, 152, 370.9
BK_NTO3	360	40	1.5	130, 229, 328
BK_NTO4	360	40	1.5	130, 210.9, 389.4
BK_NTO5	360	35	1.5	130, 155
BK_NTO6	360	40	1.5	130, 152, 210.5, 381.4
BK_NTO7	360	40	1.5	129
BK_3NT	360	40	1.5	n.d.
BK_CsAzOT	360	20	1.5	129, 152, 225
BK_BNGT	360	40	1.5	130
BK_DNQ	360	40	1.5	128

n.d. = not determined

Table 21 Sensitivity data of Black Knight formulations (continued).

Formulation	FS [N]	IS [J]	ESD [J]	DSC [°C]
BK_TNBI1	360	40	1.5	n.d.
BK_TNBI2	360	40	1.5	129, 329.1
BK_TNBI3	360	40	1.5	130, 152
BK_TNBI4	360	40	1.5	129
BK_TNBI5	360	40	1.5	n.d.
BK_TNBI6	360	40	1.5	n.d.
BK_DETT	n.d.	n.d.	1.5	132, 199, 331.3, 383
BK_DETT1	n.d.	n.d.	1.5	128, 330, 365.5
BK_EDD	n.d.	n.d.	1.5	131, 331, 353.2
BK_DETP	360	35	1.5	128, 322
BK_KBMTT	360	40	1.5	129, 315.4
BK_CsBMTT	360	40	1.5	129, 329
BK_BTO1	360	40	1.5	n.d.
BK_BTO2	360	40	1.5	n.d.
BK_BT1	360	20	1.5	128
BK_BT2	360	20	1.5	129, 152
BK_RDX	360	7	1.5	129, 180.2, 329
BK_RDX1	360	7	1.5	129, 159.8, 330
BK_HMX	360	35	1.5	129, 331
BK_BOX1	360	40	1.5	129, 152, 223
BK_BOX2	360	40	1.5	130, 151
BK_BOX3	360	40	1.5	129
BK_DNT1	360	40	1.5	129, 330
BK_DNT2	360	40	1.5	129, 152
BK_DNT3	360	40	1.5	129, 330

n.d. = not determined

Combustion Data

Pyrotechnic reactions are primarily solid-solid, solid-liquid, or solid-gaseous state redox reactions. The basic pyrotechnic reaction can be displayed as:

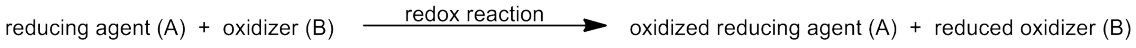

Schema 14 Basic pyrotechnic reaction; (A) e. g. elemental metal powders (Mg, Al, Magnalium, B, Si, Hf, Zr, Ti), (B) e. g. alkaline earth chromates, (per)chlorates, nitrates.[5,50]

The understanding of this redox system can be very difficult. Depending on the fuel (or other ingredients') pyrotechnic reactions take place at high temperatures (1500–4000°C) and the chemistry behind is not comparable with normal inorganic redox reactions in solution and at room temperature.

Multiple important parameters influence the reaction and make the development of new formulations to an unexhausted task and needs further a lot of experience. Normally, only one parameter should be varied while the others a held constant. Variations by preparing new formulations are possible by changing the reducing agent, the oxidizer (oxygen balance), the additives (binders, burn rate modifiers), the particle size of the single compounds and of the formulation etc. Modifications of only one of the above mentioned parameters can influence the pyrotechnic effect dramatically. Therefore: before changing the composition several important parameters have to be brought up in the work and understanding of pyrotechnics and must be considered in advance:[50,54]

- Reaction rate [m s^{-1}] (experimental)
- Heat of reaction [J g^{-1}] (calculated)
- Reaction temperature [°C] (calculated or experimental)
- Thermal behavior (DSC, TGA)
- Ignition temperature [°C] (DSC)
- Evolved gas (calculated or DSC/MS)
- Reaction products (calculated or DSC/MS/XRD)
- Emitted light (experimental)

[54] J. A. Conkling, Chemistry of Pyrotechnics – Basic Principles and Theory, Marcel Dekker Inc. USA, **1985**.

Suitable theoretical models for calculating the above mentioned parameters exists e. g. ICT code[55], NASA code[56], EKVI code[57] but they did not consider factors like the particle size, impurities or oxidation layers on the surface of the fuel.[50] Obviously, the investigation of all listed parameters is time consuming and needs large amounts of explosive material. Due to the large amount of material which would be necessary, a comprehensive evaluation of several terms like the oxygen balance or burn time was not performed yet. Only tendencies are mentioned.

As noted before, pyrotechnic formulations can be altered by numerous parameters. This thesis is based on the addition of new materials, especially potassium and/or cesium salts of a high nitrogen containing compounds. As a consequence, the amount of remaining ingredients is changed. This raises the question of whether the amount of oxidizer or the amount of fuel (Si or hexamine) should be adjusted. Because the oxygen balance of all synthesized compounds is negative they are also referred as fuels. First test were performed with a reduced amount of oxidizer followed by experiments with a reduced amount of hexamine and a combination of hexamine and lactose (Table 16–19).

From the experimental combustion experiments (chapter 7) it was noticed that, compared to the reference formulation, a couple of new compositions show different burning behavior. Some of them were impossible to light (DETT, 5,5´-azotetrazolate) others combust with very small flames and NIR emission (RDX, DETP, 5-aminotetrazole). To understand these natures' thermodynamic performance calculations using the ICT code[56] were executed for new formulations and the results compared with the data obtained for reference 1 and 4 (summarized in Table 22 and 23). The main intention of these calculations was to find any correlation between the theoretical combustion data, mainly the oxygen balance of the flare and experimental burning times and burning behaviors (flame size).

The investigated characteristic variables received from the ICT code are the previously mentioned oxygen balance (OB) Ω, the linked equivalence ratio (ER) and the fuel to oxidizer ratio (O/F). Absence data within Table 22 and 23 are due to missing crystal structures and hence missing densities and heat of formations of the high nitrogen compound. Consequently no calculations were conducted for 3NT, BNGT, DNQ, EDD, BTO1, both BMTT and BT formulations, BOX2, 3 and DNT1 and 2.

[55] S. Gordon, B. McBride, NASA CEA code, USA, **1994**.
[56] F. Volk, H. Bathelt, ICT Thermochemical Code, Fraunhofer ICT, Pfinztal, **2005**.
[57] B. Noläng, Ekvi System 3.2, BeN Systems, Balinge, Sweden, **2004**.

Oxygen balance Ω, Equivalence ratio and Oxidizer to Fuel ratio

The oxygen balance Ω (OB) is defined as the weight percent of oxygen which is necessary for complete combustion (Ω = negative) with respect to CO_2 or is still available after complete combustion (Ω = positive). Similar as for secondary explosives the oxygen balance of pyrotechnic formulations can be calculated with:

$$OB(\Omega) = 100\frac{n_{Ox}M_{Ox}u}{n_{Red}M_{Red} + n_{Ox}M_{Ox}}$$

with M_{ox} = molecular weight of oxygen, M_{red} = molecular weight of reducing agent, u = number of oxygen atoms within the oxidizer, n = number of moles.[50]

The oxygen balance influences several parameter e. g. the reaction rate and also the heat of reaction. An example for the redox system titanium/potassium perchlorate indicate that a OB of zero shows the highest heat of reactions [J g^{-1}] but not the highest reaction rate [m s^{-1}].[50] This phenomenon can be explained because pyrotechnics undergo mainly solid-solid redox reaction. Further influences of the OB are described for MTV flares. The color ratio of the mixture increases with increasing oxygen balance of the fuel but decreases also the spectral efficiency.[20] However, most pyrotechnic formulations have negative oxygen balances because there are overbalanced by fuel. A large amount of energy comes from oxidation of the fuel by air (see chapter 9).

Calculated OBs of NIR pyrotechnics are in the range of -26 to -39% for references and between +3 and -42 for new formulations (Table 22 and 23). The OBs for pure synthesized potassium and cesium compounds as well as for nitrate and perchlorate salts, RDX or HMX are listed separately within Table 22 and 23

The equivalence ratio is correlated to the oxygen balance Ω and correspond to Ω = 0 (stoichiometric) for ER = 1, to an oxygen deficit (Ω = negative) for ER < 1 and conform to an oxygen excess (Ω = positive) with ER > 1. Only BK_RDX and DETT have values larger than 1 and therefore positive oxygen balances.[56]

Another term which is obtained from calculations is the oxidizer to fuel ratio (O/F) and is self-explanatory. Formulations with an O/F value of 1 consist of 50% oxidizer and 50% fuel. Compositions listed in Table 22 and 23 having a lower O/F value than 2.33 (refers to 70/30) are reduced in the amount of oxidizer. Due to the fact that several mixtures burn very fast and others in turn burn very long or distinguish tremendous in the size of the flame, a closer inspection of these three values was of particular interest.

Burn time

The classical *Black Knight* formulations consist of 70% oxidizer (potassium or potassium/cesium nitrate), 10% fuel (silicon), 16% hexamine, and 4% binder.

Formulations with oxygen balances about -40% (ref. 2, 5, BTA4, NTO6, TNBI4) showing similar burn times of 14 – 18 s and flares with OBs between 3.44 to -11% (RDX, 5AT, ATR) have long burn times from 30 to larger than 35 s. The estimation that formulations with more positive Ω values then -30% burn faster than these with values below -30% could not be confirmed for the tested formulations. These results could be influenced by the non-homogeneity or particle size of the composition.

Replacing the total amount of 16% hexamine by 5-aminotetrazole, aminotriazole, DETT, DETP, EDD, RDX, and HMX results in long burning times (above 35 s) but also in very low flame surfaces and poor emission values (chapter 7). Moreover flares containing 5AT and ATR produce small sparks during combustion which is an unrequested property (Figure 23).

Substituting hexamine by the same amount of lactose the burn time decreases dramatically from 25 s to 11 s. This can be explained, because lactose acts as readily combustible material in pyrotechnics. Moderate values of 18 s for a 10 g charge were obtained by a ratio of 8% hexamine and 8% lactose. To avoid too fast burning the maximum amount of lactose was therefore 8%.

Flares substituted by 16% DETT were not possible to light. Another compound which was added in ratios of 6, 10.5 and 15 weight% and pressed as 15 g pellets was potassium and cesium 5,5´azotetrazolate (**24a**, **b**). Both compositions were not listed in Table 16, 20 and 22 because they were impossible to light by a sparkler and even not by a pole burner. Only a crackling noise was observed by treating the pellet directly with the hot flame of the burner. Pure salts of azotetrazolate detonate in the bunsen burner. In combination with the binder a complete detonation was suppressed, leading only in a sizzle and chunking of small pieces of the flare. A reason why both flares do not burn might be the formation of large amounts of nitrogen which extinguish the flame.

From radiometric results it was observed that an ER of 2.33 results in sufficient burn times and NIR output, except BTA1 with an ER of 1.5. Therefore further experiments should be carried out with a fix O/F ratio of 70/30.

Figure 23 Formation of sparks during combustion of BK_5AT (left) and BK_ATR (right).

Table 22 Combustion data of Black Knight formulations.

Formulation	Mass [g]	Density [g cm^{-3}]	Burn time [s]	ER[1]	O/F[2]	Ω (flare)	Ω (CO_2) (HNC)
Reference1	9.8	1.57	25	0.52	2.33	-25.97	39.56
Reference2	9.6	2.22	15	0.27	2.33	-39.30	20.52
Reference3	9.1	2.00	18	0.35	2.33	-34.68	27.12
Reference4	9.6	1.85	19	0.37	2.33	-33.59	
Reference5	9.5	2.10	14	0.30	2.33	-37.32	
BK_L	10.0	1.63	11	0.71	2.33	-11.05	
BK_5AT	9.6	1.66	36	0.88	2.33	-3.63	-65.83
BK_ATR	9.5	1.61	30	0.71	2.33	-11.37	-105.93
BK_LH	9.8	1.63	18	0.60	2.33	-18.51	
BK_BTA1	9.9	1.56	21	0.42	1.50	-33.48	-55.04(K)
BK_BTA2	10.0	1.64	22	0.69	2.33	-12.38	
BK_BTA3	9.6	1.54	21	0.48	1.50	-26.02	-25.90(Cs)
BK_BTA4	9.7	1.63	16	0.49	1.50	-25.04	
BK_BTA5	9.6	2.11	15	0.25	1.50	-42.28	
BK_BTA6	9.7	2.12	16	0.29	1.50	-34.82	
BK_BTA7	9.9	2.10	18	0.29	1.50	-39.56	
BK_NTO1	9.6	1.88	22	0.34	1.50	-31.80	-33.30(K)
BK_NTO2	9.7	1.94	15	0.34	1.50	-31.51	-21.34(Cs)
BK_NTO3	9.8	1.61	33	0.47	1.86	-28.81	
BK_NTO4	9.7	1.64	26	0.43	1.50	-31.07	
BK_NTO5	9.8	1.91	23	0.36	2.03	-34.72	
BK_NTO6	9.8	1.90	18	0.29	1.22	-39.33	
BK_NTO7	9.8	1.53	18	0.43	1.50	-31.64	
BK_3NT	9.9	1.57	28	-	-	-	-47.32(K)
BK_CsAzOT	9.9	2.07	23	0.41	2.33	-28.71	-20.78
BK_BNGT	9.9	1.56	35	-	-	-	-44.16/-29.09[3]
BK_DNQ	9.8	1.57	33	-	-	-	-8.55/-5.69[3]

[1] ER = equivalence ratio = 1 (Ω = 0), <1 (Ω = negative), >1 (Ω = positive), calculated with ICT-code[56]
[2] O/F = oxidizer to fuel ratio; Ω = oxygen balance ; HNC = high nitrogen compound;
Mass, density and burn time values are mean values (5 pellets); [3]potassium/cesium

Table 23 Combustion data of Black Knight formulations (continued).

Formulation	Mass [g]	Density [g cm^{-3}]	Burn time [s]	ER[1]	O/F[2]	Ω (flare)	Ω (HNC)
BK_TNBI1	9.7	1.60	19	0.43	1.50	-31.98	-32.79(K)
BK_TNBI2	9.9	1.74	22	0.43	1.50	-31.31	-22.15(Cs)
BK_TNBI3	9.7	2.01	14	0.34	1.50	-30.85	
BK_TNBI4	9.9	2.00	17	0.28	1.86	-39.37	
BK_TNBI5	10.0	1.63	15	0.57	2.03	-20.31	
BK_TNBI6	9.9	2.10	14	0.42	2.03	-27.16	
BK_DETT	9.9	1.79	-	1.03	2.33	0.77	-38.33
BK_DETT1	9.9	1.69	>35	0.69	2.33	-12.60	
BK_EDD	10.0	1.71	>35	-	-	-	-25.79
BK_DETP	9.8	1.61	>35	0.73	2.33	-10.33	-9.89
BK_KBMTT	9.8	1.56	28	-	-	-	-83.81
BK_CsBMTT	9.8	1.57	34	-	-	-	-50.64
BK_BTO1	9.9	1.68	>35	-	-	-	-38.98(K)
BK_BTO2	9.8	1.70	>35	0.39	2.33	-31.64	-22.13(Cs)
BK_BT1	9.9	1.73	25	-	-	-	-31.25(K)
BK_BT2	9.8	1.97	11	-	-	-	-31.85(Cs)
BK_RDX	9.8	1.69	>35	1.14	2.33	3.44	-21.61
BK_RDX1	9.9	1.64	30	0.71	2.33	-11.26	
BK_HMX	9.8	1.63	>35	0.59	2.33	-19.54	-21.61
BK_BOX1	9.8	1.97	11	0.52	2.33	-18.63	-51.98(K)
BK_BOX2	9.9	2.11	10	-	-	-	-29.75(Cs)
BK_BOX3	9.9	1.71	28	-	-	-	
BK_DNT1	9.9	1.61	17	-	-	-	-16.23(K)
BK_DNT2	9.9	1.98	17	-	-	-	-10.99(Cs)
BK_DNT3	9.9	1.66	17	0.71	2.33	-11.16	

[1] ER = equivalence ratio = 1 (Ω = 0), <1 (Ω = negative), >1 (Ω = positive), calculated with ICT-code[56]
[2] O/F = oxidizer to fuel ratio; Ω = oxygen balance; HNC = high nitrogen compound
Mass, density and burn time values are mean values (5 pellets)

Calculated reaction products[56]

Pyrotechnic compositions form solid, liquid and of course gaseous reaction products. The formed products are normally not the same as would be expected for a reaction at standard conditions. It was observed that compositions with long combustion times and small flames produce less or different residues (visual) compared to standards or formulations with good burning behavior (Figure 24). For that reason additional calculations for selected compositions were carried out for possible reaction products at explosion temperature. The reaction temperature is influenced by the chosen oxidizer and reducing agent and can vary between 1000 and 4000°C.

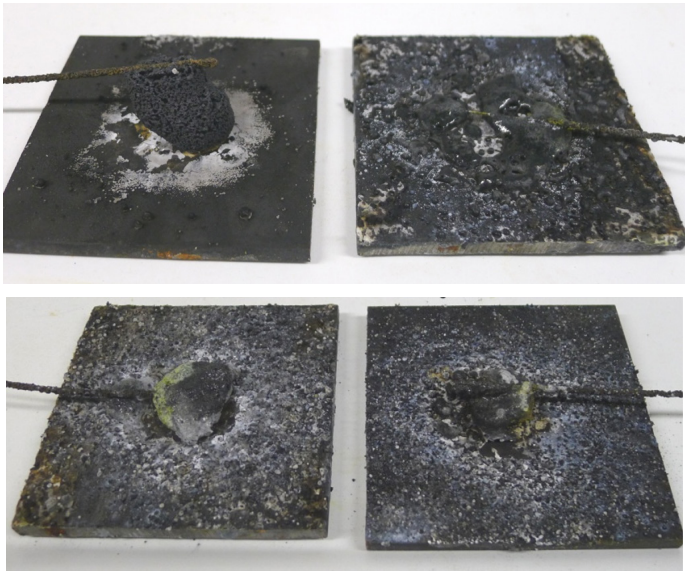

Figure 24 Residues of reference 4 (top left), BK_L (top right), BK_5AT (bottom left), and BK_ATR (bottom right).

Because all formulations containing similar and/or the same oxidizer and fuel the calculated temperatures vary only between 2100–2860 K. From literature known T-Jump/FTIR spectroscopy[58] and GC/MS experiments[59] with compounds having a similar chemical structure than the tested ones (tetrazine, azotetrazolate) the formation of e. g. HCN, NH_3, H_2O, carbon (di)oxide and of course N_2 is confirmed. Considering that, gaseous products with mole numbers smaller then 10^{-6} (at 2000 K) were excluded from the calculation.

[58] B. Tappan, S. Son, Decomposition and Ignition of the High-Nitrogen Compound Triaminoguanidinium Azotetrazolate (TAGzT), *Propellants, Explosives, Pyrotechnics* **2006**, *31*, 163.
[59] J. C. Oxley, J. L. Smith, Thermal decomposition of high nitrogen energetic compounds – dihydrazido-S-tetrazine salts salts, *Thermochimica Acta* **2002**, *384*, 91.

Because new compounds were added to form large amounts of nitrogen and improve the intensity and flame surface it raises the question if weather an excess of nitrogen release leads to the converse effect.
Diagrams for reference 1 and 4, TNBI, NTO and some selected formulations with small flames/intensities are displayed in Figure 25–28. Reaction products which are from particular interest are highlighted in red.

It becomes apparent that reference compositions (Fig. 25), TNBI (Fig. 26) and NTO (Fig. 28) formulations produce similar w% of nitrogen (between 9-16%). Formulations with weak combustion behavior form slightly more (DETT1, DETP) (Fig. 27) than reference 4 and similar w% than reference 1. Obviously more w%, up to 23%, were released during combustion of BK_5AT. Because the intensity values for TNBI and DNT formulations are just slightly better or comparable to reference intensities it can be assumed that from theoretical aspects a high nitrogen content of new additives is not obligatory for larger flame surfaces and higher radiant intensities.

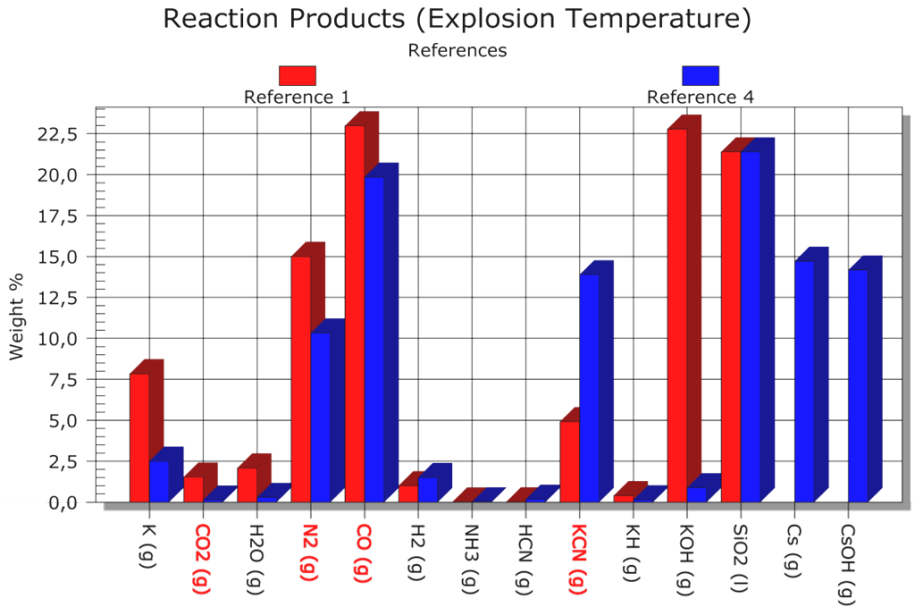

Figure 25 Calculated reaction products for reference 1 and 4.[56]

Although both references contain the same amount of hexamine but differ in the amount of potassium nitrate (70% for ref.1 and 30% for ref. 4) reference 4 form twice as much toxic potassium cyanide (13%) than reference 1 (5%). Similar values (1–10%) were obtained for TNBI formulations and the highest amount of potassium cyanide was observed for NTO6 which also contain the highest amount of the cesium salt of the high nitrogen compound

(15%). A faint smell after combustion also proves the formation of cyanide. Even though TNBI1 and 2 contain the same amount of either potassium or cesium salt (10%) the calculated amount of potassium cyanide for TNBI2 is very low and the amount of potassium hydroxide is very high and reverses for TNBI1.

As it is given for the Boudouard reaction the amount of carbon monoxide is much higher for formulations with normal combustion properties and temperatures than the amount of carbon dioxide. Formulations with poor combustion behavior e. g. RDX and DETT produce mainly CO_2 instead of CO and due to the different burning behavior it can be assumed that the combustion temperature is much lower. For the evidence of the calculated reaction products further mass spec (GC/MS) or gaseous IR experiments might be of interest.

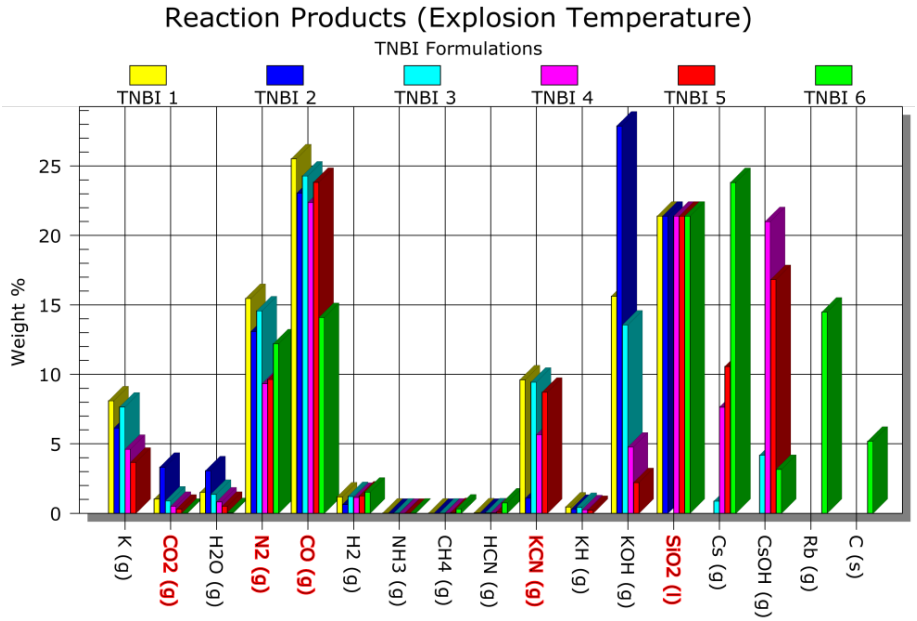

Figure 26 Calculated reaction products for TNBI formulations.[56]

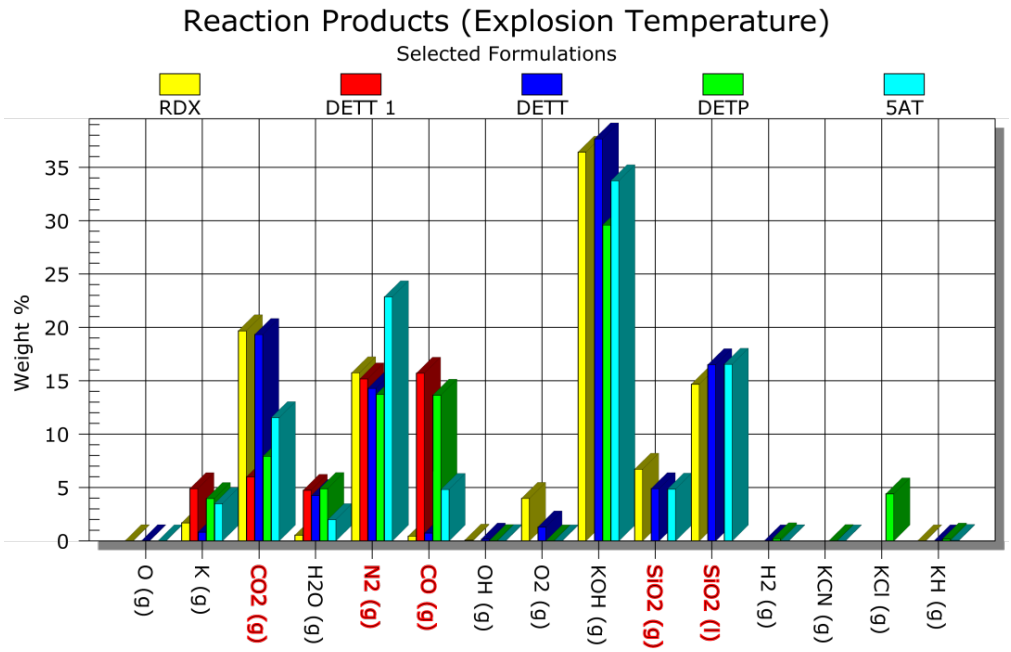

Figure 27 Calculated reactions products for selected formulations.[56]

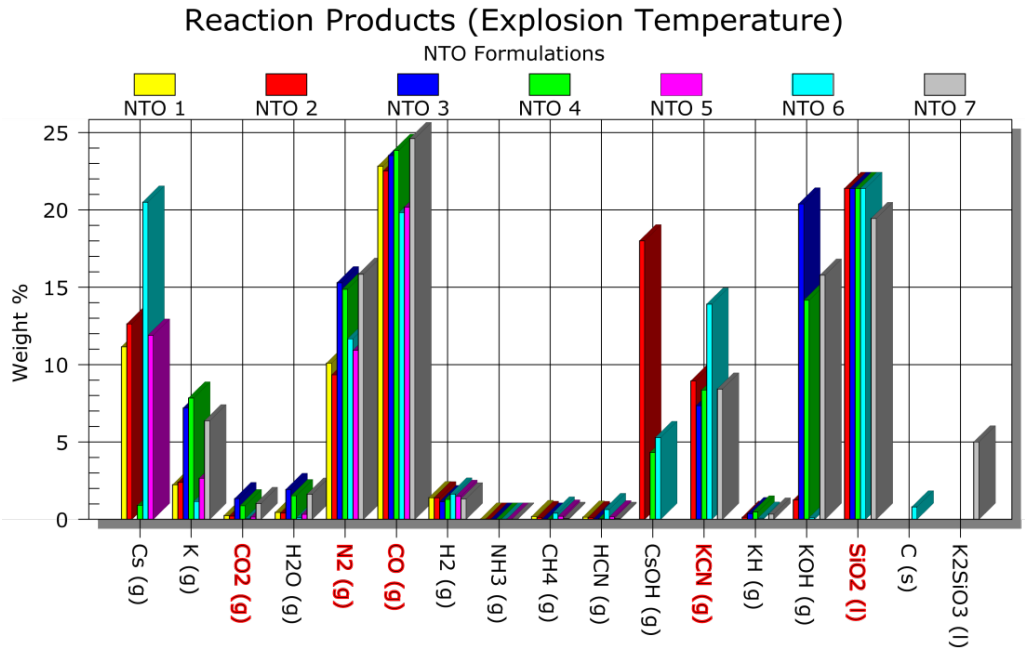

Figure 28 Calculated reactions products for NTO formulations.[56]

Discussion – Radiometric Measurements

Experimental set up

The first aim prior to executing radiometric calculations was the development of an experimental set up under the consideration of several influencing variables, otherwise the experiment will not be reproducible and comparable with other measurements at a different time and place.

Radiometric emissive properties of new *Black Knight* formulations were characterized using a *HR2000+ES* spectrometer (serial number: HR+C1888) with an ILX511B linear silicon CCD-array detector, UV2/OFLV-5 filter, L2 lens, 10 µm slit and included software from OCEAN OPTICS. The spectrometer was calibrated by OCEAN OPTICS for radiometric measurements.
For intensity measurements the optical fiber was coupled with a CC-3-UV cosine corrector (= irradiance probe) with a diameter of 3900 microns and a field of view (FOV) of 180° in order to consider angular incident light correctly to the calculations. The intensity of light was measured normal to the probe surface.

The radiometric term Irradiance E_e was already mentioned in chapter 3. In this regard the connection to the Radiance L_e should be drawn. The Radiance L_e of an emitting body is a measure of the flux density per unit solid angle and is expressed in W cm^{-2} sr^{-1}. Because the sample area increases with distance and therefore cancelling the inverse square losses, the radiance is independent of the distance of the light source. The Irradiance E_e, at any distance of the light source, is related to the Radiance L_e by the relationship given below, and depends only on the subtended central viewing angle $\boldsymbol{\theta}$ of the radiance detector:[15]

$$E_e = \pi\, L\, sin^2\left(\frac{\theta}{2}\right) \qquad (1)$$

Although radiometric measurements are sometimes performed with large distances between the emitting source and detector, the distance for the set up used within this thesis was 1 m, beginning from the end of the irradiance probe to the mid of the flare or flame, respectively (Figure 29a & b). Atmospheric influences on the emission date like air humidity can be therefore neglected choosing short distances between light area and sensing device.

To avoid light traps it should be leave as much space between the optical path, walls and ceilings as possible. Because all measurements were carried out in a fume hood the available space was limited. Usually, objects which are far away of the set up have low influences on the measurements because of the inverse square law. Therefore all objects near to the light

source and detector were removed from the field of view or were covered with black panels or color to avoid reflection. Further, to exclude the influence of the formed soot and smoke which can dim the radiant characteristics, indoor irradiance experiments were carried out using a good ventilated fume hood in the basement of the university. In contrast, outdoor irradiance measurements were carried out on an open field with a Night-Max® M5 night vision device from GUTZEIT GmbH in combination with a Sony NEX C3 digital camera. The flare was placed in the middle of a 2 x 1 m metal penal. The distance between night vision device and a 10 g pellet was 70 m.

The silicon detector of the spectrometer comprises a wavelength region from 200–1100 nm, in which the measurements for NIR calculations were in the range of 400–1050 nm. To avoid signal saturation the integration time for the measurement has to be adjusted for each specified light source. The shortest integration time which is technical possible is 1 ms. The chosen integration time was 100 ms because lower values leads to weak signals. If the intensity signal is lower than 50% the integration time should be changed as long as a maximum intensity of 85% is reached (try 200 ms). The selected scan time for all emission experiments was 35 s (350 scans). However, the average burn time of a pyrotechnic formulation was 20–25 s. Therefore, for correct calculations it is possible to exchange the set scan time to the real scan time within the MATLAB code afterwards. In order to obtain a good signal to noise ratio the 'scan to average' value should set to values above 1. To gain higher temporal resolution of the flame the spectra were not averaged ('scan to average' = 1). To avoid data loss of the intensity of the flame the boxcar-width was set to '0'. Every single experiment was performed with the exclusion from light and after recording a dark spectrum in advance. A user guide for irradiance measurements with the OCEAN OPTICS spectrometer is attached.

The second task of the radiometric experiments comprises the evaluation of the obtained intensity data. Compared to experiments using static lights like LEDs or light bulbs the combustion of pyrotechnic formulations lasts several seconds to minutes and cannot be switched-on or of ad libitum. The Irradiance E is generally obtained following equation 1. Using a calibrated spectrometer, E is calculated according to equation 2. This means, the obtained spectra, given in counts were multiplied with the detector response file (calibration file), divided by the integration time and integrated over the wavelength. As previously mentioned, the Radiance L_e is independent from the inverse square law, whereas the radiant Intensity I_e is dependent from the inverse square law. The obtained Irradiance E_e is converted into the radiant Intensity I_e according to equation 3. This results in the unit counts $\rightarrow$ W m^{-2} $\rightarrow$ W sr^{-1}.

$$E_e = \int_{\lambda_1}^{\lambda_2} dE_\lambda \, d\lambda \qquad (2)$$

$$I_e = E_e \times d^2 \qquad (3)$$

with E = Irradiance, E_λ = Spectral Radiant Flux Density, I = Radiant Intensity and d = Distance.

In addition to the maximum and mean intensities the concealment index χ is calculated according to equation 4:

$$\chi = \frac{I_{NIR}}{I_{Vis}} \qquad (4)$$

with λ_{NIR} = 700–1000 nm and λ_{VIS} = 400–700 nm, previously mentioned in chapter 3.

The obtained data for new formulations were compared to standard *Black Knight* compositions containing either potassium nitrate (reference 1) or potassium and cesium nitrate (reference 4).

a

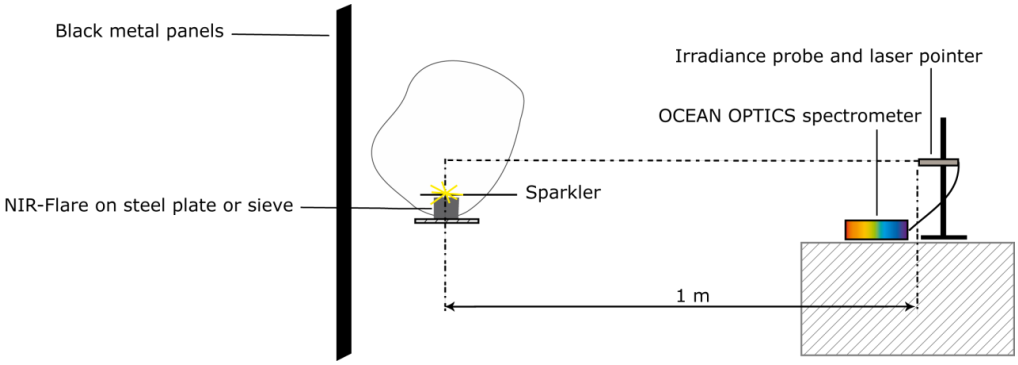

b

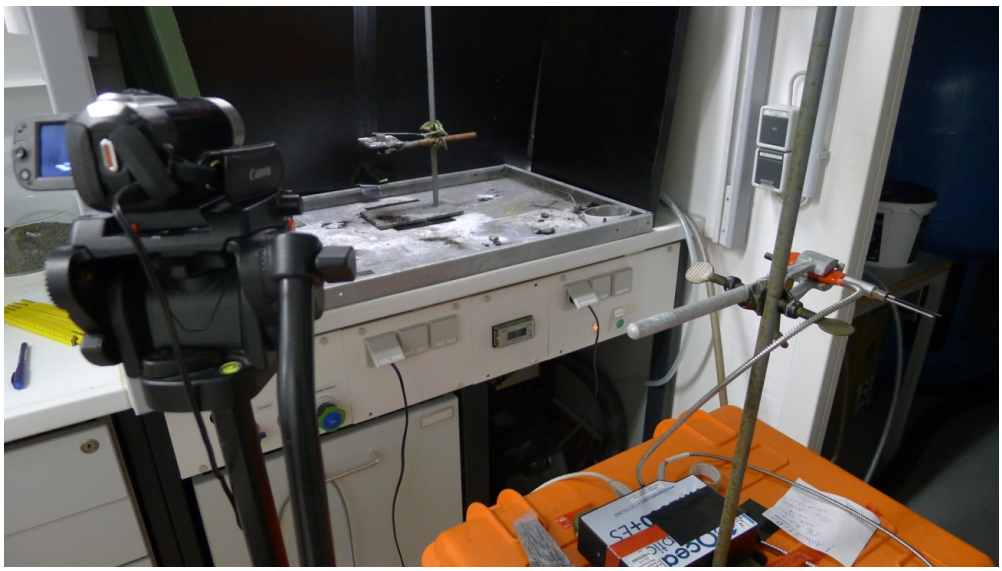

Figure 29 Experimental set up for indoor NIR measurements (a, b).

Radiometric results

Caution! *Due to safety reasons the quantity of synthesized energetic materials should be minimized. Therefore the total amount of each pure compound was 25 g. Although the impact and friction data of the formulations are determined first a further safety hazard still exists during the pressing process. Therefore the preferred charge size within this thesis was 10 g. To test the reliability of the set up only selected formulations were tested as 20 g charges.*

47 new *Black Knight* formulations and 5 reference formulations were synthesized as described in chapter 5 and investigated due to their radiant emission. Because it is described that the particle size of the used ingredients influences the burn nature of pyrotechnics, reference 1 was further synthesized in different grain sizes to test their burning quality and radiant intensity (Figure 21, 31 and 32).[50] In addition several tests were performed to test the influence of a cover charge (first fire). Although the burning character is improved using a cover (here black powder) the influence of higher amounts of visible light reduces the concealment index. As a consequence it was preferred to test the pure pellet first. After excluding compositions with poor burning properties the measurement should be repeated with a charge of 20–40 g and additional primer or first fire.

The results of the intensity measurements given in Table 24–41 are mean values of typically 5 runs á 10 g. Some of them consist of 3 runs when i) low intensities were obtained for the first run, ii) the flame surface was very low, iii) the flare was difficult to ignite. However, the data obtained for I_{vismean} or I_{NIRmean} are mean values of the complete burning times e. g. 20 s (Table 22 and 23).

Formulations which serve as standards are reference 1 and 4 and are highlighted in red. Compositions with values similar or better than the references are highlighted in blue. As mentioned above these compounds/compositions are still of interest and should be further characterized.

Reference 1–5

The spectra illustrated in Figure 30 are plots of the maximum intensity of reference 1, 4 and 5 gained after ignition. The expected emission lines for potassium at 766–769 nm, cesium at 852 and 894, and rubidium at 780 and 794 nm are displayed. Although rubidium is too expensive to use it regularly the intensity output and concealment index for a composition containing cesium and rubidium nitrate is very high due to a red-shift of about 11–28 nm for Rb and 38–128 nm for Cs compared to potassium. Therefore several formulations were

prepared with rubidium nitrate as oxidizer (Table 16 and 17). As expected it is not possible to avoid the sodium line at 589 nm, although pure compounds and oxidizers were used. Combustion products like KCN, MOH, SiO_2, H_2O, CO, CO_2, NH_3 etc. are located at higher wavelengths above 2000 to 6000 nm (M = K, Cs, Rb) and were therefore not recorded.

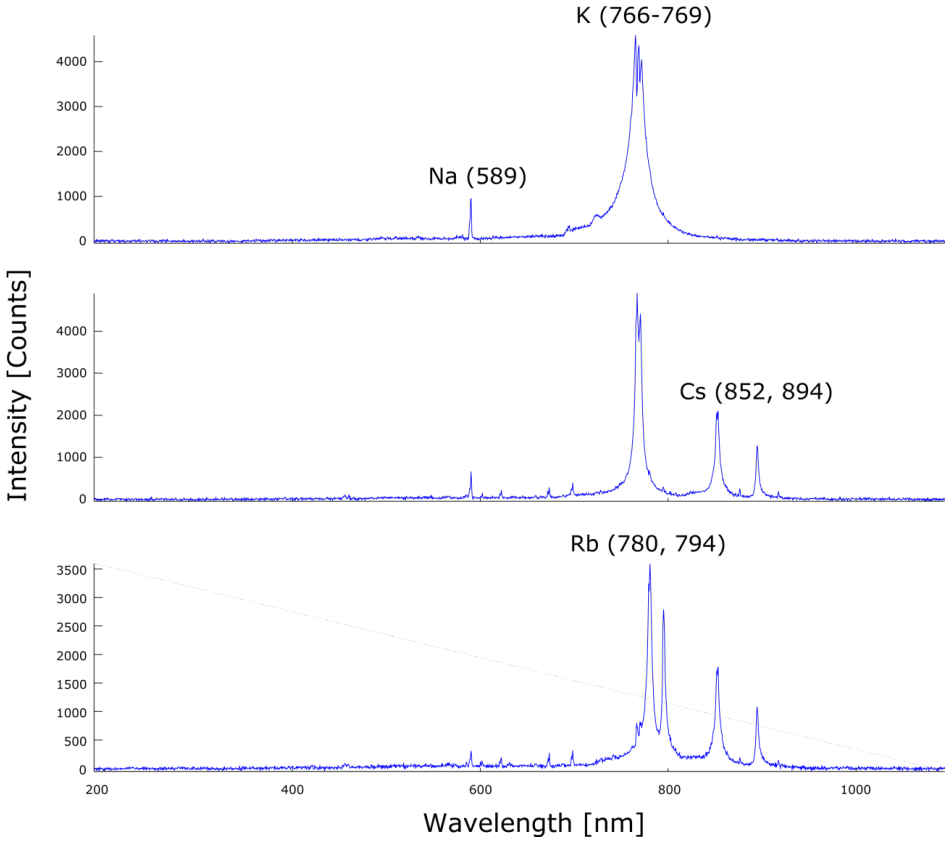

Figure 30 Intensity plots for reference 1 (top), 4 (mid) and 5 (bottom).

Figure 31 and 32 gives the comparison of reference formulations with different mixing grade. The fine composition was synthesized with ingredients mixed in a ball mill and then additionally in a mortar for 20 minutes. The rough composition was mixed for about 5 minutes in a mortar (Figure 21).

Although both formulations consist of the same wt% of the compounds the difference in their combustion behavior is obviously (Figure 31 and 32). As desired for NIR flares, the maximum IR output for the fine mixture is achieved shortly after ignition and stays nearly constant for several seconds. The maximum intensity for the rough mixture is observed not before 18 s and stays only short at his maximum. As both flares consists of the same high (2 cm), the burn rate for reference_f is 0.08 cm s^{-1} and for reference_r 0.06 cm s^{-1}. The

results of our experiment conform with results obtained in literature[50] whereas a decrease of the particle size of the fuel leads to an increase of the reaction rate. Reducing the particle size causes a higher reaction surface and a more intimate contact of fuel and oxidizer which influences the kinetic of the redox reaction.

In addition to the decrease of the burn rate both plots visualizes a significant decrease of the intensity values of 5 W sr^{-1} for the rough mixed composition compared to about 11 W sr^{-1} for the fine mixed formulation (Table 25). On this account it must be mentioned again: the mixing process of pyrotechnic formulations should be done accurate to obtain reliable data.[54]

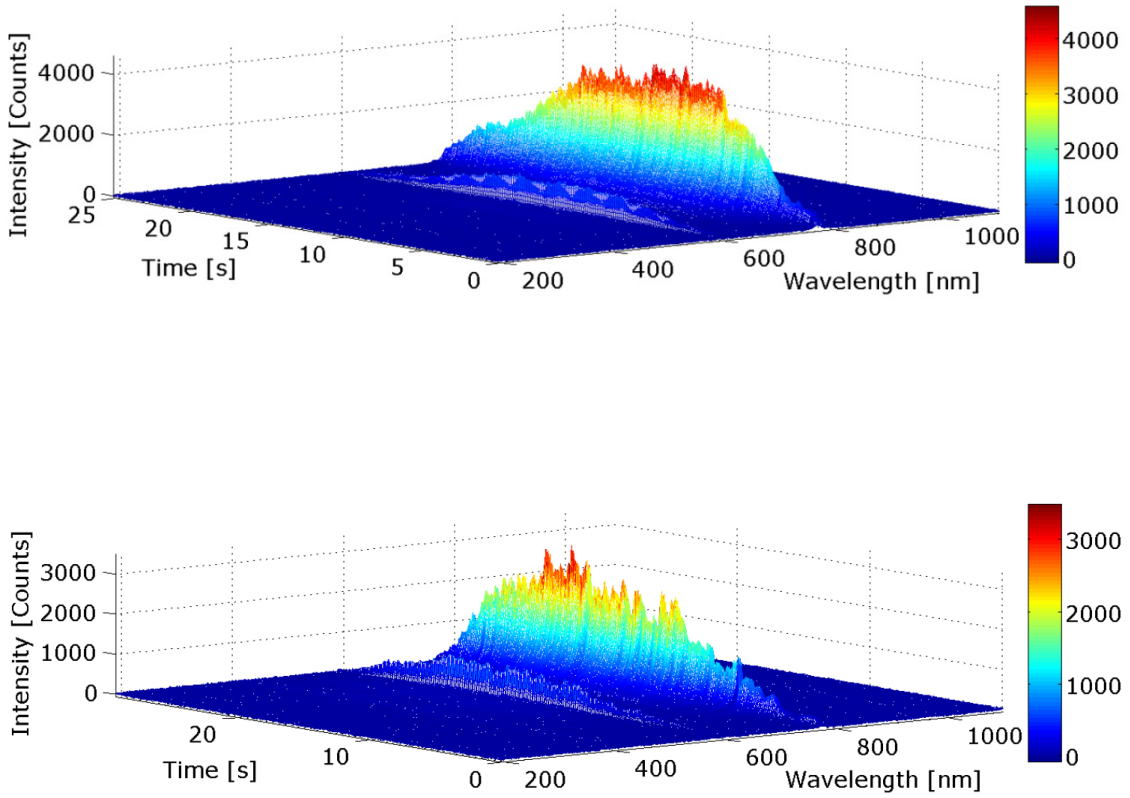

Figure 31 Intensity plot as a function of time and wavelength of reference1_f (top) and reference1_r (bottom).

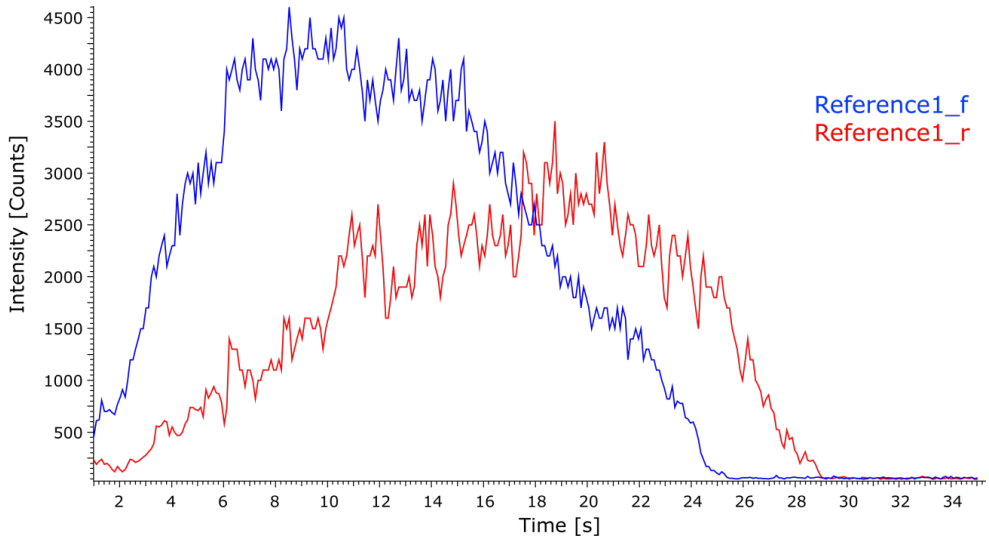

Figure 32 Intensity as a function of time for reference1_f and reference1_r.

Table 24 Radiant intensities of *Black Knight* formulations.*

Formulation	I_{VISmax} **[Cd]**	I_{VISmax} **[W/sr]**[a]	$I_{VISmean}$ **[W/sr]**	$I_{NIRmean}$ **[W/sr]**[b]
Reference1_r	129	0.19	0.10	2.77
Reference1_m	247	0.37	0.21	6.11
Reference1_f	281/264	0.42/0.39	0.20/0.25	5.37/7.71
Reference1_BP	527	0.77	0.32	8.45
Reference2	100/148	0.15/0.22	0.09/0.12	4.25/6.14
Reference3	128	0.19	0.11	5.90
Reference4	144	0.21	0.13	7.01
Reference5	121	0.18	0.11	7.57

*all values are mean values of 3-5 measurements, [a] I_{vis} = 400-700 nm

[b] I_{NIR} = 700-1000 nm; 10g / 20g batch, BP = black powder cover

Table 25 Radiant intensities of *Black Knight* formulations (continued).*

Formulation	I_{NIRmax} [W/sr][a]	I_{1max} [W/sr][b]	I_{2max} [W/sr][c]	χ
Reference1_r	5.32	5.43	4.98	28.71
Reference1_m	10.99	11.22	11.20	30.41
Reference1_f	10.96/13.15	11.21/13.40	11.38/12.85	26.82/33.98
Reference1_BP	19.36	19.87	19.77	25.60
Reference2	6.88/12.26	6.91/12.39	7.01/12.49	48.44/56.76
Reference3	10.23	10.32	10.14	54.73
Reference4	12.37	12.50	12.55	59.08
Reference5	12.59	12.69	12.76	70.98

*all values are mean values of 3-5 measurements; [a] I_{NIR} = 700-1000 nm;
[b] I_1 = 600-900 nm; [c] I_2 = 695-1050 nm; $\chi = I_{NIR}/I_{vis}$; 10g / 20g batch, BP = black powder cover

The default values for the intensities are >25 W sr^{-1} for a charge larger than 10 g (enlarged surface, higher temperature). These values are stated for the maximum intensity. Because most flares tested therein consist of 10 g, 25 W sr^{-1} are normally not reached. As it can be seen from the compared 10/20 g charges nearly the double IR output was achieved for a 20 g pellet (Table 25, 27, 35, 37, 41). Surprisingly this was observed for all new formulations but not for reference 1. One test with a 30 g charge of reference 1 and 4 results in 25 W sr^{-1} (χ = 27, I_{vismax} = 600 Cd) and 18 W sr^{-1} (χ = 57, I_{vismax} = 215 Cd), respectively. However, the data of pyrotechnic charges (mass and intensities) given in literature indicate a saturation of the intensity at a certain amount. Hence, the maximum intensity is reached at around 30 W sr^{-1} for payloads of 20 g and larger.[8] To prove this statement several additional tests should be repeated with 20, 30 and 40 g payloads.

Hexamine replacements

Interestingly the obtained data for all hexamine replacements were underperforming. DETT does not burn and only the perchlorate salt of diethylene trinitrate shows intensities of around 4 W sr^{-1} (Table 26, 27). Promising candidates like lactose, 5-aminotetrazole or amino-1,2,4-triazole show nearly no intensities. Although it is assumed that compounds like 5-aminotetrazole or DETT/DETP produce large amounts of nitrogen and lactose large amounts of carbon dioxide after decomposition the surface of the flame was not enlarged (Figure 33). As previously mentioned 5AT and ATR produces small sparks during combustion which is a further disadvantage (Figure 23). Figure 34 and 35 reflects the burning behavior

of selected flares with poor intensities and burning nature. These flares show understandably long combustion times. DETT must be lighted several times because the first contact with the flame does not support the self-sustaining of the formulation.

Both commonly used secondary explosives HMX and RDX were synthesized from hexamine as starting material. Therefore it was obvious to test both as hexamine replacement. Although both are toxic and would not find their way into industrial manufactured pyrotechnic formulations it was of interest to investigate their burning behavior and compatibleness within a pyrotechnic formulation. As it can be seen from Figure 34 it is nearly no IR output obtained for a complete exchange of hexamine by 16% RDX. Formulations with a mixture of HMX or RDX and hexamine gave also low values of around 7 W sr^{-1}.

The highly negative heat of formations of DETT, DETP and lactose (–971.70 kJ mol^{-1}, −687.01 kJ mol^{-1}, –651 kJ mol^{-1}) could be one reason for the paltry IR emission and burning nature.[20] In contrast, compounds with a similar heat of formation as hexamine (+124.06 kJ mol^{-1}) e. g. 5-AT (+207.78 kJ mol^{-1}) and ATR (+108.78 kJ mol^{-1}) showing alike performance. Because all additives are not suitable for formulations and BK_DETT, DETP and EDD are hygroscopic and not compatible with other ingredients there were not further investigated.

Table 26 Radiant intensities of *Black Knight formulations* – hexamine replacements.*

Formulation	I_{VISmax} [Cd]	I_{VISmax} [W/sr][a]	$I_{VISmean}$ [W/sr]	$I_{NIRmean}$ [W/sr][b]
Reference1_f	281/264	0.42/0.39	0.20/0.25	5.37/7.71
Reference4	144	0.21	0.13	7.01
BK_L	194	0.29	0.17	4.57
BK_5AT	28	0.04	0.04	0.83
BK_ATR	61	0.09	0.06	1.75
BK_LH	262	0.38	0.19	5.83
BK_DETT	-	-	-	-
BK_DETT1	46	0.07	0.03	0.64
BK_EDD	46	0.07	0.01	0.44
BK_DETP	122	0.18	0.08	1.59
BK_RDX	40	0.06	0.02	0.45
BK_RDX1	263/543	0.39/0.80	0.23/0.45	4.21/7.51
BK_HMX	184/527	0.27/0.34	1.13/0.77	3.05/7.09

*all values are mean values of 3-5 measurements, [a] I_{vis} = 400-700 nm

[b] I_{NIR} = 700-1000 nm; 10g / 20g batch

Table 27 Radiant intensities of *Black Knight formulations* – hexamine replacements (continued).*

Formulation	I_{NIRmax} [W/sr][a]	I_{1max} [W/sr][b]	I_{2max} [W/sr][c]	χ
Reference1_f	10.96/13.15	11.21/13.40	11.38/12.85	26.82/33.98
Reference4	12.37	12.50	12.55	59.08
BK_L	7.77	7.69	8.60	27.52
BK_5AT	1.04	1.07	1.43	25.15
BK_ATR	2.50	2.56	2.55	28.19
BK_LH	10.40	11.65	11.36	30.23
BK_DETT	-	-	-	-
BK_DETT1	1.65	1.68	1.45	24.47
BK_EDD	1.80	1.83	1.28	26.31
BK_DETP	3.76	3.85	4.10	20.95
BK_RDX	1.15	1.18	1.43	19.86
BK_RDX1	7.11/13.65	7.29/14.05	7.41/13.97	18.45/17.16
BK_HMX	6.85/15.60	7.01/16.08	6.91/15.95	25.49/20.23

*all values are mean values of 3-5 measurements; [a] I_{NIR} = 700-1000 nm; [b] I_1 = 600-900 nm; [c] I_2 = 695-1050 nm; $\chi = I_{NIR}/I_{vis}$; 10g / 20g batch

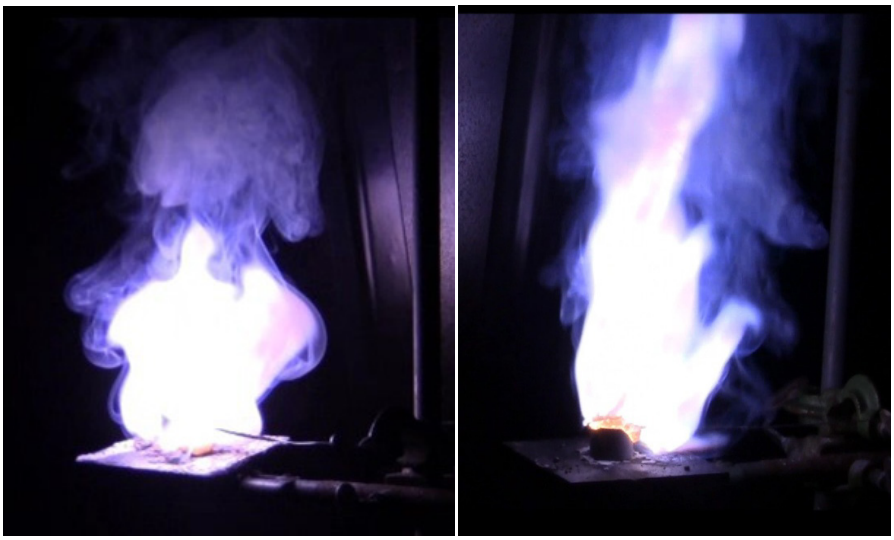

Figure 33 Flame surface of DETP (left) and reference 4 (right).

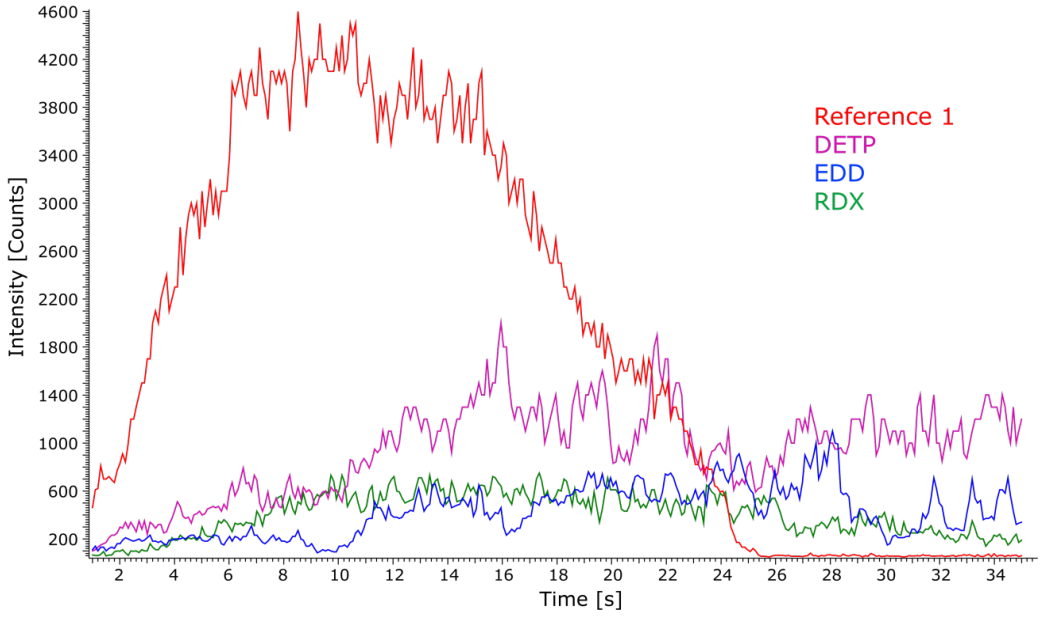

Figure 34 Selected formulations with poor burning nature.

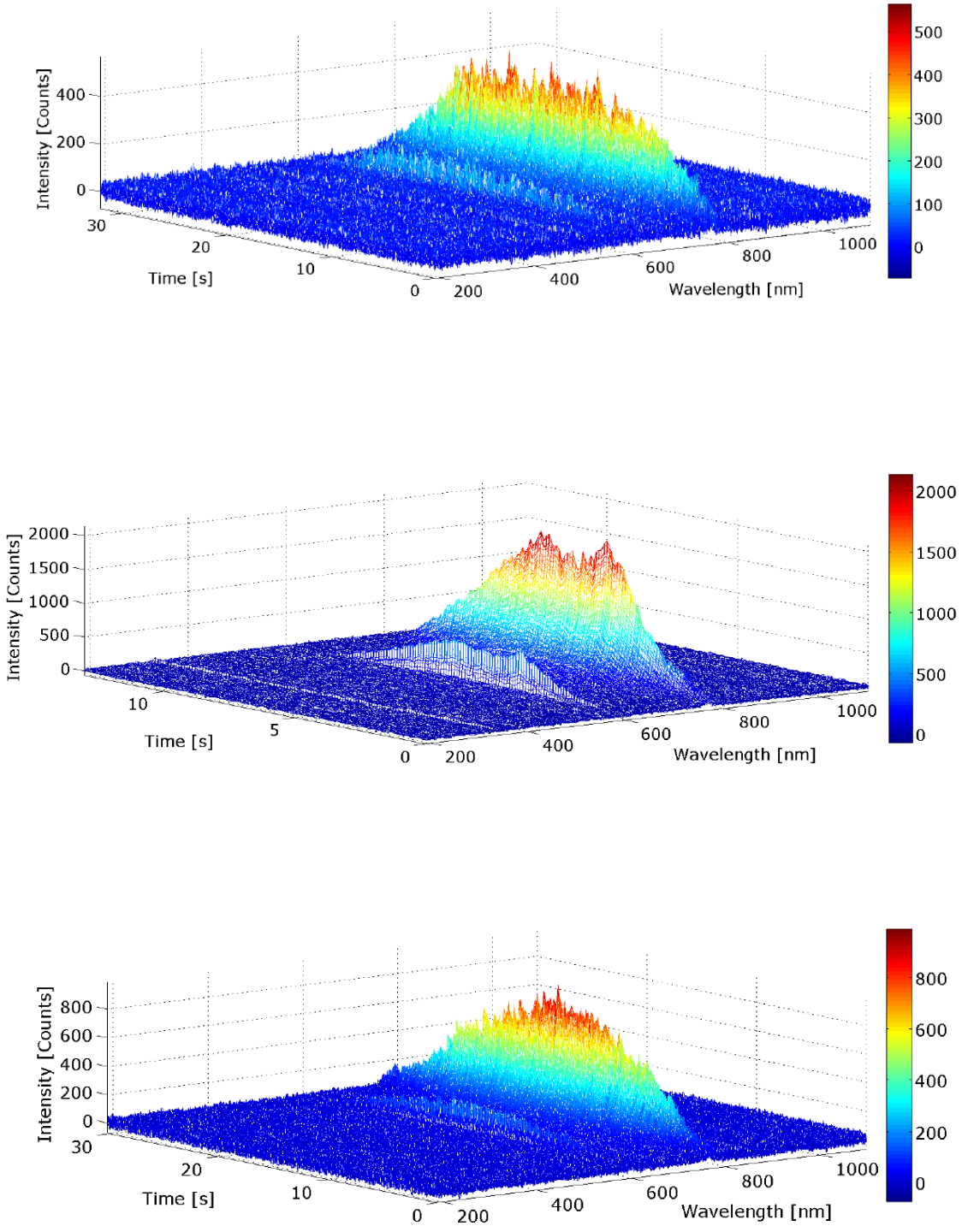

Figure 35 Intensity plots as a function of time and wavelength for BK_5AT (top), BK_L (mid) and _ATR (bottom).

BTA

All formulations containing 5-bistetrazolyl amine show good burning characteristics. The visible output for 10 g charges are below the preset emission of 350 Cd. The lowest IR output was obtained for BTA3 and BTA6 although they consist of an equal ratio of their ingredients (10% HNC, 8% lactose, 8% hexamine, 60% oxidizer). Similar values (IR, χ) as both references are obtained for BTA1, therefore this formulation would be a good candidate for further experiments. The burning behavior of BTA1 together with several selected formulations is also displayed in Figure 36. Due to the large amount of cesium and or rubidium, very high concealment indices were obtained for BTA5, 6 and 7 (Table 28 and 29).

Table 28 Radiant intensities of *Black Knight* formulations - BTA.*

Formulation	I_{VISmax} [Cd]	I_{VISmax} [W/sr][a]	$I_{VISmean}$ [W/sr]	$I_{NIRmean}$ [W/sr][b]
Reference1_f	281/264	0.42/0.39	0.20/0.25	5.37/7.71
Reference4	144	0.21	0.13	7.01
BK_BTA1	218	0.32	0.18	6.46
BK_BTA2	304	0.44	0.25	5.10
BK_BTA3	67	0.10	0.06	4.10
BK_BTA4	102	0.15	0.10	3.76
BK_BTA5	74	0.11	0.06	4.50
BK_BTA6	37	0.05	0.03	3.62
BK_BTA7	81	0.10	0.08	4.44

*all values are mean values of 3-5 measurements, [a] I_{vis} = 400-700 nm

[b] I_{NIR} = 700-1000 nm; 10g / 20g batch

Table 29 Radiant intensities of *Black Knight* formulations - BTA (continued).*

Formulation	I_{NIRmax} [W/sr][a]	I_{1max} [W/sr][b]	I_{2max} [W/sr][c]	χ
Reference1_f	10.96/13.15	11.21/13.40	11.38/12.85	26.82/33.98
Reference4	12.37	12.50	12.55	59.08
BK_BTA1	11.74	11.95	12.05	36.94
BK_BTA2	8.98	9.26	9.18	20.22
BK_BTA3	4.17	4.17	4.04	41.73
BK_BTA4	6.67	6.77	7.08	45.46
BK_BTA5	8.74	8.80	9.06	81.12
BK_BTA6	4.83	4.86	5.51	97.94
BK_BTA7	8.11	7.63	7.83	75.81

*all values are mean values of 3-5 measurements; [a] I_{NIR} = 700-1000 nm;
[b] I_1 = 600-900 nm; [c] I_2 = 695-1050 nm; $\chi = I_{NIR}/I_{vis}$; 10g / 20g batch

NTO

As stated within chapter 1 new results of commonly used explosives in pyrotechnic formulations display good properties.[20] NTO as another secondary explosive was therefore tested within NIR compositions (Table 30 and 31).

Most NTO compositions show low intensity values. Only NTO4 and 6 are in the range of 10 W sr^{-1}. The concealment indices for most compositions are comparable with the references only NTO1 and 2 have very high values of around 98. Although the oxygen balances of the formulations are in the range of references (-28 – -39 %), the O/F values are between 1.22–2.03. As mentioned previously good intensity values are obtained for an O/F of 2.33. Because NTO4 and 6 formulations consist of 10-15 w% of the high nitrogen compound it would be meaningful to repeat this measurement with 70% oxidizer and a decreased amount of hexamine instead of the nitrates.

Table 30 Radiant intensities of Black Knight formulations - NTO.*

Formulation	I_{VISmax} [Cd]	I_{VISmax} [W/sr][a]	$I_{VISmean}$ [W/sr]	$I_{NIRmean}$ [W/sr][b]
Reference1_f	281/264	0.42/0.39	0.20/0.25	5.37/7.71
Reference4	144	0.21	0.13	7.01
BK_NTO1	23	0.03	0.02	1.80
BK_NTO2	45	0.05	0.04	3.08
BK_NTO3	168	0.25	0.08	3.24
BK_NTO4	116	0.16	0.08	4.78
BK_NTO5	84	0.12	0.07	4.24
BK_NTO6	92	0.10	0.07	4.58
BK_NTO7	108	0.16	0.07	2.62

*all values are mean values of 3-5 measurements, [a] I_{vis} = 400-700 nm

[b] I_{NIR} = 700-1000 nm; 10g / 20g batch

Table 31 Radiant intensities of Black Knight formulations - NTO (continued).*

Formulation	I_{NIRmax} [W/sr][a]	I_{1max} [W/sr][b]	I_{2max} [W/sr][c]	χ
Reference1_f	10.96/13.15	11.21/13.40	11.38/12.85	26.82/33.98
Reference4	12.37	12.50	12.55	59.08
BK_NTO1	3.09	3.11	3.30	98.00
BK_NTO2	5.25	5.30	5.51	98.94
BK_NTO3	8.53	8.69	8.55	39.01
BK_NTO4	8.89	9.00	9.55	50.18
BK_NTO5	8.38	8.46	8.65	66.77
BK_NTO6	8.94	9.03	9.44	66.39
BK_NTO7	6.07	6.16	6.28	38.43

*all values are mean values of 3-5 measurements; [a] I_{NIR} = 700-1000 nm;

[b] I_1 = 600-900 nm; [c] I_2 = 695-1050 nm; $\chi = I_{NIR}/I_{vis}$; 10g / 20g batch

TNBI

Formulations containing the potassium and/or cesium salt of tetranitro bisimidazole showing a very good burning behavior. The intensity values of TNBI2, 5 and 6 are similar to both references whereas formulation 5 and 6 contain only 3 w% of the potassium or cesium salt (Table 32 and 33). TNBI2 consists of 10 w% of the cesium salt and gives slightly lower values then 5 and 6. Although TNBI flares had the largest flame sizes compared to all others the intensity output was not improved. Values obtained for formulation 4 (5/5 % potassium and cesium HNCs) are lower than of 1 and 2 (10 % either K or Cs). The reason for that might be the addition of lactose or the decreased amount of oxidizer. The intensity output of 5 and 6 is not obviously better compared to the standard and only a low amount of TNBI was added. Figure 36 illustrates the burn time of several formulation, including TNBI1, compared to reference 1.

Table 32 Radiant intensities of *Black Knight* formulations - TNBI.*

Formulation	I_{vismax} [Cd]	I_{vismax} [W/sr][a]	$I_{vismean}$ [W/sr]	$I_{NIRmean}$ [W/sr][b]
Reference1_f	281/264	0.42/0.39	0.20/0.25	5.37/7.71
Reference4	144	0.21	0.13	7.01
BK_TNBI1	162	0.24	0.13	4.78
BK_TNBI2	163	0.24	0.13	5.58
BK_TNBI3	65	0.09	0.05	3.95
BK_TNBI4	81	0.12	0.08	5.23
BK_TNBI5	266	0.39	0.20	5.30
BK_TNBI6	129	0.19	0.11	5.08

*all values are mean values of 3-5 measurements, [a] I_{vis} = 400-700 nm

[b] I_{NIR} = 700-1000 nm; 10g / 20g batch

Table 33 Radiant intensities of *Black Knight* formulations - TNBI (continued).*

Formulation	I_{NIRmax} **[W/sr]**[a]	I_{1max} **[W/sr]**[b]	I_{2max} **[W/sr]**[c]	χ
Reference1_f	10.96/13.15	11.21/13.40	11.38/12.85	26.82/33.98
Reference4	12.37	12.50	12.55	59.08
BK_TNBI1	8.75	8.91	8.98	39.97
BK_TNBI2	10.68	10.83	10.87	44.69
BK_TNBI3	7.18	7.24	7.67	75.67
BK_TNBI4	9.09	9.15	9.41	76.67
BK_TNBI5	10.93	11.21	11.50	27.99
BK_TNBI6	10.54	10.66	11.00	55.94

*all values are mean values of 3-5 measurements; [a] I_{NIR} = 700-1000 nm;

[b] I_1 = 600-900 nm; [c] I_2 = 695-1050 nm; $\chi = I_{NIR}/I_{vis}$; 10g / 20g batch

BOX

Good values for the maximum intensity were obtained for BOX1 which comprises 8% of the potassium salt and a decreased amount of hexamine. Because the total amount of oxidizer (70%) and high nitrogen compound (8%) are equal for all three BOX formulations, the addition of lactose and the combination of the potassium and cesium salt (4/4%) reduces the NIR output by half for BOX2 and 3. The concealment index for 1 and 2 is moderate due to the amount of cesium nitrate. Because BOX3 contain only potassium nitrate and only 4% of the cesium salt χ is considerably lower (55 *vs.* 24). Similar as for BTA1 further test should be carried out with larger amounts of BOX1 in addition with a first fire. Because the visible output for a 20 g charge is higher than requested it should be further tested if the visible emission could be adjusted by a varied ratio of the single components.

Table 34 Radiant intensities of *Black Knight* formulations - BOX.*

Formulation	I_{vismax} [Cd]	I_{vismax} [W/sr][a]	$I_{vismean}$ [W/sr]	$I_{NIRmean}$ [W/sr][b]
Reference1_f	281/264	0.42/0.39	0.20/0.25	5.37/7.71
Reference4	144	0.21	0.13	7.01
BK_BOX1	172/432	0.25/0.63	0.17/0.37	6.44/14.29
BK_BOX2	94/206	0.14/0.30	0.09/0.17	3.34/6.17
BK_BOX3	216/361	0.32/0.53	0.14/0.31	3.38/7.00

*all values are mean values of 3-5 measurements, [a] I_{vis} = 400-700 nm

[b] I_{NIR} = 700-1000 nm; 10g / 20g batch

Table 35 Radiant intensities of *Black Knight* formulations - BOX (continued).*

Formulation	I_{NIRmax} [W/sr][a]	I_{1max} [W/sr][b]	I_{2max} [W/sr][c]	χ
Reference1_f	10.96/13.15	11.21/13.40	11.38/12.85	26.82/33.98
Reference4	12.37	12.50	12.55	59.08
BK_BOX1	11.80/26.15	11.97/26.60	12.21/28.03	46.92/41.31
BK_BOX2	5.87/12.52	5.96/12.47	6.58/14.07	43.00/41.50
BK_BOX3	7.78/12.87	7.96/13.17	7.86/13.49	24.56/24.32

*all values are mean values of 3-5 measurements; [a] I_{NIR} = 700-1000 nm;

[b] I_1 = 600-900 nm; [c] I_2 = 695-1050 nm; $\chi = I_{NIR}/I_{vis}$; 10g / 20g batch

DNT

The IR output for all DNT formulations is comparable with the emission of references 1 and 4. The visible light of a 20 g charge is much higher, although only 2–5% of DNT were added. Due to the low amount of DNT all formulations deviate only slightly from the reference formulation, therefore the high amount of visible light might be from the decomposition of DNT. Because DNT2 formulations showing good intensity values (slightly better than both references) it might be useful to performed further tests and higher amounts of DNT within the formulation.

Table 36 Radiant intensities of *Black Knight* formulations - DNT.*

Formulation	I_{vismax} [Cd]	I_{vismax} [W/sr][a]	$I_{vismean}$ [W/sr]	$I_{NIRmean}$ [W/sr][b]
Reference1_f	281/264	0.42/0.39	0.20/0.25	5.37/7.71
Reference4	144	0.21	0.13	7.01
BK_DNT1	285/713	0.42/1.04	0.23/0.53	5.04/11.22
BK_DNT2	178/398	0.26/0.58	0.14/0.30	6.36/12.10
BK_DNT3	277/789	0.41/1.16	0.22/0.61	4.98/11.07

*all values are mean values of 3-5 measurements

[a] I_{vis} = 400-700 nm; [b] I_{NIR} = 700-1000 nm; 10g / 20g batch

Table 37 Radiant intensities of *Black Knight* formulations - DNT (continued).*

Formulation	I_{NIRmax} [W/sr][a]	I_{1max} [W/sr][b]	I_{2max} [W/sr][c]	χ
Reference1_f	10.96/13.15	11.21/13.40	11.38/12.85	26.82/33.98
Reference4	12.37	12.50	12.55	59.08
BK_DNT1	10.05/23.40	10.33/24.13	10.30/24.73	24.11/22.43
BK_DNT2	12.70/24.94	12.85/25.30	13.18/26.32	48.90/42.75
BK_DNT3	10.00/22.11	10.24/22.86	10.50/23.48	24.76/19.15

*all values are mean values of 3-5 measurements; [a] I_{NIR} = 700-1000 nm;

[b] I_1 = 600-900 nm; [c] I_2 = 695-1050 nm; $\chi = I_{NIR}/I_{vis}$; 10g / 20g batch

BTO and BT

All compositions containing either BTO or BT show lower intensity values than reference formulations. Although the IR output for BT2 is around 12 W sr^{-1} for a 10 g payload the formulations consist of only 3% of potassium BT. The visible emission for 10 g charges are in a good range for both BTO flares (10 and 20 g) and for BT2. Only BT1 exceeds the 350 Cd benchmark. Because of the low values obtained for BT1 (10 w% cesium salt) further experiments might be not useful.

Table 40 Radiant intensities of *Black Knight* formulations – BTO and BT.*

Formulation	I_{vismax} [Cd]	I_{vismax} [W/sr][a]	$I_{vismean}$ [W/sr]	$I_{NIRmean}$ [W/sr][b]
Reference1_f	281/264	0.42/0.39	0.20/0.25	5.37/7.71
Reference4	144	0.21	0.13	7.01
BK_BTO1	78/139	0.11/0.20	0.05/0.10	1.31/2.54
BK_BTO2	136/299	0.20/0.44	0.08/0.25	2.71/7.91
BK_BT1	216/411	0.32/0.60	0.14/0.36	2.93/7.38
BK_BT2	153/207	0.23/0.30	0.14/0.23	6.00/10.43

*all values are mean values of 3-5 measurements

[a] I_{vis} = 400-700 nm; [b] I_{NIR} = 700-1000 nm; 10g / 20g batch

Table 41 Radiant intensities of *Black Knight* formulations – BTO and BT (continued).*

Formulation	I_{NIRmax} [W/sr][a]	I_{1max} [W/sr][b]	I_{2max} [W/sr][c]	χ
Reference1_f	10.96/13.15	11.21/13.40	11.38/12.85	26.82/33.98
Reference4	12.37	12.50	12.55	59.08
BK_BTO1	3.20/4.96	3.27/5.09	3.13/4.74	28.31/23.35
BK_BTO2	6.82/14.64	6.94/14.90	5.94/15.06	34.25/33.52
BK_BT1	6.72/12.62	6.89/12.95	7.07/12.59	21.21/20.97
BK_BT2	11.52/17.10	11.67/17.30	12.21/18.44	51.64/56.31

*all values are mean values of 3-5 measurements; [a] I_{NIR} = 700-1000 nm;

[b] I_1 = 600-900 nm; [c] I_2 = 695-1050 nm; $\chi = I_{NIR}/I_{vis}$; 10g / 20g batch

Figure 36 displays the intensity as a function of time for reference 1 and 4 as well as for BTA1, TNBI1 and BTO1 is displayed in Figure 36. BTA1 and TNBI1 are constituted of 10 wt% potassium HNC and 60 % potassium nitrate as oxidizer. It can be seen BK_BTA1 and TNBI1 show good intensity values and burn times between both references. Similar as the references the maximum intensity output is close after ignition but the radiant emission of about 8 W sr^{-1} for TNBI 1 is unexpected low. Compared to BTO1 which comprises only 5 wt% of potassium BTO and 65% potassium nitrate the burning behavior and intensity output differs dramatically, although the burning time is larger than 35 s. One reason for this characteristic might be a too high nitrogen content of the compound. Due to the high formation of nitrogen the produced heat which is necessary for the burn rate and intensity emission is dissipated.

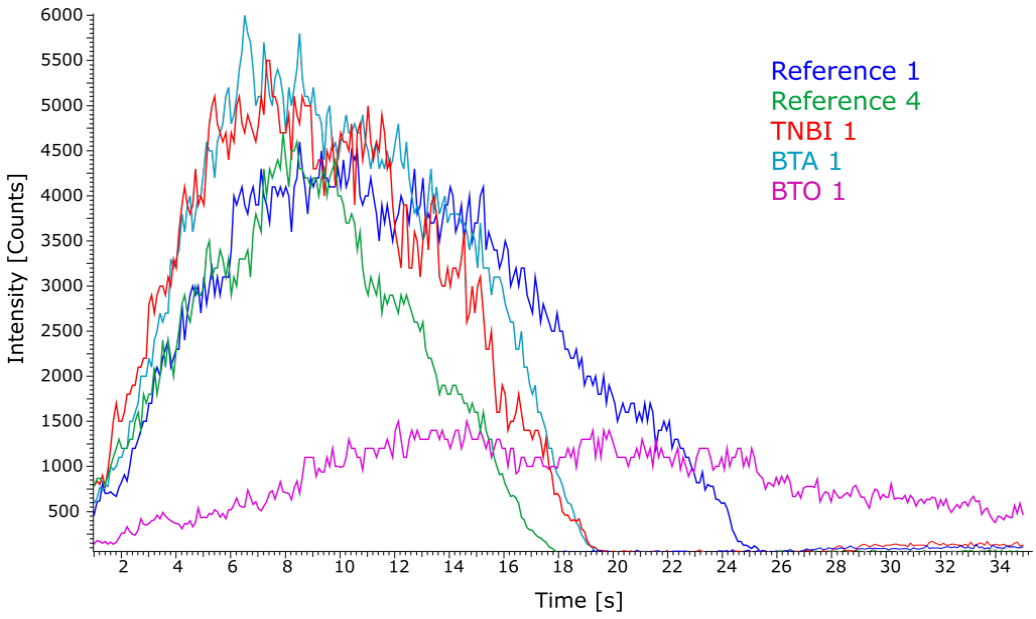

Figure 36 Intensity as a function of time for selected formulations.

The intensity plot for several selected formulations with different burn times is illustrated below. As desired, all composition reaches their maximum intensity shortly after ignition. However, the burn time decreases dramatically from 25 s to 10 s for BT2. TNBI6 and BT2 consist of similar ingredients and w% and differ therefore only slightly in burn time and radiant output.

Because lactose is added in pyrotechnics as readily combustible material it accelerates the combustion process of TNBI6 and BT2; both combust within 10–14 s.

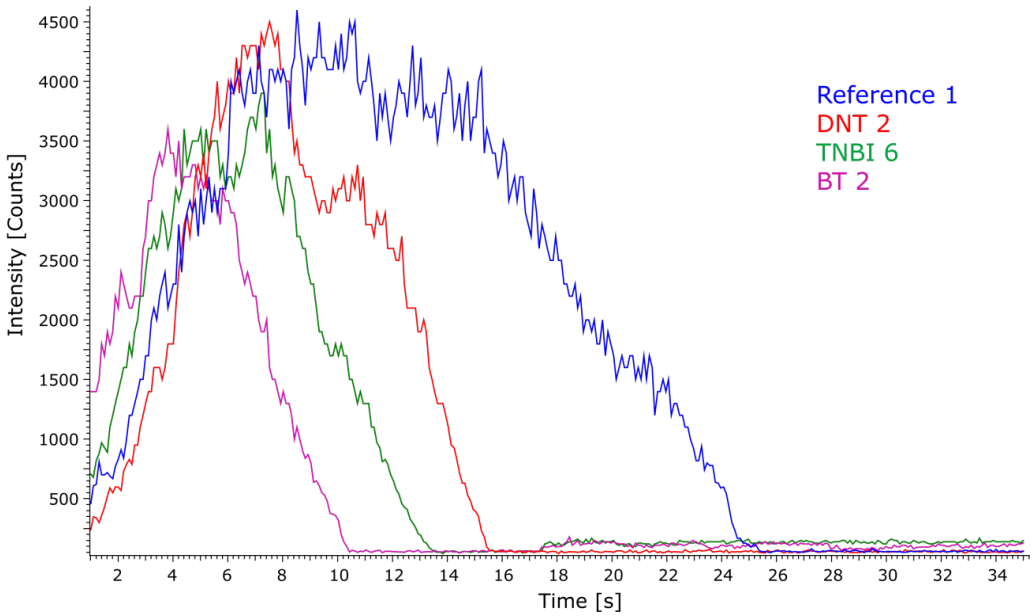

Figure 37 Intensity as a function of time for selected formulations.

Individual tests

The obtained data for 3NT, CsAzOT, DNQ, and BNGT are not satisfying. Although the visible output for all formulations is in a good range (< 350 Cd) the IR output with around 9 W sr^{-1} and the concealment index of 55 is only for CsATzO acceptable. Due to the sensitivity data of the formulation (chapter 6) the use of CsAtzO as a possible additive would be further questionable. Because the synthesis of DNQ is ambitious and the neutral compound decomposes after several days, the synthesis of larger scales of DNQ is also not profitably.

Table 38 Radiant intensities of *Black Knight* formulations - Selected.*

Formulation	I_{VISmax} [Cd]	I_{VISmax} [W/sr][a]	$I_{VISmean}$ [W/sr]	$I_{NIRmean}$ [W/sr][b]
Reference1_f	281/264	0.42/0.39	0.20/0.25	5.37/7.71
Reference4	144	0.21	0.13	7.01
BK_KBMTT	217	0.32	0.16	4.26
BK_CsBMTT	179	0.26	0.12	3.57
BK_3NT	237	0.35	0.15	3.55
BK_CsATzO	115/221	0.17/0.32	0.09/0.18	4.53/8.77
BK_BNGT	166	0.24	0.12	3.21
BK_DNQ	137	0.20	0.09	2.53

*all values are mean values of 3-5 measurements, [a] I_{vis} = 400-700 nm

[b] I_{NIR} = 700-1000 nm; 10g / 20g batch

Table 39 Radiant intensities of *Black Knight* formulations - Selected (continued).*

Formulation	I_{NIRmax} [W/sr][a]	I_{1max} [W/sr][b]	I_{2max} [W/sr][c]	χ
Reference1_f	10.96/13.15	11.21/13.40	11.38/12.85	26.82/33.98
Reference4	12.37	12.50	12.55	59.08
BK_KBMTT	8.69	8.88	9.14	27.42
BK_CsBMTT	8.08	8.24	8.25	30.96
BK_3NT	7.71	7.92	8.05	22.36
BK_CsATzO	9.20/18.09	9.30/18.30	9.3/18.87	55.04
BK_BNGT	6.67	6.80	6.83	27.31
BK_DNQ	5.27	5.39	5.23	26.77

*all values are mean values of 3-5 measurements; [a] I_{NIR} = 700-1000 nm;

[b] I_1 = 600-900 nm; [c] I_2 = 695-1050 nm; $\chi = I_{NIR}/I_{vis}$; 10g / 20g batch

NIR pyrotechnics produce purple flames because of the formation of excited potassium and cesium ions. However the interesting emission is not visible with the human eye. Therefore several flares were tested outside with a night vision device. The first photo series illustrates the illumination close to the flame (Figure 38). The area next to the flare is considerably more illuminated compared to the area with extinct flame. The second photo series features the different view with and without NIR device (Figure 39). After a few seconds the IR output reaches his maximum. Because of the overexposure of the camera by filming the flame directly the desired effect is only slightly visible. Because NIR flares fulfill their work in high altitudes these pictures give only an impression of the influence of the NIR emission at ground level and less dihedral angle. Nevertheless, in combination with their calculated intensities they are still more informative then just the visible purple flame.

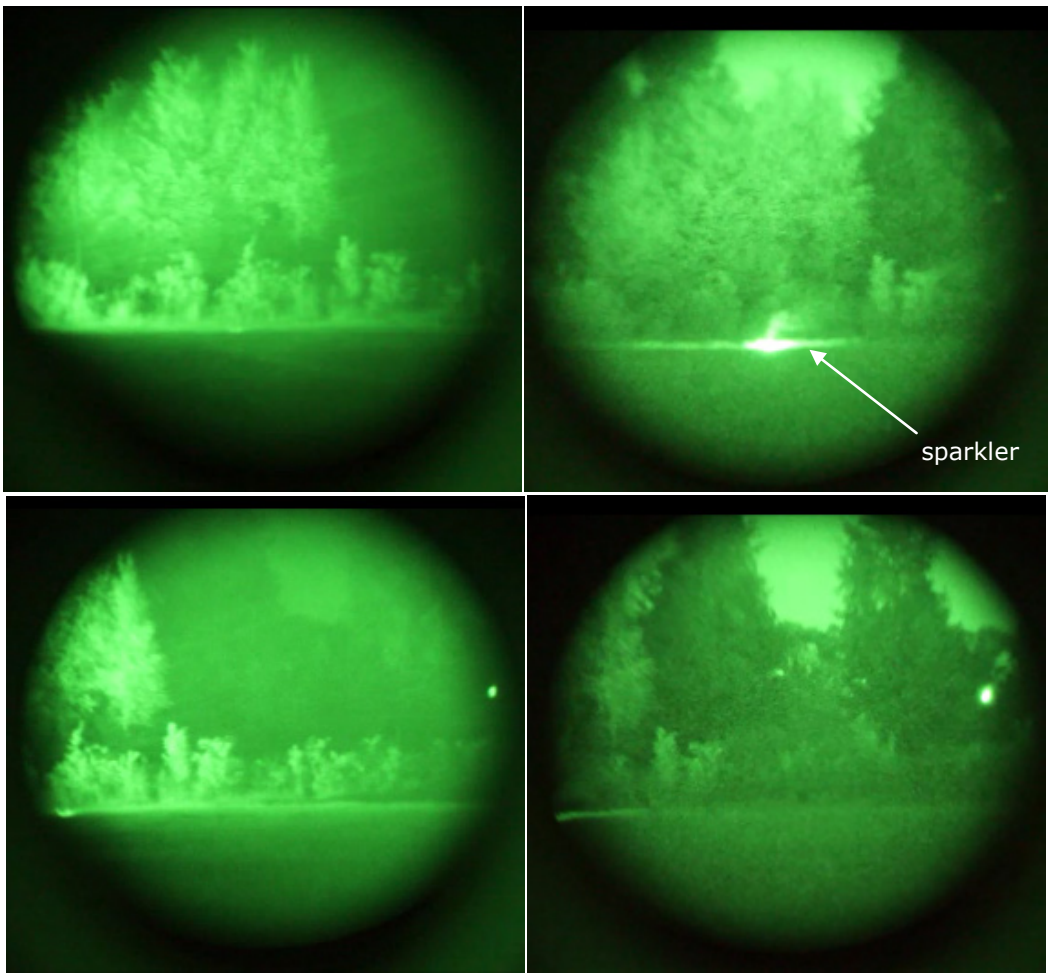

Figure 38 Outdoor NIR experiments with burning pellet (first column, left) and extinguished pellet (second column, right).

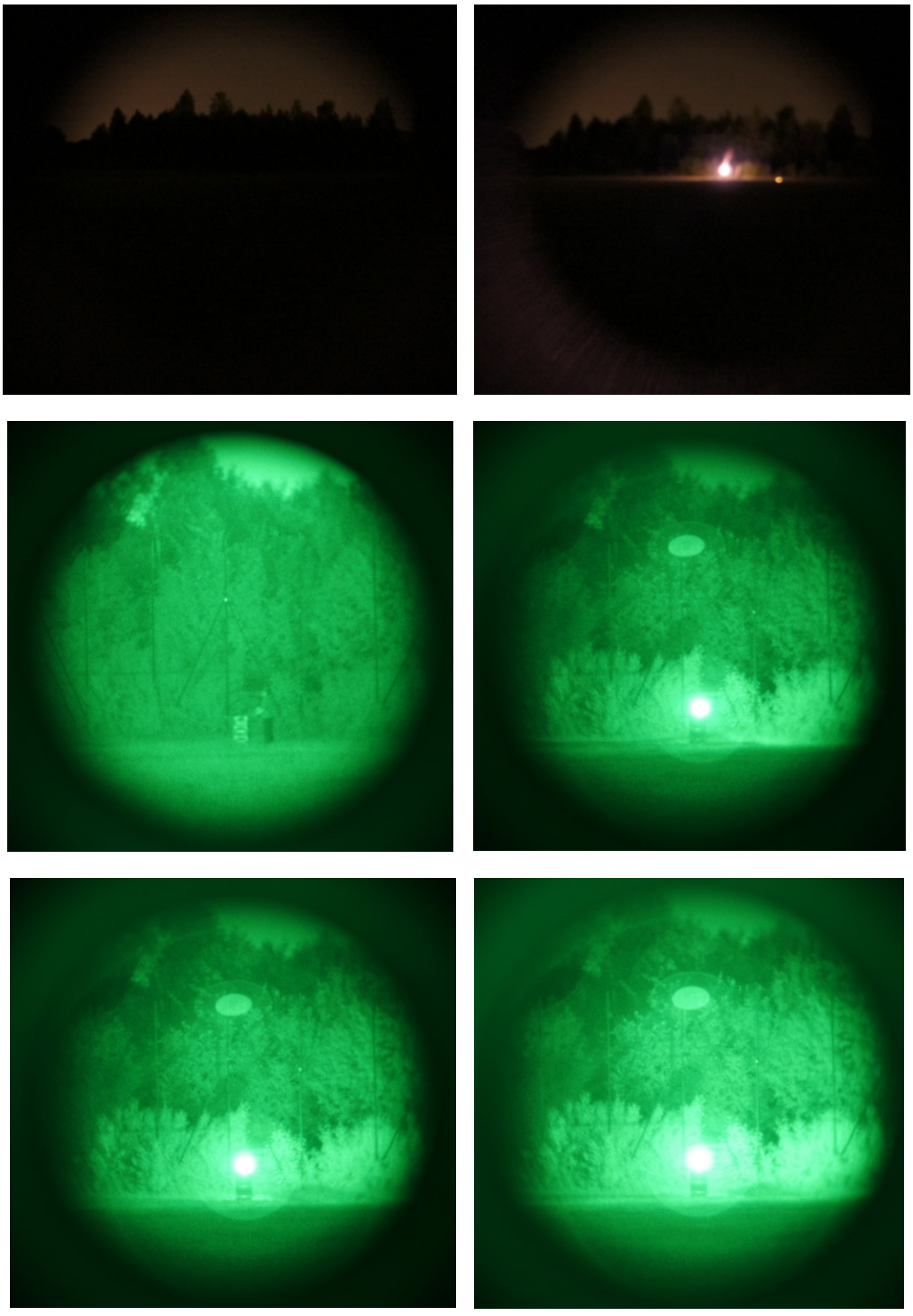

Figure 39 Outdoor NIR experiments (with and without NVD).

Conclusion

Several energetic materials like potassium and cesium 3,5-dinitro-1,2,4-triazolate or 3-nitro-1,2,4-triazol-5-(4*H*)-one were successfully synthesized. Selected salts were investigated as possible additives in near infrared pyrotechnic formulations, so called *Black Knight* compositions. Before executing radiometric measurements, all formulations were tested due to their sensitivity and combustion behavior. Exclusively all formulations are insensitive against friction and electric discharge and only few are moderate or less sensitive against impact e. g. BK_RDX or BK_CsAzOT. Additionally, thermodynamic calculations using the ICT code were performed to compare parameters like the oxygen balance or combustion products of the new formulations with the standard *Black Knight* composition. Because the main intention of this thesis was the establishment of a new set up for radiometric measurements investigations of possible influences on the burning behavior or burn rate and trends in combination with e. g. the oxygen balance were not observed. However, this work is now on progress.

The set up of the new OCEAN OPTICS spectrometer was successfully established in our research group. 46 new formulations were tested due to their radiant intensity and burning behavior and compared mainly with reference formulations containing either potassium or a combination of potassium and cesium nitrate as oxidizer. The results of the measurements showing the same scale as for flares stated in literature therefore their maximum intensities are comparable.

Most of the new tested formulations show similar or lower maximum intensity values as both references. Several additional tests might be carried out with DNT2, BTA1, BT2, TNBI5 or BOX1 which shows good burning behaviors and acceptable IR output.

Experimental Section

Equipment

Caution! *Although no problems occurred during the synthesis and handling of the materials studied in this work, some of the neutral compounds and their salts are sensitive energetic materials. Safety equipment such as Kevlar® gloves, leather coat, wrist protection, face shield, ear protection, grounded equipment, and shoes are mandatory.*

General Method. All chemicals and solvents were used as received (Sigma–Aldrich, Fluka, Acros Organics) unless stated otherwise. MELTING POINTS were measured with a Linseis PT10 DSC, calibrated with standard pure zinc and indium. Measurements were performed at a heating rate of 5°C min^{-1} in a closed aluminum sample pan with a 1 µm hole on top for gas release and under a nitrogen flow of 20 mL min^{-1} with an empty identical aluminum sample pan as reference. The values were checked by a Büchi Melting Point B-450 apparatus. The M. p. values are not corrected. MASS SPECTROMETRY was conducted on a JEOL MStation JMS 700 machine. All NMR SPECTRA were recorded with a Jeol Eclipse 270, Jeol EX 400, or a Jeol Eclipse 400 instrument. The chemical shifts are quoted in ppm relative to TMS (^{1}H, ^{13}C), and $MeNO_2$ (^{14}N, ^{15}N). For NMR signals the common abbreviations were used: s (singlet), d (duplet), t (triplet), q (quartet), and m (multiplet). INFRARED (IR) SPECTRA were recorded with a Perkin–Elmer Spektrum One *FT-IR Spectrum BXII* with *Smith ATR Dura Sample IRII* instrument. The absorption is given in wave numbers (cm^{-1}) with a range of 100–4000 cm^{-1}. Transmittance values are qualitatively described as very strong (vs), strong (s), medium (m), weak (w), and very weak (wv). RAMAN SPECTRA were measured with a Bruker MULTIRAM 1064 2000R NIR FT-Raman instrument equipped with a Nd:YAG laser (1064 nm). The intensities are given in percentages of the most intense peak and are given in parenthesis. ELEMENTAL ANALYSES (C, H, N, I) were performed with a Vario El and Netsch STA 429 Simultaneous Thermal Analyzer. SENSITIVITY DATA were determined using a BAM drop hammer, BAM Friction tester, and an OZM electrical discharge testing device.[52,53]

Potassium and cesium salts were synthesized using p. a. alkaline bases (KOH and CsOH) or their carbonates (K_2CO_3, $KHCO_3$ and Cs_2CO_3), respectively. Typically CsOH was used as a 50 w% solution (5.74 mol L^{-1}) and KOH pellets of 99.95% purity. The salts were obtained depending on their solubility from acetone, ethanol or water.

For crystallographic data the molecular structure in the crystalline state were determined using an Oxford Xcalibur3 diffractometer with a Spellman generator (voltage 50 kV, current 40 mA) and a KappaCCD detector. The data collection was performed using the CrysAlis CCD software,[60] the data reduction with the CrysAlis RED software.[61] The structures were solved with SIR-92,[62] and SHELXS-97,[63] refined with SHELXL-97[64] and finally checked using the PLATON software.[65] In all structures, the hydrogen atoms were located and refined. The absorptions were corrected by a SCALE3 ABSPACK multi-scan method.[66]

All relevant data and parameters of the X-ray measurements and refinements are given in Table 50. Thermal ellipsoids in figures of crystal structures were drawn to 50% probability.

[60] CrysAlis CCD, Oxford Diffraction Ltd., Version 1.171.27p5 beta (release 01-04-2005 CrysAlis171 .NET) (compiled April 1 **2005**, 17: 53: 34).
[61] CrysAlis CCD, Oxford Diffraction Ltd., Version 1.171.27p5 beta (release 01-04-2005 CrysAlis171 .NET) (compiled April 1 **2005**, 17: 53: 34).
[62] A. Altomare, G. Cascarano, C. Giacovazzo, A. Guagliardi, A Program for Crystal Structure Solution, SIR-92, *J. Appl. Cryst.* **1993**, *26*, 343.
[63] G. M. Sheldrick, Program for Crystal Structure Solution, SHELXS-97, University Gottingen, **1997**.
[64] G. M. Sheldrick, Program for the Refinement of Crystal Structures, SHELXS-97, University of Göttingen, Germany, **1997**.
[65] A. L. Spek, A Multipurpose Crystallographic Tool, PLATON, Utrecht University, Utrecht, The Netherlands, **1999**.
[66] SCALE3 ABSPACK – An Oxford Diffraction program (1.0.4,gui:1.0.3) (C) **2005** Oxford Diffraction Ltd.

Synthesis

Synthesis of 3-nitro-1,2,4-triazole (1), potassium and cesium 3-nitro-1,2,4-triazolate (1a & 1b)

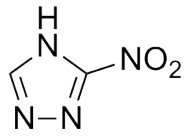

3-Amino-1,2,4-triazole (10.00 g, 119 mmol) was dissolved in 22 mL 37% HCl. The solution was added via a dropping funnel and under ice cooling within 45 min to a solution of sodium nitrite (23.00 g, 333 mmol) in 100 mL water. After one hour the ice bath was removed and the solution was stirred for a further hour at room temperature. Afterwards the mixture was heated to 55°C and stirred for 1.5 h and then cooled to r. t. The pH was adjusted from five to one with 4.60 mL 37% HCl. The excess of nitrite was removed by adding a solution of 7.00 g urea in 40 mL water. After 1 h stirring the solid was filtered off and washed with 4 x 30 mL ice water. The beige powder **1** was dried at 90°C over night. Yield: 10.30 g (75%) **M. p.** 212–214°C (Lit: 210–214°C), **EA** ($C_2H_2N_4O_2$, 114) found(calc.): C 21.02(21.06), H 1.67(1.77), N 49.20(49.12) %; **^{1}H NMR** (d_6 DMSO, 25°C): δ = 8.85, 7.92; **^{13}C NMR** (d_6 DMSO, 25°C): δ = 163.6, 146.7; **^{14}N NMR** (d_6 DMSO, 25°C): δ = -26; **IR** (ATR): $\tilde{\nu}$ = 3854 (w), 3746 (w), 3676 (w), 3650 (w), 3630 (w), 3162 (w), 3093 (w), 3025 (w), 2962 (w), 2849 (w), 2775 (w), 2700 (w), 2649 (w), 2361 (w), 2338 (w), 1772 (w), 1734 (s), 1379 (s), 1310 (s), 1269 (s), 1180 (m), 1107 (m), 1018 (m), 980 (s), 917 (m), 879 (m), 834 (s), 772 (w); **Raman** (200 mW): $\tilde{\nu}$ = 3162 (12), 2859 (5), 1578 (6), 1481 (19), 1425 (100), 1382 (858), 1312 (14), 1271 (12), 1177 (25), 1108 (13), 1020 (19), 983 (6), 835 (11), 774 (8), 535 (4), 449 (10), 278 (4), 246 (13).

4.00 g (35.1 mmol) of **1** were solved in 1.97 g (35.1 mmol) KOH in 20 mL water and stirred for 20 min at r. t. The cesium salt was obtained from 3.50 g (30.7 mmol) of **1** in 6.12 mL CsOH solution (50 w%) and 20 mL water. After the solvent was evaporated both salts could be recrystallized from EtOH/H_2O. Yield 4.82 g (90%) potassium salt (**1a**) and 7.77 g (90%) cesium salt (**1b**).

Potassium 3-nitro-1,2,4-triazolate (**1a**) **EA** ($C_2HKN_4O_2$, 152) found(calc.): C 16.16(15.79), H 0.85(0.66), N 37.97(36.82) %; **^{1}H NMR** (d_6 DMSO, 25°C): δ = 7.73; **^{13}C NMR** (d_6 DMSO, 25°C): δ = 166.4, 152.2; **^{14}N NMR** (d_6 DMSO, 25°C): δ = -18; **IR** (ATR): $\tilde{\nu}$ = 3366 (w), 3139 (m), 2649 (w), 1567 (s), 1549 (vs), 1490 (vs), 1417 (m), 1394 (vs), 1362 (vs), 1310 (m), 1290 (s), 1258 (m), 1170 (m), 1080 (m), 1060 (s), 982 (m), 960 (m), 903 (m), 837 (vs), 686 (m); **Raman** (200 mW): $\tilde{\nu}$ = 3126 (12), 1534 (10), 1492 (4), 1408 (7), 1393 (70), 1376 (2), 1364 (100), 1292 (10), 1259 (8), 1168 (54), 1080 (4), 1065

(48), 1022 (7), 984 (3), 903 (1), 842 (10), 771 (1), 542 (3), 280 (2), 249 (2); **Sensitivity data**: IS 40 J, FS 288 N, ESD 0.5 J; grain size: 100-200 µm.

Cesium 3-nitro-1,2,4-triazolate monohydrate (**1b**) **EA** ($C_2H_3CsN_4O_3$, 263.9) found(calc.): C 9.06(9.10), H 1.04(1.15), N 21.21(21.22) %; **^{1}H NMR** (d_6 DMSO, 25°C): δ = 7.74; **^{13}C NMR** (d_6 DMSO, 25°C): δ = 162.6, 152.2; **^{14}N NMR** (d_6 DMSO, 25°C): δ = -18; **IR** (ATR): $\tilde{\nu}$ = 3369 (vs), 3140 (vs), 1668 (m), 1521 (vs), 1480 (vs), 1394 (vs), 1356 (vs), 1293 (m), 1259 (m), 1163 (m), 1073 (s), 984 (m), 890 (m), 836 (s); **Raman** (200 mW): $\tilde{\nu}$ = 3121 (15), 1529 (7), 1471 (3), 1390 (63), 1357 (100), 1291 (5), 1260 (7), 1162 (49), 1070 (64), 1026 (8), 986 (3), 834 (4), 765 (2), 541 (1), 250 (4); **Sensitivity data**: IS 40 J, FS 240 N, ESD 0.4 J; grain size: 100–200 µm.

Synthesis of potassium and cesium 3,5-dinitro-1,2,4-triazolate (DNT) (2a & 2b)

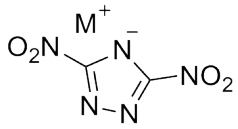

4.95 g (0.05 mol) 3,5-diaminotriazole was dissolved in 115 mL 1 M sulfuric acid and 35 mL water. The solution was slowly added within 1 h to an ice/salt cooled solution of 34.50 g (0.5 mol) sodium nitrite in 150 mL water. Afterwards the suspension was stirred for 1 h at 0°C and a further hour at r. t. The suspension was heated to 65°C and kept at this temperature until it became a clear red solution. It was cooled again with an ice/salt bath and 60 mL 30% sulfuric acid was added. After 15 min a solution of 6 g urea in 30 mL water was added and the red mixture was stirred for 1 h at r. t. and then extracted with 12 x 100 mL diethyl ether. The solvent was removed to a total volume of 4-5 mL and a small excess (0.055) of KOH in ethanol (0.5 M) or 2 M KOH was added. The orange solid was filtered off and washed with ice water. The cesium salt was obtained by adjusting the pH to 6–7 with a small excess of CsOH (0.1 M) or Cs_2CO_3. The alkaline salts precipitated after a few hours. Yield: 4.9 g (50%) potassium salt, 7.3 (50%) cesium salt.

Potassium DNT dihydrate (**2a**) **EA** ($C_2KN_5O_4 \cdot 2\ H_2O$, 197.15) found(calc.): C 10.08(10.30), H 1.38(1.73), N 29.61(30.03) %; **^{1}H NMR** (d_6 DMSO, 25°C): δ = 3.39 (H_2O); **^{13}C NMR** (d_6 DMSO, 25°C): δ = 163.4; **^{14}N NMR** (d_6 DMSO, 25°C): δ = -21; **IR** (ATR): $\tilde{\nu}$ = 3603 (s), 3415 (vs), 2361 (w), 1642 (m), 1535 (vs), 1492 (vs), 1390 (vs), 1355 (vs), 1301 (vs), 1111 (m), 1050 (m), 845 (s); **Raman** (200 mW): $\tilde{\nu}$ = 1543 (5), 1494 (2), 1404 (90), 1394 (3), 1358 (15), 1309 (3), 1113 (100), 1031 (2), 834 (8), 768 (3), 298 (2); **Sensitivity data**: IS 40 J, FS 144 N, ESD 0.30 J; grain size: 100-200 µm.

Cesium DNT monohydrate (**2b**) **EA** ($C_2CsN_5O_4$, 290.90) found(calc.): C 7.75(7.77), H 0.22(0.65), N 22.55(22.67) %; **^{1}H NMR** (d_6 DMSO, 25°C): δ = 3.37 (H_2O); **^{13}C NMR** (d_6 DMSO, 25°C): δ = 163.3; **^{14}N NMR** (d_6 DMSO, 25°C): δ = -25; **IR** (ATR): $\tilde{\nu}$ = 3358 (vs), 2358 (w), 1547 (s), 1489 (vs), 1384 (vs), 1351 (vs), 1294 (vs), 1097 (m), 1047 (m), 844 (s), 829 (s); **Raman** (200 mW): $\tilde{\nu}$ = 3610 (1), 1524 (2), 1495 (4), 1427 (5), 1397 (100), 1353 (16), 1306 (4), 1096 (79), 1015 (4), 832 (5), 768 (3), 517 (2), 312 (3); **DSC** (5°C min^{-1}): T = 208°C (M. p.), 368°C (dec.); **Sensitivity data**: IS 40 J, FS 144 N ESD 0.15 J; grain size: 100–200 µm.

Synthesis of potassium and cesium 3,3'-bis(1,2,4-oxadiazol-5-dion) (BOX) (5a & 5b)[27]

Synthesis of diaminoglyoxime (3)

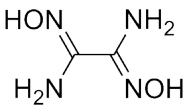

To a solution of 140 g (3.50 mol) sodium hydroxide in 400 mL ice water was added slowly under ice cooling 250 g (3.60 mol) hydroxylamine hydrochloride. The solution was treated with 46.40 g (0.80 mol, 92 mL) glyoxal (40% solution in water), stirred for 10 min at 0°C and then refluxed for 12 h. The yellow mixture was kept in a fridge for 36 h to crystallize. The beige solid was filtered off and dried under high vacuum. Yield: 52.25 g (56%) of diaminoglyoxime (**3**). **^{1}H NMR** (d_6 DMSO, 25°C): δ = 5.14, 9.75; **^{13}C NMR** (d_6 DMSO, 25°C): δ = 145.8; **IR** (ATR): $\tilde{\nu}$ = 3463 (vs), 3363 (vs), 2803 (m), 1637 (s), 1601 (m), 1571 (m), 1441 (m), 1418 (m), 1296 (w), 1111 (w), 935 (m), 736 (w), 714 (w).

Synthesis of oxamiddioxim dicarboxylic acid diphenylester (4)

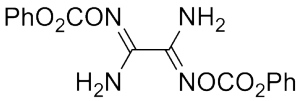

To a solution of **3** (10.00 g, 84.7 mmol) in 250 mL THF was added 27.40 g (175 mmol, 22.1 mL) phenyl chloroformate in 25 mL THF. Under ice cooling was added slowly via a dropping funnel 20.00 g (197.6 mmol, 27.4 mL) triethylamine. The solution was stirred for 4 h at r. t. and the solid (triethylammoniumchloride) was filtered off and washed with 3 x 40 mL THF. The filtrate was treated with 500 mL water and **4** precipitated as a colorless solid which was washed with 4 x 30 mL diethyl ether and dried under high vacuum. Yield: 25.59 g (89%). **^{1}H NMR** (d_6 DMSO, 25°C): δ = 7.05, 7.28, 7.29, 7.48; **^{13}C NMR** (d_6 DMSO, 25°C): δ = 115.4, 121.4, 126.5, 126.7, 129.5, 129.9, 130.0, 150.8, 151.3, 151.9.

Synthesis of 3,3'-bis(1,2,4-oxadiazol-5-one) (5) (BOX)

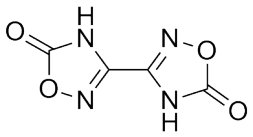

26.60 g (74.2 mmol) of **4** was added to 300 mL of a 5% sodium hydroxide solution. The suspension was refluxed over night. A color change from yellow to green to dark red was observed. After cooling to r. t. a black solution was obtained. The product **5** precipitated after adding 100 mL of 6 M HCl under ice cooling. The solution was stirred for further 5 h; afterwards the brown solid filtered off and washed with 3 x 40 mL 2 M HCl and 4 x 30 mL water. Yield 7.55 g (60%). **EA** ($C_4H_2N_4O_4$, 170.0) found(calc.): C 27.89(28.25), H 1.04(1.19), N 32.77(32.94) %; **^{1}H NMR** (d_6 DMSO, 25°C): δ = 11.15; **^{13}C NMR** (d_6 DMSO, 25°C): δ = 148.2, 168.6; **Raman** (200 mW): $\tilde{\nu}$ = 1840 (9), 1757 (16), 1687 (5), 1635 (100), 1574 (10), 1539 (4), 1323 (13), 1239 (13), 1040 (6), 1029 (5), 970 (51), 927 (15), 766 (16), 759 (18), 695 (4), 596 (9), 393 (13), 328 (10), 328 (10),213 (13), 161 (16); **MS**: m/z (DEI$^+$): 170 [M], 112 (59), 70 (28), 44 (37), 41 (14).

Synthesis of potassium and cesium BOX (5a & 5b)

4.73 g (27.8 mmol) of **5** was solved in 0.16 g KOH (55.6 mmol) and 10 mL water, or 5.70 g (33.5 mmol) of **5** was solved in CsOH (50 wt%, 0.585 mL, 67 mmol) and 10 mL water, respectively. After the water was evaporated both salts were recrystallized from EtOH/water and dried under HV.

Potassium BOX (**5a**) **EA** ($C_4K_2N_4O_4$, 246.26) found(calc.): C 19.33(19.51), H 0.0(0.0), N 22.67(22.75) %; **^{13}C NMR** (d_6 DMSO, 25°C): δ = 141.1, 160.3; **Raman** (200 mW): $\tilde{\nu}$ = 1779 (3), 1611 (48), 1572 (100), 1552 (2), 1517 (7), 1498 (1), 1401 (1), 1256 (2), 1210 (9), 1076 (2), 953 (9), 936 (35), 906 (10), 877 (1), 778 (19), 752 (2), 728 (1), 606 (4), 408 (7), 342 (4), 249 (3); **IR** (ATR): $\tilde{\nu}$ = 2322 (w), 2218 (w), 1660 (vs), 1465 (m), 1281 (s), 1213 (m), 956 (w), 931 (m), 867 (m), 781 (m) 733 (w); **DSC** (5°C min^{-1}): no phase transition, M. p. or T_{dec}; **Sensitivity data**: IS 40 J, FS 360 N, ESD 1 J; grain size: 100–200 µm.

Cesium BOX (**5b**) **EA** ($C_4Cs_2N_4O_4$, 433.88) found(calc.): C 11.05(11.07), H 0.0(0.0), N 12.88(12.91) %; **^{13}C NMR** (d_6 DMSO, 25°C, ppm): δ = 140.3, 158.2; **Raman** (200 mW): $\tilde{\nu}$ = 1673 (2), 1563 (100), 1501 (8), 1471 (3), 1199 (19), 1072 (3), 923 (17), 878 (10), 771 (19), 748 (3), 600 (5), 405 (14), 334 (10), 248 (4); **IR** (ATR): $\tilde{\nu}$ = 2280 (w), 2198 (vw), 1655 (vs), 1456 (m), 1278 (m), 1194 (m), 967 (w), 920 (m), 844 (m), 782 (m), 756 (w); **DSC** (5°C min^{-1}): T = 386°C (dec.); **Sensitivity data**: IS 40 J, FS 360 N, ESD 1 J; grain size: 100–200 µm.

Synthesis of potassium and cesium 3-nitro-1,2,4-triazol-5(4*H*)-one (NTO) (7a & 7b)

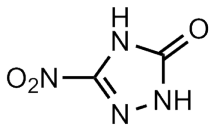

115 mL (423 mmol) 85% acetic acid was heated to 70°C and semicarbazide (112 g, 1 mol) was added. The reaction mixture was refluxed at 110°C for 7 h and afterwards the solvent was evaporated. The solid was treated with 200 mL water which was again evaporated. The procedure was repeated two more times. The damp crude product was recrystallized from 120 mL boiling water, then filtered off and washed with water, ethanol, diethyl ether and dried under high vacuum. Yield: 51.9 g (61%) of 1*H*-1,2,4-triazol-5(4*H*)-one (**TO**) (**6**).
EA ($C_2H_2N_3O$, 85.06) found(calc.): C 28.29(28.24), H 3.39(3.55), N 49.17(49.40) %.
Under ice cooling 6.00 g (71 mmol) of **6** was added slowly to a solution of 8.67 mL (274 mmol) 100% nitric acid and 2 mL water. After 2 h the cooling was removed and the

mixture was stirred at r. t. over night. The solid was filtered off, washed with a small amount of ice water, ethanol and diethyl ether and dried under high vacuum. Yield: 2 g (23%) **NTO** (**7**) as colorless crystals.

1.00 g (7.7 mmol) of **7** was solved in 10 mL ethanol and 0.43 g (7.7 mmol KOH or 1.02 mL) CsOH solution (50 wt%), respectively. After 20 min the salts precipitated and after isolation recrystallized from ethanol/water. Yield: 1.23 g potassium NTO dihydrate (**7a**) and 1.66 g cesium NTO monohydrate (**7b**) as yellow crystals.

Potassium NTO dihydrate (**7a**) **EA** ($C_2H_5KN_3O_5$, 204.18) found(calc.): C 11.88(11.76), H 1.83(2.27), N 27.47(27.44) %; **M. p.** 172°C, **DSC** (5°C min^{-1}): T = 248°C (dec.); **^{1}H NMR** (d_6 DMSO, 25°C): δ = 11.45, 3.41; **^{13}C NMR** (d_6 DMSO, 25°C): δ = 165.4, 160.6; **Raman** (200 mW): $\tilde{\nu}$ = 1538 (3), 1494 (6), 1376 (100), 1303 (7), 1111 (31), 1049 (18), 1017 (6), 846 (1), 783 (2), 484 (2); **IR** (ATR): $\tilde{\nu}$ = 3342 (m), 3239 (m), 3095 (w), 2995 (w), 2785 (w), 2489 (w), 2422 (w), 2271 (w), 1696 (m), 1587 (s), 1540 (w), 1500 (vs), 1412 (m), 1377 (m), 1309 (m), 1115 (m), 1045 (s), 1011 (m), 847 (m), 809 (m), 774 (vs), 744 (s), 719 (m), 671 (m); **MS** (FAB^- m/z): 129.00 (100), 130.01 (3); **Sensitivity data**: IS 40 J, FS 360 N, ESD 0.3 J; grain size: 100–200 µm.

Cesium NTO monohydrate (**7b**) **EA** ($C_2H_3CsN_3O_4$, 261.96) found(calc.): C 8.40(8.58), H 1.05(1.08), N 19.46(20.01) %; **DSC** (5°C min^{-1}): T = 250.9°C (dec.); **^{1}H NMR** (d_6 DMSO, 25°C): δ = 11.27, 3.39; **^{13}C NMR** (d_6 DMSO, 25°C): δ = 165.3 (s, 1 C, C=O), 160.6 (s, 1 C, C-NO_2); **Raman** (200 mW): $\tilde{\nu}$ = 1550 (4), 1495 (7), 1377 (100), 1302 (3), 1268 (2), 1101 (24), 1044 (20), 1010 (7), 843 (1), 783 (2), 488 (2), 263 (1); **IR** (ATR): $\tilde{\nu}$ = 3349 (s), 3244 (m), 3094 (m), 2999 (m), 2796 (m), 2498 (w), 2433 (w), 2280 (w), 1675 (m), 1591 (s), 1504 (vs), 1413 (m), 1375 (m), 1309 (m), 1040 (m), 1004 (m), 818 (m), 769 (s), 740 (s) 668 (m); **MS** (FAB^- m/z): 129.00 (100), 130.01 (3); **Sensitivity data**: IS 40 J, FS 360 N, ESD 0.3 J; grain size: 100–200 µm.

Synthesis of potassium and cesium bis(1-methyl-tetrazole-5-yl)-triazenate (8a & 8b)

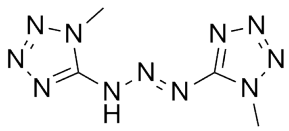

1-Methyl-5-aminotetrazole (9.91 g, 100 mmol) was solved in 50 mL water and stirred under ice cooling. 37% HCl (4.80 mL) was added until a clear solution was obtained. Within 1 h a solution of sodium nitrite (3.50 g, 5.50 mmol) in 20 mL water was added with a dropping funnel and the mixture was stirred for 24 h at 0°C. The solid was filtered off and washed with 4 x 20 mL ice water. Yield: 3.36 g (32 %) of **8** · H_2O (colorless powder).
1.60 g of **8** · H_2O was solved in 10 mL ethanol and two equivalents of KOH (0.79 g, 14.1 mmol) or CsOH solution (50 w%, 1.86 mL, 14.1 mmol) were added. After 30 min both salts precipitated, were filtered off and washed with cold EtOH and Et_2O. Yield: 1.9 g of the potassium salt (**8a**) and 2.3 g of the cesium salt (**8b**) (yellow powder).

Potassium bis(1-methyl-tetrazol-5-yl)-triazene (**8a**) **EA** ($C_4H_6KN_{11}$, 247.26) found(calc.): C 18.29(19.43), H 2.38(2.45), N 57.70(62.31) %; **^{1}H NMR** (d_6 DMSO, 25°C): δ = 3.87, 3.34 (H_2O); **^{13}C NMR** (d_6 DMSO, 25°C): δ = 162.0, 33.2; **Raman** (200 mW): $\tilde{\nu}$ = 3016 (2), 2962 (8), 1538 (100), 1465 (12), 1398 (3), 1339 (24), 1285 (8), 1270 (2), 1206 (10), 1119 (16), 1007 (3), 952 (2), 707 (5), 497 (10), 404 (4), 351 (1), 268 (4), 230 (7); **IR** (ATR): $\tilde{\nu}$ = 3420 (m), 2322 (m), 2299 (m), 1512 (s), 1477 (m), 1307 (vs), 1194 (m), 1096 (m), 1013 (m), 751 (m), 705 (m); **Sensitivity data**: IS 35 J, FS 360 N, ESD 30 mJ; grain size: 100–200 µm.

Cesium bis(1-methyl-tetrazol-5-yl)-triazene (**8b**) **EA** ($C_4H_8CsN_{11}O$, 359.08) found(calc.): C 13.35(13.38), H 2.11(2.25), N 42.88(42.91) %; **^{1}H NMR** (d_6 DMSO, 25°C): δ = 3.84, 3.33 (H_2O); **^{13}C NMR** (d_6 DMSO, 25°C): δ = 161.9, 33.1; **Raman** (200 mW): $\tilde{\nu}$ = 2956 (4), 1534 (100), 1463 (8), 1412 (6), 1331 (25), 1281 (8), 1200 (23), 1124 (19), 1010 (3), 948 (3), 702 (3), 497 (12), 405 (4), 218 (3); **IR** (ATR): $\tilde{\nu}$ = 3378 (m), 2300 (w), 2266 (w), 1653 (m), 1500 (s), 1473 (m), 1461 (m), 1440 (m), 1261 (vs), 1195 (vs), 1037 (m), 803 (m), 753 (m), 699 (m); **Sensitivity data**: IS 35 J, FS 288 N, ESD 30 mJ; grain size: 100–200 µm.

Synthesis of triaminoguanidinium hydrochloride (TAG-HCl) (9)

Aminoguanidinium bicarbonate (136.11 g, 1.0 mol) was added slowly to 500 mL 2 M HCl until no more CO_2 release was observed. The mixture was stirred for 1 h at r. t. The solvent was removed *in vacuo* and the crude product (aminoguanidinium hydrochloride (AG-HCl)) was recrystallized from 200 mL EtOH and 30 mL water. AG-HCl was filtered off, dried under high vacuum, and added to 500 mL dioxane in a two neck SCHLENK flask. 108 mL (2.2 mol) hydrazine monohydrate solution was added and the mixture was stirred for 6 h at 90°C. Nitrogen was bubbled to the solution and ammonia release (pH paper) indicated the end of the reaction. The solvent was removed and the precipitate recrystallized from 200 mL ethanol and 250 mL water. Yield: 95.6 g (68%) **9** as a colorless powder. **EA** (CH_9ClN_6, 140.5) found(calc.): C 8.46(8.48), H 6.42(7.12), N 59.57(59.36) %; **^{1}H NMR** (d_6 DMSO, 25°C): δ = 8.60, 4.52; **^{13}C NMR** (d_6 DMSO, 25°C): δ = 160.3.

Synthesis of 3,6-bis(3,5-dimethylpyrazol-1-yl)-1,2-dihydo-1,2,4,5-tetrazine (10)

10.42 g (74.2 mmol) of **9** was solved in 80 mL water. Within 1 h 16 mL acetyl acetone (155 mmol) was added and the suspension stirred for 1 h at r. t. The yellow solution was heated to 75°C and stirred for 5 h whereas **10** precipitated. After cooling to r. t. the solid was filtered off and washed with a large amount of cold water. Yield: 13.34 g (66%) of a light yellow powder. **^{1}H NMR** ($CDCl_3$, 25°C): δ = 2.20, 2.46, 5.94, 8.03; **^{13}C NMR** ($CDCl_3$, 25 °C): δ = 13.6, 13.9, 110.0, 142.5, 145.8, 150.1.

Oxidation of 10 to 3,6-bis(3,5-dimethylpyrazol-1-yl)-1,2,4,5-tetrazine (11)

13 g (48 mmol) of **10** was added to 50 mL *N*-methyl-2-pyrrolidone (NMP). The suspension was stirred for 30 min under ice/salt cooling. Afterwards 3.2 mL (100 mmol) liquid NO_2 was added slowly and the red suspension stirred for 2 h at r. t. To remove the excess of NO_2 nitrogen was bubbled through the mixture. The solid was filtered off and washed with water. Yield: 10.6 g (83%) of **11**. **EA** ($C_{12}H_{14}N_8$, 270) found(calc.): C 53.27(53.32), H 5.09(5.22), N 41.09(41.46) %; **^{1}H NMR** ($CDCl_3$, 25°C): δ = 2.34, 2.69, 5.99; **^{13}C NMR** ($CDCl_3$, 25°C): δ = 13.8, 14.5, 110.0, 142.4, 145.6, 149.9.

Synthesis of potassium 3,6-bis-nitroguanidyl-1,2,4,5-tetrazine (12a)

Potassium methoxide (2.10 g, 30 mmol) was solved in 50 mL methanol. Nitro guanidine (1.44 g, 13.8 mmol) was added and the mixture heated to 55°C. After the solution became clear (45 min), 1.80 g (6.67 mmol) of **11** was added slowly. After 10 min a dark red solid was obtained and the mixture was stirred for further 3 h at 55°C. After cooling to r. t. the solid was filtered off and washed with 4 x 30 mL methanol. The crude product was dried at 60°C over night and then recrystallized from 20 mL water. Yield 0.8 g (33%) of **12a** as a red powder.

Potassium 3,6-bis-nitroguanidyl-1,2,4,5-tetrazine (**12a**) **EA** ($C_4H_4K_2N_{12}O_4$, 362.35) found(calc.): C 13.28(13.26), H 1.85(1.11), N 45.21(46.39) %; **^{1}H NMR** (d_6 DMSO, 25°C): δ = 8.66; **^{13}C NMR** (d_6 DMSO, 25°C): δ = 163.3, 160.9; **Raman** (200 mW): $\tilde{\nu}$ = 2928 (10), 2915 (5), 1627 (6), 1598 (3), 1556 (2), 1474 (100), 1434 (4), 1416 (4), 1404 (2), 1395 (5), 1356 (13), 1345 (2), 1103 (36), 1049 (4), 953 (8), 869 (14), 757 (19), 666 (3), 609 (1), 602 (5), 585 (3), 440 (3); **IR** (ATR): $\tilde{\nu}$ = 3345 (vs), 3247 (vs), 2361 (m), 2338 (m), 1575 (s), 1450 (s), 1247 (s), 1247 (s), 1041 (m), 935 (w), 844 (vw), 778 (vw), 760 (vw), 726 (vw), 685 (vw); **Sensitivity data**: IS 40 J, FS 240 N, ESD 0.6 J; grain size: 100–200 µm.

Synthesis of 3,6-bis-nitroguanidyl-1,2,4,5-tetrazine (12)

The crude product **12a** (1.3 g, 3.6 mmol) was solved in 20 mL water and the pH adjusted to 1 with 6 M HCl. The mixture was stirred for 1 h at r. t., the solid filtered off and washed with 3 x 30 mL water. Yield: 0.76 g (74%) of **12** as a pink powder.

3,6-Bis-nitroguanidyl-1,2,4,5-tetrazine (**12**) **EA** ($C_4H_6N_{12}O_4$, 286.15) found(calc.): C 16.25(16.79), H 2.41(2.11), N 54.82(58.73) %; **^{1}H NMR** (d_6 DMSO, 25°C): δ = 11.63, 9.42, 8.75; **^{13}C NMR** (d_6 DMSO, 25°C): δ = 159.4, 157; **Raman** (200 mW): $\tilde{\nu}$ = 3215 (4), 1912 (6), 1622 (21), 1582 (9) 1503 (100), 1396 (3), 1302 (20), 1222 (22), 1112 (30), 1027 (10), 962 (86), 886 (40), 808 (2), 785 (28), 754 (5), 613 (29), 491 (3), 411 (15); **IR** (ATR): $\tilde{\nu}$ = 3361 (s), 3180 (s), 2360 (m), 2322 (m), 1620 (m), 1546 (s), 1333 (s), 1221 (vs), 1062 (w), 1026 (m), 937 (m); **MS** (DCI) m/z: 287 (M+H), 257 (M+H-NO); **Sensitivity data**: IS 8.5 J, FS 240 N, ESD 0.1 J; grain size: 100–200 µm.

Synthesis of cesium 3,6-bis-nitroguanidyl-1,2,4,5-tetrazine (12b)

12 (1 g, 3.5 mmol) was solved in acetone and 1.2 mL CsOH solution was added. The solvent was evaporated on air. Yield: 1.54 g (80%) of **12b**.

Cesium 3,6-bis-nitroguanidyl-1,2,4,5-tetrazine (**12b**) ($C_4H_4Cs_2N_{12}O_4$, 549.8): **^{1}H NMR** (d_6 DMSO, 25°C): δ = 9.22; **^{13}C NMR** (d_6 DMSO, 25°C): δ = 165.2, 157.7; **IR** (ATR): $\tilde{\nu}$ = 3364 (s), 3169 (s), 2355 (m), 2331 (m), 1609 (m), 1547 (m), 1334 (m), 1261 (m), 1049 (w), 948 (w); **Sensitivity data**: IS 40 J, FS 288 N, ESD 0.6 J; grain size: 100–200 µm.

Synthesis of 3,6-dihydrazino-1,2,4,5-tetrazine (13)

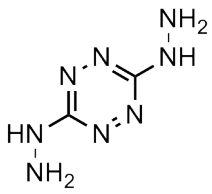

11 (2 g, 7.41 mmol) was added to 30 mL acetonitrile. Hydrazine monohydrate (0.8 mL, 16.3 mmol) was added slowly to the suspension and the mixture was stirred for 30 min at r. t. Afterwards the solution was refluxed for 4 h and the solid filtered off. Yield: 0.76 g of **13** (72%) as a dark red powder. **^{1}H NMR** (d_6 DMSO, 25°C): δ = 8.39, 4.38; **^{13}C NMR** (d_6 DMSO, 25°C): δ = 164.2; **MS** ($C_2H_6N_6$) (DEI) m/z: 142 (87), 57 (100), 43 (23), 31 (46).

Synthesis of 3,6-dichloro-1,2,4,5-tetrazine (14)

20 mL acetonitrile and 0.75 g (5.28 mmol) of **13** were added in a SCHLENK flask. *Via* a glas tube chlorine was bubbled through the mixture. The excess of chlorine was passed into a 2 M sodium hydroxide solution (in between 3 washing flasks). After 30 min a color change from red to orange occurred. The mixture was stirred for further 15 min and then chlorine was replaced by nitrogen for 20 min to get rid of the excess of chlorine. Afterwards the solution was concentrated but not dried at high vacuum to avoid sublimation of the product. Yield: 610 mg (76%) of **14** as an orange powder. **^{13}C NMR** ($CDCl_3$, 25°C): 168.0.

Synthesis of 3,6-diamino-1,2,4,5-tetrazine (16)

13.60 g (0.05 mol) of **11** was added to 50 mL NMP in a 250 mL autoclave. A stirring bar was added and the autoclave was closed with 10 N, and cooled with liquid nitrogen. After 20 min the container was evacuated. A flask with defined volume (2.746 L) was connected to the steel vacuum line and ammonia (3 x 0.1 mol) was passed into it. The ammonia was condensed into the autoclave and after 30 min cooling with liq. N_2 the autoclave was allowed to come to r. t., and then heated to 100°C in an oil bath for 10 h. The less excess of ammonia was released, the solution added to 150 mL isopropyl alcohol and cooled in a fridge over night. The precipitate was filtered off and washed with 4 x 30 mL cold isopropyl alcohol. Yield: 4.9 g (60%) of **16** as a red powder. **EA** ($C_2H_4N_6$, 112.09) found(calc.): C 21.72(21.43), N 74.50(74.97), H 3.54(3.60) %; **^{1}H NMR** (d_6 DMSO, 25°C): δ = 6.70, **^{13}C NMR** (d_6 DMSO, 25°C): δ = 162.3.

Synthesis of potassium and cesium 3-amino-6-nitrimino-1,2,4,5-tetrazine (17a & b)

Under ice-cooling 1 g (8.9 mmol) 3,6-diamino-1,2,4,5-tetrazine was added in small portions to 25 mL 60% nitric acid. After stirring for 2 h the ice bath was removed and the solution allowed coming to room temperature. The precipitate was washed with 3 x 30 mL ice water and dried on air. Yield: 1.05 g (75%) of an orange-red powder (**17**). EA ($C_2H_3N_7O_2$, 157.54) found(calc.): C 15.52(15.29), N 60.91(62.41), H 1.92(1.92) %; **^{1}H NMR** (d_6 DMSO, 25°C): δ = 8.45; **^{13}C NMR** (d_6 DMSO, 25°C): δ = 163.0.

1.00 g of **17** was treated with 10 mL acetone and 1.10 mL CsOH solution (50 w%) or 6.37 mL 1M KOH respectively were added. The water was evaporated and both salts were obtained in good yields. 1.40 g (77%) of **17a** and 1.10 g (88%) of **17b**.

Potassium 3-amino-6-nitrimino-1,2,4,5-tetrazine (**17a**) ($C_2H_2K_2N_7O_2$, 195.1), **^{1}H NMR** (d_6 DMSO, 25 °C): δ = 7.38; **^{13}C NMR** (d_6 DMSO, 25°C): δ = 164.3, 162.2; **^{14}N NMR** (d_6 DMSO, 25°C): δ = -13; **Raman** (200 mW): $\tilde{\nu}$ = 1574 (4), 1436 (100), 1400 (16), 1368 (58), 1335 (10), 1303 (16), 1043 (41), 961 (5), 891 (6), 853 (16), 806 (4), 754 (16), 653 (5), 394 (4), 363 (10); **IR** (ATR): $\tilde{\nu}$ = 3410 (m), 3326 (m), 1651 (m), 1574 (s), 1435 (s), 1375 (vs), 1335 (s), 1251 (m), 1053 (s), 1033 (m), 1040 (m), 959 (m), 849 (w), 805 (w), 757 (w), 752 (w), 670 (w); **Sensitivity data**: IS 23 J, FS 252 N, ESD 0.5 J; grain size: 500–1000 µm.

Cesium 3-amino-6-nitrimino-1,2,4,5-tetrazine (**17b**) **EA** ($C_2H_2Cs_2N_7O_2$, 288.9) **^{1}H NMR** (d_6 DMSO, 25°C): δ = 7.38; **^{13}C NMR** (d_6 DMSO, 25°C): δ = 164.0, 162.2; **^{14}N NMR** (d_6 DMSO, 25°C): δ = -13; **Raman** (200 mW): $\tilde{\nu}$ = 1537 (7), 1504 (15), 1427 (100), 1380 (31), 1336 (24), 1306 (23), 1027 (57), 959 (5), 896 (21), 862 (46), 803 (6), 769 (19), 737 (12), 669 (7), 590 (7), 490 (8), 423 (13), 390 (13); **IR** (ATR): $\tilde{\nu}$ = 3280 (m), 3123 (m), 1634 (m), 1514 (s), 1451 (s), 1370 (vs), 1331 (s), 1661 (s), 1025 (m), 957 (m), 861 (w), 813 (w), 767 (w), 742 (w), 670 (w); **Sensitivity data**: IS 2 J, FS 160 N, ESD 0.3 J; grain size: 500–1000 µm.

Synthesis of 2,4,5-trinitro-1*H*-imidazole (21)

Synthesis of 1,4-dinitroimidazole (18)

Glacial acetic acid (12 mL, 210 mmol) and acetic anhydride (9 mL, 95 mmol) were added under ice/salt cooling in a 50 mL flask. After 45 min 4.1 mL (98 mmol) 100% nitric acid was added slowly. The solution was stirred for 2 h and afterwards 5 g (44 mmol) 4-nitroimidazole was added in small portions. The reaction mixture was stirred for 48 h at r. t., then poured onto 40 mL ice water and stirred for further 30 min whereas **18** precipitated. The solid was filtered off, washed with 3 x 30 mL ice water and dried under HV. Yield: 3 g (43%) of **18** as a colorless powder. **^{1}H NMR** (d_6 DMSO, 25°C): δ = 9.40, 8.97; **^{13}C NMR** (d_6 DMSO, 25°C): δ = 144.8, 133.2, 116.5.

Isomerization of 16 to 2,4-dinitroimidazole (18)

18 (7.8 g, 49.3 mmol) was added to 75 mL chloro benzene and the suspension stirred for 24 h at 115°C. After cooling to r. t. **19** precipitated, was filtered off and dried under high vacuum. The pure compound could not be isolated.

Synthesis of 2,4,5-trinitro-1*H*-imidazole (21) from 2,4,5-triiodo-1*H*-imidazole (20)

Synthesis of 2,4,5-triiodo-1*H*-imidazole (20)

20.32 g (0.08 mol) Iodine and 26.56 g (0.16 mol) potassium iodide were solved in 150 mL water. The solution was added slowly to a solution of 1.36 g (0.02 mol) 1*H*-imidazole in 200 mL (22.44 g) potassium hydroxide. The mixture was stirred for 24 h at r. t. and afterwards 25 mL 25% acetic acid was added to adjust the pH to 7. The yellow precipitate was filtered off, washed with water and recrystallized from a small amount of ethanol. After two days in the fridge the solid was filtered off. Yield: 1.20 g (13%) of **20** as brown crystals. The filtrate was added to 100 mL water and further precipitate was obtained which was solved in 100 mL 4 M KOH. To the mixture was added 12.70 g (0.05 mol) Iodine and 16.60 g (0.1 mol) KI and then the solution stirred for further 24 h at r. t. The pH was again adjusted to 7 with 50 mL 25% acetic acid. The precipitate was filtered off, washed with 100 mL water, was added to 150 mL 1 M sodium thiosulfate solution and stirred for 1 h at r. t. The solid was filtered off and washed with 3 x 50 mL water. Yield: 4.8 g (54%) of **20** (powder). **EA** ($C_3HI_3N_2$, 445.77) (crystals), found(calc.): C 8.08(8.08), H 0.21(0.23), N 6.37(6.28) %; **EA** (powder), found(calc.): C 7.88(8.08), H 0.17(0.23), N 6.18(6.28) I 85.97(85.41); **MS** (DEI) m/z: 446 (52) [M], 319 (25) [M-I], 253 (100) [I_2], 192 (6) [M-I_2], 127 (19) [I].

Synthesis of 2,4,5-trinitro-1*H*-imidazole (21) from 2,4,5 triiodo-1*H*-imidazole (20)

18 (2 g, 4.5 mmol) was added under ice cooling slowly to 2 mL (48 mmol) 100% HNO_3. The mixture was stirred for 1 h at 0°C and then heated to 80°C for 10 min. The solution was poured onto ice and neutralized with sodium bicarbonate. Afterwards a few drops of 100% HNO_3 were added and the solution extracted with 6 x 20 mL diethyl ether. The solvent was removed and a small amount of water was added to the oily residue. The pH was adjusted to 9 with potassium carbonate and saturated with potassium chloride. No precipitate was observed. **18** could not be isolated.

Synthesis of potassium and cesium 4,4′,5,5′-tetranitro-2,2′-bis-1*H*-imidazole (TNBI) (23a & 23b)

Synthesis of 2,2′-bis-1*H*-imidazole (22)

183 g (1.75 mol) sodium bisulfite was solved in 800 mL water and 500 mL ethanol. 128 g (0.88 mol) 40 w% glyoxal solution was added. The suspension was stirred for 1.5 h at r. t., the residue was filtered off and washed with a large amount of EtOH and Et_2O. The product was dried at 60°C for 1 h. Yield: 50.6 g of glyoxal bisodium bisulfite monohydrate. The solid was added to 1.4 L 25% ammonia and 50 g ammonium carbonate. The mixture was stirred for 4 h at 80 °C. A color change from clear to yellow to brown was observed. The solution was cooled to r. t. and the precipitate was filtered off, washed with 3 x 50 mL water and 3 x 50 mL acetone. Yield: 12 g (40% based on Glyoxal). **EA** ($C_6H_6N_4$, 134.14) found(calc.): C 53.50(53.72), H 4.16(4.51), N 41.54(41.77) %; **^{1}H NMR** (d_6 DMSO, 25°C): δ = 12.58, 7.13, 7.00; **^{13}C NMR** (d_6 DMSO, 25°C): δ = 139.8, 128.8, 117.9.

Synthesis of 4,4′,5,5′-tetranitro-2,2′-bis-1*H*-imidazole (23)

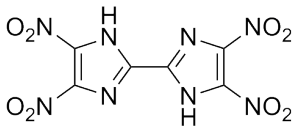

18 g (0.21 mol) sodium nitrate was solved under ice cooling in 30 mL 96% sulfuric acid. A catalytic amount of urea was added and thereupon 5 g (0.04 mol) of **22**. The solution was stirred for 30 min at 0°C, 1 h at r. t. and then heated to 85°C over night. The mixture was cooled to r. t. and poured onto ice. The solid was filtered off and washed with water (or 2 M HCl). **23** precipitated after a few hours, was then filtered off and washed with a small amount of ice water. The filtrate of **23** was extracted with diethyl ether, concentrated and an excess of potassium hydroxide in ethanol was added to obtain further product. Yield: 8 g (70%). **EA** ($C_6H_2N_8O_8 \cdot 2\ H_2O$, 314.13) found(calc.): C 21.08(20.58), N 32.22(32.00); H 1.40(1.73) %; **^{1}H NMR** (d_6 DMSO, 25°C): δ = 8.95; **^{13}C NMR** (d_6 DMSO, 25°C): δ = 135.2, 138.9, 139.6; **Raman** (200 mW): $\tilde{\nu}$ = 1626 (43), 1553 (50), 1531 (30), 1514 (17), 1481 (5) 1443 (3), 1373 (17), 1340 (19), 1303 (100), 1275 (20), 1115 (2), 1016 (16), 866 (7), 765 (2), 742 (2), 521 (1), 389 (2); **IR** (ATR): $\tilde{\nu}$ = 3361 (s), 3180 (s), 2360 (m), 2322 (m), 1620 (m), 1546 (s), 1333 (s), 1221 (vs), 1062 (w), 1026 (m), 937 (m); **Sensitivity data**: IS 40 J, FS 240 N, ESD 1.0 J; grain size: 100–200 µm.

2 g (6.4 mmol) of **23** in 50 mL water was treated with two equivalents of KOH, KOH in ethanol (0.5 M), CsOH (50 wt%), or Cs_2CO_3, respectively. The potassium salt was recrystallized from ethanol/water. The cesium salt was obtained as an orange powder. Yield: 1.6 g (65%, K), 2.9 g (80%, Cs).

Potassium TNBI (**23a**) **EA** ($C_6K_2N_8O_8$, 390.33): found(calc.): N 28.43(28.71), C 18.32(18.46) %, **DSC** (5°C min^{-1}): T = 312°C (dec.); **^{1}H NMR** (d_6 DMSO, 25°C): no signal; **^{13}C NMR** (d_6 DMSO, 25°C): δ = 144.9, 141.0; **^{14}N NMR** (d_6 DMSO, 25 °C): δ = -25; **Raman** (200 mW): $\tilde{\nu}$ = 1562 (100), 1538 (3), 1529 (8), 1494 (5), 1472 (28), 1390 (9), 1349 (16), 1307 (44), 1248 (93), 1021 (13), 870 (10), 769 (5), 759 (4), 396 (6); **IR** (ATR): $\tilde{\nu}$ = 1510 (m), 1489 (s), 1469 (vs), 1394 (s), 1367 (s), 1302 (s), 1230 (s), 1112 (m), 944 (m), 854 (m), 809 (s), 754 (m), 704 (m); **Sensitivity data**: IS 40 J, FS 360 N, ESD 1.0 J; grain size: 100–200 µm.

Cesium TNBI (**23b**) **EA** ($C_6Cs_2N_8O_8$, 577.93): found(calc.) C 12.81(12.47), N 19.09(19.39); **^{13}C NMR** (d_6 DMSO, 25°C, ppm): δ = 144.9, 141.0; **^{14}N NMR** (d_6 DMSO, 25°C, ppm): δ = -34; **IR** (ATR): $\tilde{\nu}$ = 1506 (m), 1488 (s), 1436 (m), 1379 (s), 1354 (m), 1307 (s), 1193 (vs), 1104 (w), 940 (m), 857 (m), 810 (s), 755 (m), 702 (m); **Sensitivity data**: IS 9 J, FS 192 N, ESD 0.1 J; grain size: 100–200 µm.

Synthesis of potassium and cesium 5,5´-azotetrazolate (24a & 24b)[67]

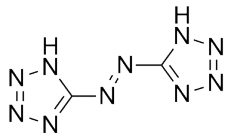

50 g (0.59 mol) 5-aminotetrazole was solved in 500 mL 10% potassium hydroxide or cesium hydroxide solution and over a period of 45 min 65 g (0.41 mol) potassium permanganate was added at 65°C. The solution was stirred for 2 h. Afterwards 400 mL ethanol was added and the solution refluxed for 15 minutes. The precipitate (MnO_2) was filtered off from the hot solution with a warm suction filter. The yellow solution was kept in the fridge over night. The solid was filtered off and washed with ethanol and diethyl ether. Yield: 44.91 g (55.7%)

Potassium 5,5´-azotetrazolate pentahydrate (**24a**) **EA** ($C_2H_{10}K_2N_{10}O_5$, 278.32) found(calc.): C 7.2(7.3), H 3.0(3.1), N 42.1(41.7) %; **^{13}C NMR** (d_6 DMSO, 25°C): δ = 172.0; **Raman** (200 mW): $\tilde{\nu}$ = 1500 (21), 1481 (44), 1411 (11), 1394 (50) 1374 (100), 1185 (2), 1155 (1), 1078 (13), 1059 (10), 1050 (16), 1037 (14), 922 (5), 348 (1); **IR** (ATR): $\tilde{\nu}$ = 3641 (m), 3260 (w), 2925 (m), 2850 (w), 2411 (m), 2356 (m), 2090 (m), 1965

[67] A. Hammerl, *European Journal of Inorganic Chemistry* **2002**, 834.

(w), 1673 (w), 1480 (w), 1447 (m), 1400 (m), 1182 (m), 1156 (m), 866 (m), 770 (m), 727 (m), 340 (w); **DSC** (5°C min^{-1}): T = 239°C (dec.); **Sensitivity data**: IS 50 J, FS 360 N, ESD 1.2 J; grain size: 100–200 µm.

Cesium 5,5´-azotetrazolate dihydrate (**24b**) **EA** ($C_2H_4Cs_2N_{10}O_2$, 465.93) found(calc.): C 5.2(5.3), H 0.9(1.2), N 30.1(29) %; **^{13}C NMR** (d_6 DMSO, 25°C): δ = 173.0; **Raman** (200 mW): $\tilde{\nu}$ = 1483 (44), 1464 (4), 1406 (12), 1371 (100), 1282 (2), 1072 (22), 1044 (25), 913 (5), 890 (2); **IR** (ATR): $\tilde{\nu}$ = 3641 (m), 3260 (w), 2925 (m), 2850 (w), 2411 (m), 2356 (m), 2090 (m), 1965 (w), 1673 (w), 1480 (w), 1447 (m), 1400 (m), 1182 (m), 1156 (m), 866 (m), 770 (m), 727 (m), 340 (w); **DSC** (5°C min^{-1}):T = 231°C (dec.); **Sensitivity data**: IS 1 J, FS 5 N, ESD 0.02 J; grain size: 100–200 µm.

Synthesis of potassium and cesium bistetrazolyl amine (25a & 25b)[68]

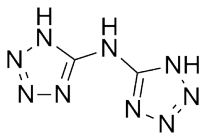

A 2 L three-neck reaction flask contained a refluxing suspension of sodium dicyanamide (44.5 g, 0.5 mol), sodium azide (65 g, 1.0 mol), ethanol (400 mL), and water (250 mL). 2 M HCl (750 mL) was added over the course of five hours. The reaction mixture was refluxed for 48 h. After cooling to 0°C in an ice bath and addition of conc. HCl (80 mL) **25** · H_2O was obtained as a fine colorless precipitate. The solid was filtered off and washed with small amounts of ethanol and diethyl ether and dried under vacuum. Yield: 75 g (88%). The product was recrystallized from HCl. **^{1}H NMR** (d_6 DMSO) δ = 11.92, 9.53; **^{13}C NMR** (d_6 DMSO) δ = 154.7; **DSC** (5°C min^{-1}) T = 250°C (dec.); **IR** (KBr): $\tilde{\nu}$ = 3456 (s), 3028 (s), 2932 (s), 2858 (s), 2671 (m), 2438 (m), 1796 (w), 1656 (vs), 1611 (s), 1556 (s), 1454 (m), 1352 (m), 1337 (m), 1282 (m), 1263 (m), 1154 (w), 1110 (m), 1072 (s), 1501 (s), 1036 (m), 1003 (m), 899 (m), 819 (m), 790 (m), 738 (m), 690 (m), 503 (m), 406 (w); **Raman** (200 mW): $\tilde{\nu}$ = 3328 (11), 3120 (8, br), 1649 (9), 1618 (34), 1552 (54), 1480 (22), 1455 (17), 1370 (17), 1346 (15), 1267 (25), 1226 (26), 1151 (15), 1128 (15), 1073 (100), 1039 (42), 838 (7), 794 (17), 736 (9), 670 (7), 421 (22), 409 (48), 381 (9), 348 (20), 321 (48), 172 (100), 147 (46).

25 · H_2O (10 g, 0.06 mol) was added to 150 mL water and the mixture was heated to 80°C. Potassium carbonate (8.28 g, 0.06 mol) was added and the solution stirred for 1 h. The solvent was evaporated and the solid recrystallized from water/ethanol. Yield: 90%.

[68] J. Weigand, *Journal of Material Chemistry* **2008**, *18*, 5248.

Potassium BTA (**25a**) **DSC** (5°C min^{-1}): T = 349°C (dec.); **^{1}H NMR** (d_6 DMSO): δ = 7.6; **^{13}C NMR** (d_6 DMSO): δ = 162; **Raman** (200 mW): $\tilde{\nu}$ = 1524 (57), 1420 (10), 1405 (6), 1305 (5), 1217 (66), 1114 (23), 1063 (10), 1051 (100), 1000 (10), 569 (5), 403 (14), 348 (14), 306 (16); **IR** (ATR): $\tilde{\nu}$ = 3395 (s), 3262 (s), 3036 (s), 2897 (m), 1684 (w), 1625 (m), 1509 (m), 1392 (w), 1303 (w), 1213 (w), 1154 (w), 1137 (w), 1110 (w), 1008 (w), 855 (w), 749 (w), 729 (w); **Sensitivity data**: IS 40 J, FS 288 N, ESD 1.5 J; grain size: 250 –500 µm.

25 · H_2O (10 g, 0.06 mol) was added to 150 mL water and the mixture was heated to 80°C. Cesium carbonate (19.44 g, 0.06 mol) was added and the solution stirred for 1 h. The solvent was evaporated and the solid recrystallized from water/ethanol. Yield: 90%.

Cesium BTA (**25b**) **DSC** (5°C min^{-1}): T = 274°C (dec.); **^{1}H NMR** (d_6 DMSO): δ = 7.4; **^{13}C NMR** (d_6 DMSO): δ = 162; **Raman** (200 mW): $\tilde{\nu}$ = 1521 (55), 1413 (10), 1400 (6), 1221 (22), 1212 (44), 1123 (21), 1113 (23), 1051 (100), 1006 (11), 400 (17), 345 (14), 306 (24); **IR** (ATR): $\tilde{\nu}$ = 3300 (s), 3246 (s), 2877 (w), 1591 (m), 1490 (m), 1409 (w), 1390 (w), 1299 (w), 1211 (w), 1121 (w), 1001 (w), 848 (w); **Sensitivity data**: IS 40 J, FS 240 N, ESD 1.5 J; grain size: 250 –500 µm.

Mid Infrared Pyrotechnics

[69]

Abstract: *Infrared decoy flares serve the protection of aerial platforms such as helicopters, fixed wing and jet propelled planes against infrared guided air-to-air and surface-to-air missiles. These flares are jettonised from the craft at high speed and upon combustion develop a strong infrared signature in the infrared band between λ = 1–5 µm. Decoy flares developing a blackbody type signature often comprise magnesium, polytetrafluoroethylene, $(C_2F_4)_n$ (Teflon®) and vinylidene fluoride - hexafluoropropene copolymer $(C_{10}F_{13}H_7)_n$ (Viton®) and are hence called MTV flares. It has now been found that pyrolants containing magnesium and e. g. ammonium or guanidinium 5-(perfluoropropyl)-5H-tetrazolate as oxidizers yield superior spectral efficiency compared to MTV. Several similar compounds like cesium trifluoromethyl tetrazolate or their chlorine derivatives are of further interest as new additives in pyrotechnic formulations.*

[69] Eurocopter AS532UL Cougar dispensing flares at Axalp 2010, © Édouard Puginier – http://tazintosh.com [Stand: 10.11.2012]

Introduction

Similar as NIR illuminants belong 'decoy flares' to the category of light-producing pyrotechnics. A (decoy) flare is an aerial infrared countermeasure to counter an infrared homing (passive missile guidance system) surface-to-air or air-to-air missile. Such flares are based on very hot burning metals with burning temperatures equal or hotter than an engine exhaust. The favored fuel is magnesium. Standard decoy flares are so called 'MTVs'. They consist of magnesium (fuel), Teflon® (oxidizer), and Viton® (Binder).

An example for one of the first heat-seeking, short range, air-to-air missile is the sidewinder AIM-9. The infrared detector of the sidewinder exists of lead sulfide and lead selenide. The lead sulfide seeking-head detected radiance in the range of 2–3 microns, whereas the lead selenide seeking-head detected radiance between 3–5 microns. These both IR ranges are referred as α (2–3 microns) and β-band (3–5 microns). Until now, IR detectors of air-to-air or surface-to-air missiles were improved tremendously.[70]

The IR signature of an aircraft is generated by several components of the metal cover and the engine exhaust (Figure 40). Radiation between 3–5 microns is emitted from hot exhausts (H_2O, CO, CO_2), whereas hot jet engines emit in the range of 2–2.5 microns. The aircraft fuselage emit primarily between 8-10 microns, due to sun and earth radiation or friction. An IR seeking missiles detect the combined radiation and identify the aircraft as a potential target.[70,71,72]

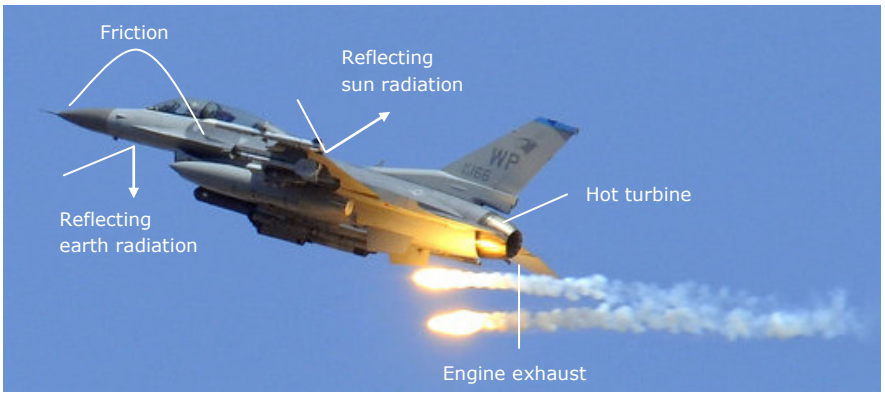

Figure 40 Complete infrared signature of a fighter jet.[73]

[70] S. P. Mahulikar, H. R. Sonawane, *Progress in Aerospace Sciences* **2007**, *43*, 218.
[71] J. S. Acetta, D. L. Shumaker, The Infrared and Electro-Optical Systems Handbook, *Vol. 5*, Passive Electro-Optical Systems, SPIE Optical Engineering Press, Bellingham, **1996**, 220.
[72] H. Radies, PhD thesis, Ludwig-Maximilians-University Munich, **2009**.
[73] http://3.bp.blogspot.com/_J4nYRGAodHs/TQIkpMVGZSI/AAAAAAAAAgs/6HS8p2Q_IdI/s1600/us_kampfjet.jpg [Stand: 2.11.2012]

An example for the IR signature of the MIG 29 is illustrated in Figure 41.

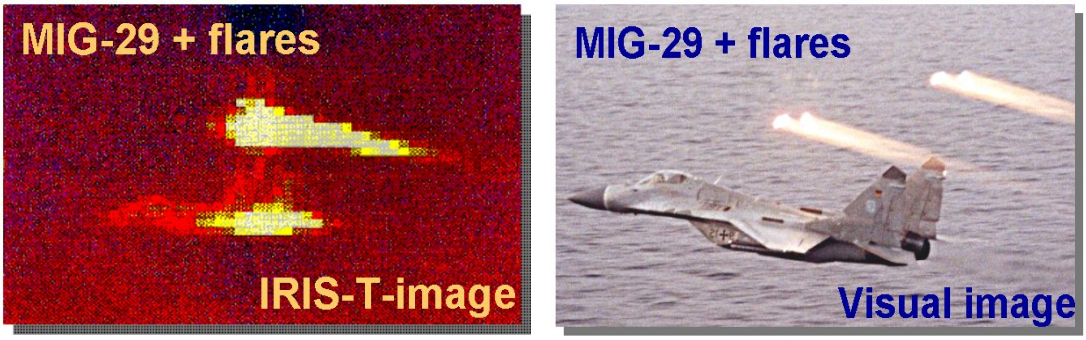

Figure 41 FPA image and visual image of MIG 29 expelling flares.[74]

Heat-seeking missiles normally searching for radiation emitted from the aircraft between the α and β band. New weapon systems are able to differ between the several radiation sources. For tactical reasons the aircraft can ignite decoy flares to prescind adversarial missiles from the aircraft to the burning flare. These pyrotechnic compositions should burn with similar radiation and higher intensity as the aircraft. An example of a missile attack and the use of decoys of a fighter jet are illustrated in Figure 42.

[74] E.-C. Koch, Pyrotechnic Countermeasures II, *Propellants, Explosives, Pyrotechnics* **2006**, *31*, 3.

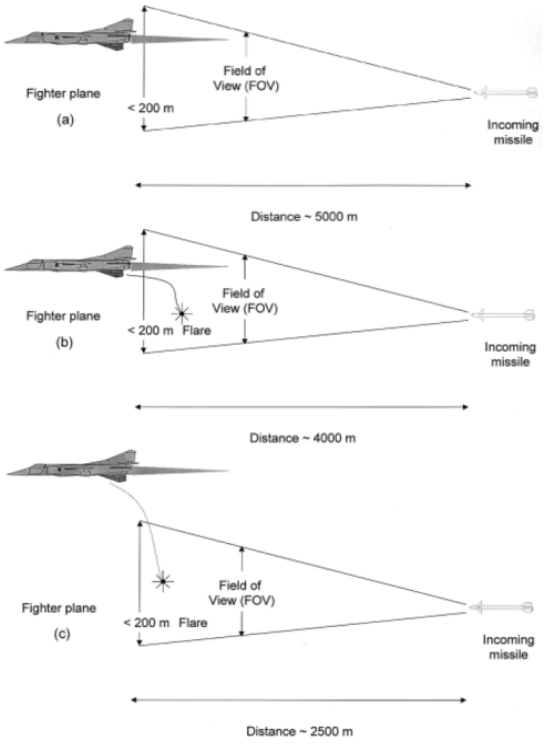

Figure 42 Scenario of a missile attack.[75]

Radiometric principles

On the research of IR emitting compositions it is important to compare the signature of aircrafts and decoy flares. The dimensionless parameter *θ* is useful discussing the intensity of (new) formulations. Term *θ* gives the ratio of the intensity in the α band to the intensity of the β band (equation 1).

$$\theta = \frac{I_\alpha}{I_\beta} \qquad (1)$$

with α = 2–3 μm and β = 3–5 μm. As mentioned before hot components emit between the α band and the exhaust emit in the β band. Theta values of an aircraft are in the range of 0.7. New decoy flares should have values very close to the aircraft to avoid adverse attacks.

Figure 43 illustrates the radiant intensity of an aircraft compared to the mainly used MTV flares.

[75] E.-C. Koch, Review on Pyrotechnic Aerial Infrared Decoys, *Propellants, Explosives, Pyrotechnics* **2001**, *26*, 3.

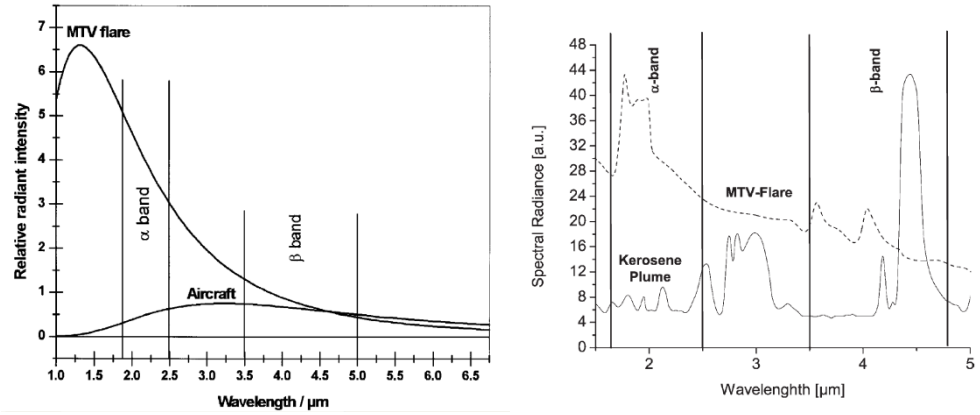

Figure 43 Comparison of relative magnitude of MTV and target (left)[75] and kerosene plume and MTV flare in 2–5 microns range (right).[74]

The physical principles of decoy flares are based on black body radiation, due to high burning temperatures and combustion products (soot) which add as black (grey) emitters. According to PLANCK´S law, the emitted radiation can be described mathematically as:[75,76]

$$W_\lambda = \frac{2\pi hc^2}{\lambda^5} \; \frac{1}{e^{hc/\lambda kT} - 1} \qquad (2)$$

were W_λ = spectral radiant emittance in W cm^{-2} µm^{-1}, λ = wavelength in microns, h = PLANCK´S constant 6.626 x 10^{-34} W s^{-2}, T = absolute temperature in Kelvin, c = velocity of light 2.998 x 10^{10} cm s^{-1}, and k = Boltzmann constant 1.381 x 10^{-23} W s K^{-1}.

Referred to the WIEN displacement law the emission maximum (λ_{max}) shifts to shorter wavelengths as the temperature of the radiator rises, with:

$$\lambda_{max} = 2897.756\,\mu m\,K\,T^{-1} \qquad (3)$$

As PLANCK´S law is valid for an ideal black body emitter, true decoys are rather grey bodies. To describe the deviation from the ideal case to real behavior, the emissivity ε is introduced:

$$\varepsilon = \frac{W'}{W} \qquad (4)$$

The emissivity gives the ratio of the radiant emittance W' of a real radiator to the radiant emittance W of a black body of the same temperature. ε can range from unity (black body)

[76] P. Atkins, Physikalische Chemie, Wiley-VCH, **2001**.

to zero for non radiation sources. For real grey bodies values from $0 < \varepsilon < 1$ are observed (Figure 44).

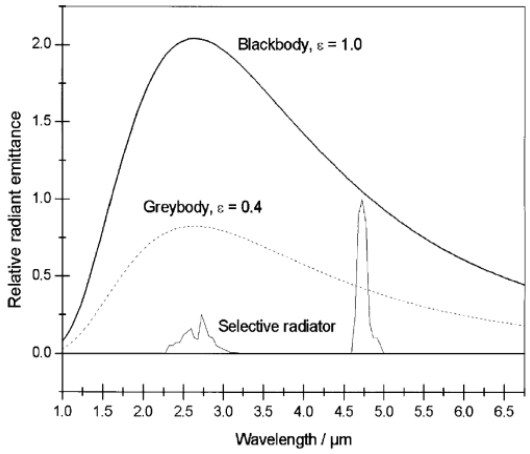

Figure 44 Radiant emittance W for 1100 K for black body, grey body, and a selective radiator.[75]

The values 0 and 1 are not included, because $\varepsilon = 0$ would be an ideal white emitter and $\varepsilon = 1$ an ideal black body. A good grey body emitter is soot ($\varepsilon = 0.95$) which is formed during combustion of MTV flares. The main intention of decoy flares based on black body principles are high ε values, high combustion temperatures and θ values between 0.5–0.8. Recent decoy flares have θ values of 1.3–1.4.

MTV composition

Typical MTV decoy flares contain an excess magnesium, fluorine combustible materials like PTFE (Polytetrafluoroethylene) and a binder like Viton® (hexafluoropropene-vinylidenefluoride-copolymer) [(-$C_5H_3F_8$)-]. The ratio of fuel to oxidizer is usually 70/30. The main part of the released energy is produced by the reaction of excess Mg with air to form MgO (Schema 15).

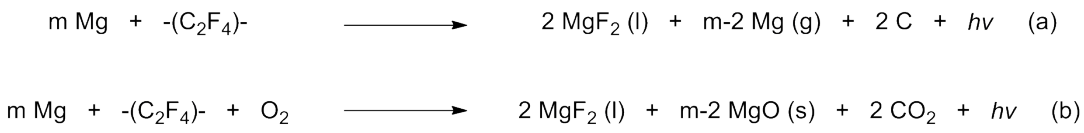

Schema 15 Combustion reaction of MTVs, whereas $m \geq 2$ for (a) and (b).

New approaches of MTV compositions are based on the addition of fluorine bearing high nitrogen compounds, such as derivatives of tetrazoles or triazoles. Several new formulations were tested within the PhD thesis of H. RADIES.[72] According to his work on new pyrotechnic formulations several attempts were carried out within this thesis to synthesize possible candidates for novel flare formulations. The major intention is to find a formulation with convenient performance data and theta values, compared to the original MTV composition. Two examples of fluorine high nitrogen compounds are given in Figure 45. Due to the positive effect of chlorine in pyrotechnic formulations it is furthermore of interest to synthesize chlorine derivatives of high nitrogen compounds and to test the effectiveness as MTV additives.

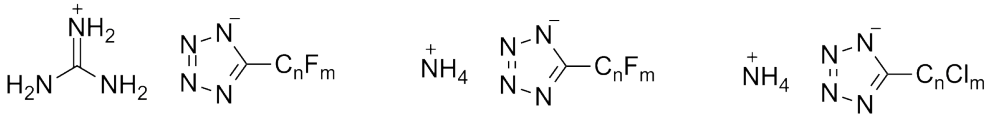

Figure 45 Guanidinium (**a**) and ammonium (**b**) 5-(perfluoroalkyl)-5*H*-tetrazolate and the corresponding chlorine derivative of the ammonium salt (**c**) (n = 1-3, m = 3, 5, 7).

Further new concepts for new decoy flare formulations are based on boron and boron-oxygen bonds or on silicon as an additive. Other novel compositions are so called 'pyro organics' and contain for instance $Al/Fe_2O_3/Sr(NO_3)_2$ and an organic binder.[72]

Research objective

An additional project adapted on pyrotechnic formulations is the synthesis of fluorine bearing high nitrogen materials. These compounds include two advantages: nitrogen release to enlarge the surface of radiation and fluorine as a strong oxidizing agent. Therefore there are possible additives or replacements for Teflon® in MTV formulations. Of major concerns are several tetrazole and triazole derivatives (Figure 46). On the basis of the PhD thesis of H. Radies[72] it was found that good candidates are the salts of trifluoromethyl tetrazole. Due to hygroscopic behavior of calcium trifluoro methyl terazolate, the corresponding potassium and cesium salts are of interest. Thus, both compounds were synthesized and characterized by analytical and spectroscopic measurements.

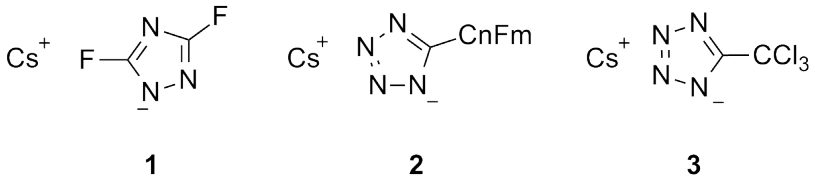

1 **2** **3**

Figure 46 Chemical structures of cesium difluoro-1,2,4-triazolate (**1**), cesium trifluoromethyl tetrazolate (n = 1, 2, 3; m = 3, 5, 7) (**2**), and the chlorine derivative (**3**) for n = 1; m = 3.

Because of the positive effect of chlorine in pyrotechnic formulations a further attempt is the synthesis of the corresponding chlorine derivatives of tetrazoles or triazoles.

Discussion – Synthesis of MTV Additives

The improvement of pyrotechnic formulations is still an extensive task. Several previously mentioned parameters, e. g. heat of formation, oxygen balance, reaction products, burning behavior, combustion temperature etc., must be considered and can be modified. A possible approach discussing MTV payloads is the replacement of Teflon® by compounds which showing a faster burning behavior and produce favorable non-luminous flames or gas like nitrogen. Nitrogen release is desired due to an expansion of the hot core zone, the dispersion of the formed soot and therefore obtaining a higher emission of radiation. A further benefit is the enlargement of the emitting body which is useful during adversely attacks. Based on the PhD thesis of H. Radies[72] several fluorine tetrazoles are of interest. The monosubstituted sodium tetrazolate with fluorinated alkyl chains are known in literature since 1962. The compound is synthesized from sodium azide and trifluoracetonitrile in acetonitrile.[77] Further tetrazole derivatives were synthesized in the group of J. M. SHREEVE in 1989.[78,79] Several other groups concentrate on disubstituted perfluoralkyl tetrazolates and also 5,5´-(hexafluoropropyl)-bis-tetrazole is already kown.[80] Due to the hygroscopicity of several perfluorinated derivatives synthesized in our research group, cesium 5-trifluoromethyl tetrazolate was synthesized and its spectroscopic properties investigated. The chlorinated derivative of 5-trifluoromethyl tetrazolate are attempted to synthesize. Further fluorinated substances, like 3,5-difluoro-1*H*-1,2,4-triazolate or 4,5-difluoro-1*H*-1,2,3-triazolate might be interesting compounds.

[77] W. P. Norris, 5-Trifluoromethyltetrazole and its Derivatives, *Journal of Organic Chemistry* **1962**, *27*, 3248.
[78] E. O. John, J. M. Shreeve, 5-(perfluoralkyl)tetrazoles: η^5 Ligands in Solution and μ-2,3- η^2 Ligands in Solid Complexes, *Inorganic Chemistry* **1989**, *28*, 893.
[79] E. O. John, J. M. Shreeve, Reaction of 5-(Perfluoralkyl)tetrazoles with cyanogens, nitrosyl, and cyanuric chlorides, *Inorganic Chemistry* **1989**, *28*, 4629.
[80] a) W. R. Carpenter, Formation of tetrazoles by the condensation of organic azides with nitriles, *Journal of Organic Chemistry* 1962, *27*, 2085. b) W. G. Finnegan, R. A. Henry, Synthesis and reaction of 1-nitroso-l-alkyl-2-guanyl and 2-carbamoylhydrazines, *Journal of Organic Chemistry* 1965, *30*, 567. c) R. J Spear, Positional selectivity of the methylation of 5-substituted tetrazolate anions, *Australian Journal of Chemistry* **1984**, *37*, 2453. d) H. C. Brown, R. J. Kassal, 5-Perfluoroalkyltetrazoles. I. Ring-opening reactions, *Journal of Organic Chemistry* **1967**, *32*, 1871.

Synthesis of sodium 5-trifluoromethyl tetrazolate (1) and the corresponding cesium (2) salt

The synthesis of **2** follows a [2+3] cycloaddition of nitriles (dipolarophile) with azides (dipole).[77] Fundamental investigations of the 1,3-dipolar cycloaddition was already carried out by HUISGEN *et al*.[81,82] Unfortunately the starting material trifluoroacetonitrile is toxic, expensive, and under normal conditions a gaseous product (bp. −64°C), which makes the synthesis of **2** unfavorable. Therefore, trifluoroacetonitrile was synthesized *in situ* from the cheap corresponding trifluoroacetamide. Two possible syntheses are known in literature for the formation of the nitrile (Schema 16 and 17).

Schema 16 Synthesis of trifluoroacetonitrile from the corresponding amide via phosphorous pentoxide.

The dehydration described in literature uses phosphouros pentoxide as desiccant and the product is obtained after heating the mixture to 100°C.[83] Alternative the product can be formed out of 2,2,2-trifluoroacetamide in pyridine, adding a mixture of trifluoroacetic anhydrate (TFAA) as desiccant.[84] Trifluoroacetonitrile can be then separated in a cooling flask.

Schema 17 Synthesis of trifluoroacetonitrile from the corresponding amide via trifluoroacetic anhydride and pyridine.

[81] R. Huisgen, 1,3-Dipolar cycloadditions. 76. Concerted nature of 1,3-dipolar cycloadditions and the question of diradical intermediates, *Journal of Organic Chemistry* **1976**, *41*, 403.
[82] R. Huisgen, Centenary lecture. 1,3-dipolar cycloadditions, *Proceedings of the Chemical Society* **1961**, 357.
[83] Y. Kobayshi, I. Kumadaki, 1,3-Dipolar cycloaddition reaction of trifluoroacetonitrile with heterocyclic ylides, *Heterocycles* **1981**, *15*, 1223.
[84] M. H. Parker, A convenient preparation of trifluoroacetonitrile. Application to the synthesis of a novel pyrimidinone building block, *Synthetic Communications* **2004**, *34*, 903.

The synthesis of trifluoroacetonitrile was performed according to Schema 17. The preparation of potassium and cesium 5-trifluoromethyl tetrazolate was carried out according to Schema 18. As stated above the nitrile is formed *in situ* in a three neck flask combined with a dropping funnel and an in- and outlet for a low nitrogen flow. The amide was solved in pyridine and while stirring a mixture of TFAA in pyridine was added very slowly. Via the nitrogen flow the formed nitrile was then condensed in a cooled flask (liquid nitrogen). The advantage of this reaction is a nearly quantitative yield of 100%. **1** was obtained after condensing the cooled nitrile into a flask with sodium azide in dry acetonitrile. The azide is provided in small excess to be sure that all of the nitrile reacts. The excess of solid sodium azide can be filtered off and after removing the solvent **1** was obtained as a white powder in good yields. For the formation of **2**, **1** was treated with 1 M HCl and then extracted with diethyl ether. The neutral compound was then treated with the corresponding hydroxide or carbonate. Compared to the cesium salt which is moderate hygroscopic potassium 5-trifluoromethyl tetrazolate is very hygroscopic and was not further investigated. Analytical data were only conducted for **2**.

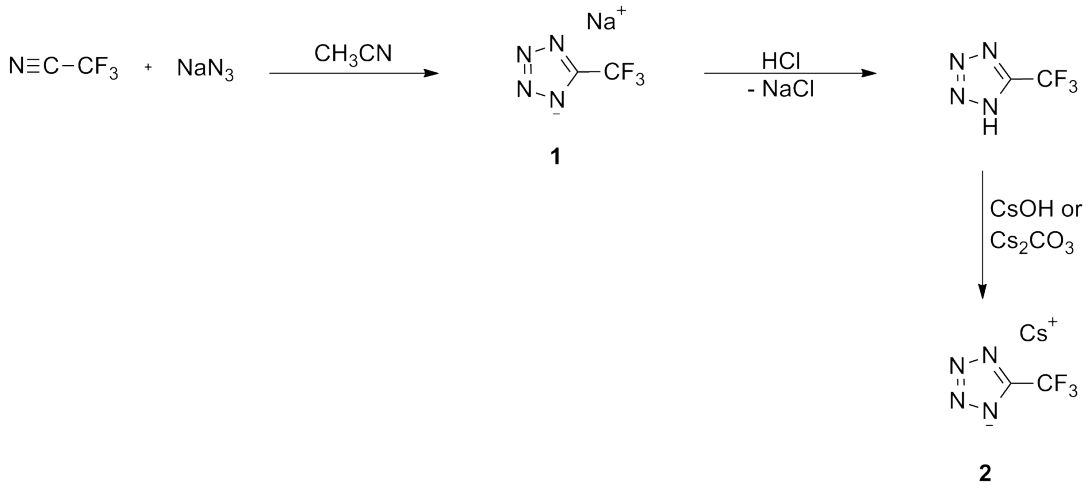

Schema 18 Synthesis of cesium 5-trifluoromethyl tetrazolate (**2**).

Analytical and physical-chemical data

Compared to other 5-perfluoroalkyltetrazolates discussed in literature,[72] the cesium salt was characterized by $\{^1H\}^{13}C$, ^{19}F, and $^{14/15}N$ NMR, DSC, mass spectra, vibrational spectroscopy, and sensitivity tests.The $\{^1H\}^{13}C$ NMR in DMSO of **2** displays two signals (Figure 47). The ring carbon is located at 154.1 ppm. Because of the nearby CF_3 group the signal is split into a quartet with a coupling constant of 33.8 Hz (^2J). The carbon signal of the CF_3 group is shifted to higher field and is located at 123.8 ppm. The signal split again into a quartet with

a coupling constant of 267.5 Hz (^1J) to the fluorine atoms. The signal for the fluorine atoms of the CF_3 group in the ^{19}F NMR appears as a singlet at -60.3 ppm. The nitrogen signals of the ring system are located at 14 (^{14}NMR) and 13.6 ppm (^{15}NMR) and at -60 ppm ($^{14/15}$NMR).

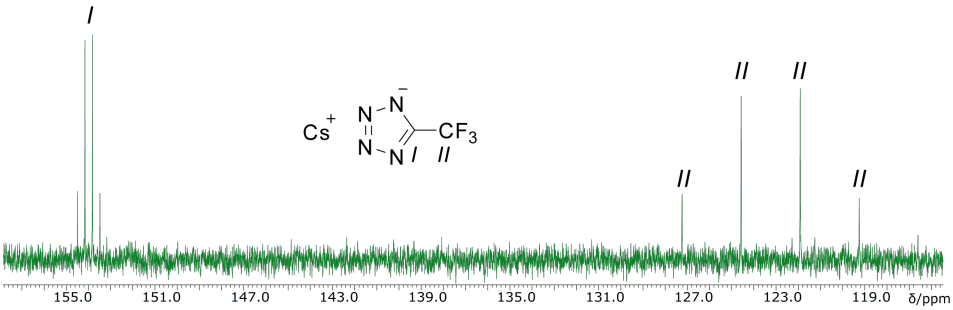

Figure 47 ^{1}H decoupled ^{13}C NMR spectra of **2**.

The decomposition temperature of the cesium salt was obtained from DSC measurements. Compound **2** loose crystal water at 132°C and decompose at 290°C. These values are comparable with decomposition temperatures found for the sodium salt of trifluoromethyl tetrazolate.[72] In addition to crystal water the structure includes sodium (from sodium azide) and therefore the decomposition point of **2** is a bit lower compared to the sodium salt (310°C).

Similar to other salts of perfluoralkyltetrazolate[72] **2** is insensitive against impact, friction and electric discharge (Table 42). Because of the hygroscopic behavior the compound is restricted in the use as pyrotechnic additive. However, **2** was synthesized as a 50 g batch and send to the Frauenhofer-Institut für Chemische Technologie (ICT) for several combustion experiments.

Table 42 Sensitivity data of cesium trifluoromethyl tetrazolate.

	2
IS / J	40
FS / N	360
ESD / J	0.5

Attempted synthesis of sodium 5-trichloromethyl tetrazolate (3)

Similar as for 5-trifluoromethyl tetrazole the synthesis of the chlorine derivative follows a 1,3-dipolar cycloaddition.[81] The chemical reaction is between a 1,3-dipole (azide) and a dipolarophile (nitrile) and forms a five-membered ring (Schema 19).

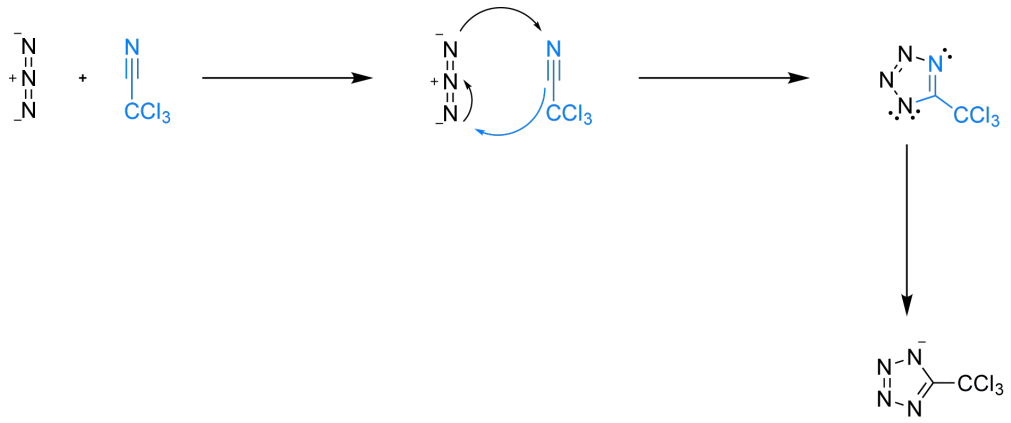

Schema 19 Reaction mechanism for the synthesis of 5-trichloromethyl tetrazolate.

Only few synthetic routes are described for the synthesis of the chloro derivative of methyl tetrazole.[85,86,87] GEISENBERGER and BECK synthesized the compound 1987 under mild conditions via cobalt(III) complexes and they also published the crystal structure.[88] Because the yields are low using cobalt(III) complexes the compound was attempted to synthesize similar as 5-trifluoromethyl tetrazole. Schema 20 describes the synthetic routes tested within this thesis to obtain the sodium salt of 5-trichloromethyl tetrazolate.

A simple method for synthesizing **3** with 75% yield is described by B. DAS.[86] Trichloro acetonitrile and sodium azide were solved in an adequate solvent like DMF or 2-butanone. Catalytically amounts of iodine or silica based sodiumhydogensulfate were added to the mixture and the solution was stirred for 3 h under refluxing conditions. After purification by column chromatography the compound could not be isolated. Only mass spec and NMR shift signals identify the crude compound in very low yields. Several attempts were carried out using the described procedure. B. DAS *et al.* also describe that nitriles bearing an electron

[85] Z. P. Demko, K.B. Sharpless, Preparation of 5-Substituted 1*H*-Tetrazoles from Nitriles in Water, *Journal of Organic Chemistry* **2001**, *66*, 7945.
[86] B. Das, C. R. Reddy, A Simple, Advantageous Synthesis of 5-Substituted 1*H*-Tetrazoles, *Synlett* **2010**, *3*, 391.
[87] F. Himo, Z. Demko, B. Sharpless, Why is Tetrazole Formation by Addition of Azides to Organic Nitriles Catalyzed by Zinc(II) Salts?, *Journal of the American Chemical Society* **2003**, *125*, 9983.
[88] J. Geisenberger, W. Beck, Synthese von Tetrazolen und Triazolen über die 1,3-dipolare Cycloaddition an die Azid-Liganden von polymeren Cobalt(III)- und Palladium(II) Komplexen. Darstellung und Struktur von 5-Trichlormethyltetrazol, *Zeitschrift für Naturforschung* **1987**, *42b*, 55.

donating group reacts faster than those with electron withdrawing groups. Therefore the reaction time was elongated from 3 h to 12 h. Further variations of solvents or temperatures were also not successful.

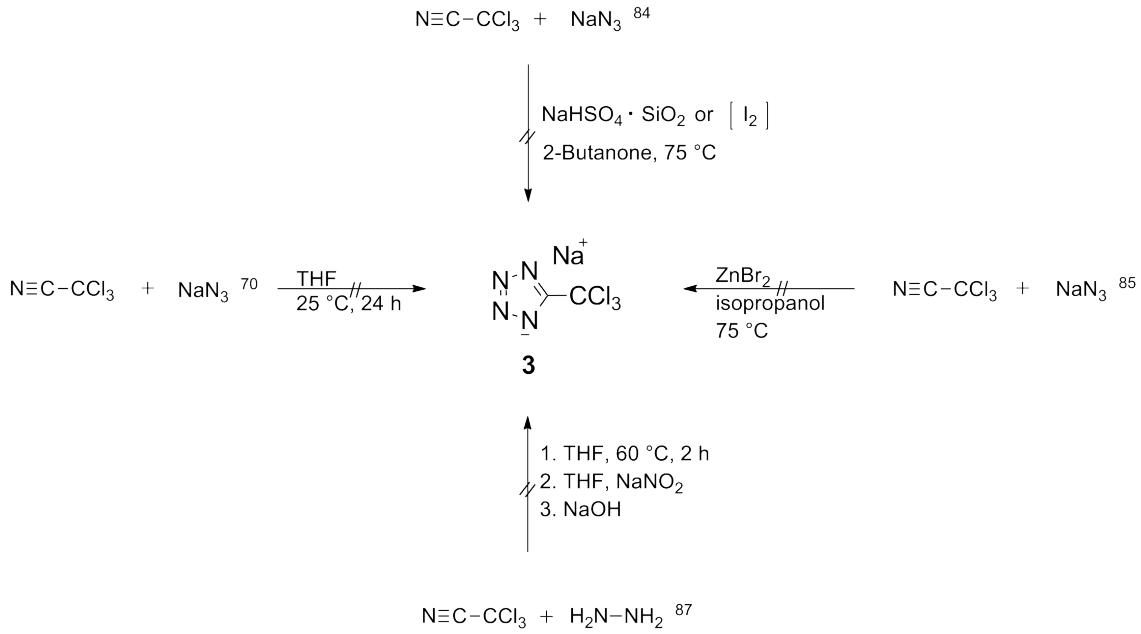

Schema 20 Attempted synthetic routes to sodium 5-trichloromethyl tetrazolate.

Another possible reaction pathway was suggested by F. HIMO[87] using zinc bromide as catalyst. They discuss only kinetic experiments using gas chromatography and did not isolate the compound. However, on this basis the compound was attempted to synthesize using trichloro acetonitrile with an excess of sodium azide and zinc bromide as lewis acid. The preferred solvent was 2-propanol instead of water, due to the formation of trichloro acetamide. The neutral zinc bromide solution inhibits the formation of toxic and explosive HN_3. Zinc bromide act as catalyst because the energy barrier which is necessary for the formation of the ring system, is lower when Zn^{2+} cations coordinate to the nitrogen of the nitrile. If the zinc ion is tetrahedral coordinated by three water molecules and one nitrile the energy barrier decreases from 132.4 to 106.0 kJ mol^{-1}. It increases if the zinc coordinates tetrahedral to water and the azide ion to 149.2 kJ mol^{-1}. Thus, the catalytically effect of zinc bromide is due to a dative bond to the nitrile (Figure 48).[87] Changing reaction times, temperatures or solvents, compound **3** could not be isolated using this procedure.

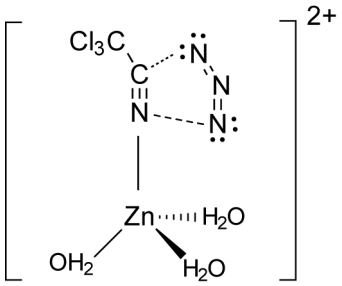

Figure 48 Tetrahedral coordination of the zinc cation.

Based on the results of H. RADIES[72] **3** was attempted to synthesize using the same procedure as for the synthesis of **2**. Dry THF was used as solvent instead of acetonitrile. The reaction was carried out at room temperature and the mixture was stirred for 24 h. The NMR of the obtained residue displays several signals. Only few of them were identified as educt. Other obtained signals could not be correlated to the desired product.

According to the patent from MASAHARU[89] **3** was attempted to synthesise *via* hydrazine in THF. The solution was added to trichloro acetonitrile and stirred for 2 h at 60°C. Afterwards sodium nitrit was added and the mixture stirred over night. The NMR of the obtained orange oil displays signals of trichloro acetonitrile and several signals which could not allocated to **3**.

Conclusion

Pyrotechnic formulations which emit light in the region between 2 and 5 microns (mid infrared) are so called MTV decoy flares. These flares consist normally of Magnesium, Teflon® and Viton®. To improve the burn rate or the size of the hot core zone Teflon® might be replaced. A possible candidate as new additive in MTV compositions is cesium trifluoromethyl tetrazolate, which was successfully synthesized. A sample of 50 g of the compound was send to the Frauenhofer Institut (ICT) for several decomposition and compatibility tests. The evaluation of the results is still in progress; therefore they could not be presented within this thesis.

Because chlorine is a useful additive in pyrotechnics, several attempts were carried out to synthesize the chlorine derivative trichloromethyl tetrazole or its salts. Although the compound is mentioned in literature the synthesis could not be reproduced.

[89] Masaharu, *European Patent Application* **2001**, EP 1136476 A2.

Experimental Section

Equipment

Caution! *Although no problems occurred during the synthesis and handling of the materials studied in this work, some of the neutral compounds and their salts are sensitive energetic materials. Safety equipment such as Kevlar® gloves, leather coat, wrist protection, face shield, ear protection, grounded equipment, and shoes are mandatory.*

General Method. All chemicals and solvents were used as received (Sigma–Aldrich, Fluka, Acros Organics) unless stated otherwise. MELTING POINTS were measured with a Linseis PT10 DSC, calibrated with standard pure zinc and indium. Measurements were performed at a heating rate of 5°C min^{-1} in a closed aluminum sample pan with a 1 µm hole on top for gas release and under a nitrogen flow of 20 mL min^{-1} with an empty identical aluminum sample pan as reference. The values were checked by a Büchi Melting Point B-450 apparatus. The M. p. values are not corrected. MASS SPECTROMETRY was conducted on a JEOL MStation JMS 700 machine. All NMR SPECTRA were recorded with a Jeol Eclipse 270, Jeol EX 400, or a Jeol Eclipse 400 instrument. The chemical shifts are quoted in ppm relative to TMS (^{1}H, ^{13}C), $MeNO_2$ (^{14}N, ^{15}N), and $CFCl_3$ (^{19}F). For NMR signals the common abbreviations were used: s (singlet), d (duplet), t (triplet), q (quartet), and m (multiplet). INFRARED (IR) SPECTRA were recorded with a Perkin–Elmer Spektrum One *FT-IR Spectrum BXII* with *Smith ATR Dura Sample IRII* instrument. The absorption is given in wave numbers (cm^{-1}) with a range of 100 to 4000 cm^{-1}. Transmittance values are qualitatively described as very strong (vs), strong (s), medium (m), weak (w), and very weak (wv). RAMAN SPECTRA were measured with a Bruker MULTIRAM 1064 2000R NIR FT-Raman instrument equipped with a Nd:YAG laser (1064 nm). The intensities are given in percentages of the most intense peak and are given in parenthesis. ELEMENTAL ANALYSES (C, H, N, I) were performed with a Vario El and Netsch STA 429 Simultaneous Thermal Analyzer. SENSITIVITY DATA were determined using a BAM drop hammer, BAM Friction tester, and an OZM electrical discharge testing device.[52,53]
For the synthesis of nitrogen rich heterocyclic fluorine and chlorine derivatives reactions were carried out under exclusion of air and moisture using the SCHLENCK technique. Argon (purity 4.6) from a 50 L compressed gas cylinder of the MESSER GRIESHEIM Company was used as inert gas. Before usage the glass flasks were heated twice to 400°C with a heat gun and in between exposed with an argon flow. The weighting of the compounds was done against an argon flow. For several reactions absolute solvents (e. g. THF, acetonitrile) were used and freshly distilled over an adequate desiccant.

Synthesis

Synthesis of cesium trifluoromethyl tetrazolate (2)

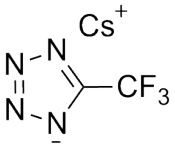

Trifluoromethyl amide (5.65 g, 0.05 mol) was added to 26 mL dry pyridine in a 100 mL three neck flask. A dropping funnel was filled with 8.5 mL dry pyridine and TFAA (7 mL, 0.05 mol) whereby the dropping funnel was cooled during the addition of TFAA. An ice bath cooled condensation trap (collects pyridine) was connected to the flask, followed by a second cold trap which was cooled to –196°C by liquid nitrogen. The second trap was connected at the end to a bubble counter to avoid the condensation of liquid oxygen. During the reaction a low to medium nitrogen flow was ran through the reaction mixture. The solution of the dropping funnel was added slowly to the trifluoromethyl amide/pyridine mixture. If no more gas formation was observed the nitrogen flow was raised for 5 min. The second cold trap, containing trifluoro acetonitrile, was removed and evacuated under cooling with liq. nitrogen. A dry 1000 mL flask with sodium azide (3.575 g, 0.055 mol) in 75 mL dry acetonitrile was connected to the cold trap and the trifluoro acetonitrile was condensed to the sodium azide solution. The reaction mixture was allowed to come to r. t. and then stirred for 48 h. The excess of sodium azide was filtered off and washed with acetonitrile. The solvent was removed and the product dried under high vacuum. Yield: 8 g (98%) of colorless crystalline sodium trifluoromethyl tetrazolate (**NaTF 1**). NaTF (6.16 g, 73 mmol) was solved in 36.5 mL 2 M HCl and afterwards extracted with 3 x 150 mL diethyl ether and 1 x 100 mL water. To the combined organic layers was added 12.72 mL CsOH, the solution was stirred for 1 h at r. t. and the solvent evaporated. Yield: 19.36 g (97%, Cs).

EA ($C_2CsF_3N_4$, 270) found(calc.):C 8.90(8.95) H 0.05(0.0) N 20.75(20.32); **^{19}F NMR** (d_6 DMSO, 25°C): δ = -60.03; **^{13}C NMR** (d_6 DMSO, 25°C): δ = 123.8, 154.1; **^{14}N NMR** (d_6 DMSO, 25°C): δ = 14.0, -60.0; **^{15}N NMR** (d_6 DMSO, 25°C): δ = 13.6, -60.0; **MS** (FAB^-) *m/z* (rel. Int.): 137.0 (100) [$C_2N_4F_3^-$]; **DSC** (5°C min^{-1}): T = 129°C, 310°C (dec.) **IR** (ATR): $\tilde{\nu}$ = 3418 (s), 1642 (m), 1508 (s), 1415 (w), 1230 (vs) 1175 (vs), 1141 (vs), 1045 (s), 980 (w), 769 (w), 750 (m), 580 (w); **Raman** (200 mW): $\tilde{\nu}$ = 1507 (100), 1242 (13), 1170 (50), 1160 (12), 1062 (80), 999 (31), 755 (90), 426 (30), 389 (84); **Sensitivity data**: IS 35 J, FS 40 N, ESD 1.5 J; grain size: 250–500 µm.

Synthesis of trichloro acetonitrile according to H. Radies[72]

Synthesis via trichloro acetamide (TCAA)

Trichloro acetamide (9.74 g, 60 mmol) in 20 mL dry pyridine was added under argon in a 250 mL three neck flask. A dropping funnel was filled under cooling with 25 mL dry pyridine and 8.51 mL (60 mmol) trichloroacetic anhydride. The solution was added within 1.5 h to the trichloro acetamide mixture. Afterwards the solution was stirred under argon over night. The brown solution was distilled under argon (ambient temperature, 100°C). A colorless liquid was obtained at 83–84 °C. **^{1}H NMR** (C_6D_6, 25°C): δ = - ; **^{13}C NMR** (C_6D_6, 25°C): δ = 113.0, 70.0; **IR**: $\tilde{\nu}$ = 3080 (vw), 3002 (vw), 1582 (m), 1482 (w), 1438 (m), 1261 (vw), 1217 (w), 1147 (vw), 1068 (w), 1030 (m), 992 (m), 786 (s), 745 (vs), 700 (vs), 664 (m).

Synthesis via trifluoro acetamide (TFAA)

The procedure as described above was repeated using TFAA instead of TCAA. **^{1}H NMR** (C_6D_6, 25°C): δ = - ; **^{13}C NMR** (C_6D_6, 25°C): δ = 114.0, 70.2; **IR** (ATR): $\tilde{\nu}$ = 3391 (w), 3080 (w), 3063 (vw), 3026 (w), 2581 (vw), 2094 (vw), 1636 (w), 1612 (w), 1598 (m), 1582 (m), 1540 (w), 1487 (m), 1438 (s), 1216 (w), 1200 (w), 1147 (w), 1068 (w), 1030 (m), 992 (m), 784 (s), 748 (s), 700 (vs), 685 (vs); **Raman** (200 mW): $\tilde{\nu}$ = 3060 (67), 2249 (35), 2306 (16), 1733 (17), 1601 (5), 1581 (28), 1217 (15),1032 (71), 992 (100), 485 (45), 264 (27), 162 (26).

Synthesis of silica gel-supported sodium hydrogen sulfate ($NaHSO_4 \cdot SiO_2$)[90]

4.14 g (0.03 mol) $NaHSO_4$ was added to 20 mL water. After the solid was dissolved 10 g (0.17 mol) silica gel (60 Å, 230–400 mesh) was added and the mixture stirred for 15 min. It was heated to 50°C and while stirring the solvent was evaporated. For further drying the solid was placed into an oven at 65°C for 3 h and at 135°C over night. The catalyst was stored in an oven and was used within 48 h. Yield: 100%.

[90] G. W. Breton, *Journal of Organic Chemistry* **1997**, *62*, 8952.

Synthesis of trichloromethyl tetrazole according to B. Das[86] by using iodine

2.2 g (34.2 mmol) sodium azide and 2.3 g (22.8 mmol) trichloro acetonitrile were solved in 60.0 mL butanone. Under argon 0.34 g (2.7 mmol) dry iodine was added and the mixture stirred for 4 h at 85°C. After cooling to r. t. 45 mL 4 M HCl and 70 mL ethyl acetate was added. The solution was stirred over night, afterwards 70 mL ethyl acetate and 50 mL water was added. The aqueous solution was extracted with 3 x 100 mL ethyl acetate. The combined organic layers were extracted with 3 x 30 mL sat. sodium thiosulfate solution and then washed with 3 x 100 mL water. The solvent was removed. The orange oil was subjected to column chromatography (silica gel; n-hexane/ethyl acetate 8:1). **^{1}H NMR** (d_6 DMSO, 25°C): δ = 8; **^{13}C NMR** (d_6 DMSO, 25°C): δ = 163.5, 93.5; **MS**: (DEI$^+$) *m/z* (rel. Int.): 187 (6) [M+H].

Attempted synthesis of trichloromethyl tetrazole according to B. Das[86] with $NaHSO_4 \cdot SiO_2$

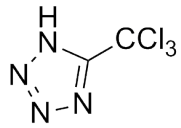

2 mL (20 mmol) trichloro acetonitrile, 1.95 g (30 mmol) sodium azide and 0.9 g (7.5 mmol) $NaHSO_4 \cdot SiO_2$ was added in a 250 mL flask. 50 mL dry butanone was added and the mixture refluxed for 4 h at 75°C under argon. After cooling to r. t. 100 mL 4 M HCl and ethyl acetate was added. After 10 min another 100 mL ethyl acetate was added. The aqueous layer was extracted with 3 x 100 mL ethyl acetate. The combined organic layers were washed with 3 x 100 mL water. In some cases brine was used for obtaining separated phases. The organic layer was dried over Na_2SO_4, the solvent was removed and 1 mL of an orange oil was obtained.

Alternative:

Using the same procedure the synthesis was repeated with different volume% of butanone and different solvents e. g. dry iso propanol. **^{1}H NMR** (d_6 DMSO): δ = 10.0; **^{13}C NMR** (d_6 DMSO, 25°C): δ = 138.0, 74.4; **IR** (ATR): $\tilde{\nu}$ = 2982 (w), 2942 (w), 2362 (vw), 1710 (s), 1650 (w), 1613 (w), 1549 (vw), 1530 (vw), 1513 (vw), 1462 (w), 1379 (m), 1262 (m), 1157 (m), 1105 (m), 1049 (m), 1025 (m), 1001(m), 947 (w), 870 (m), 815 (vs), 790 (vs), 728 (s), 695 (m).

Attempted synthesis of trichloromethyl tetrazole according to F. Himo[87]

To a solution of 1.6 g (25 mmol) sodium azide, 5.6 g (25 mmol) zink bromide in 35 mL water and 15 mL iso propanol was added 0.1 mL (1 mmol) trichloro acetonitrile. The solution was stirred over night at r. t. One fourth of the solution was added to 5 mL 1 M HCl and 25 mL ethyl acetate. The organic layer was separated and the procedure repeated with the remained solution. The solvent of all combined organic layers were removed under high vacuum. Yield: 0.5 g of a colorless and hygroscopic solid.

Alternative:
The synthesis was repeated using benzyl alcohol (1 mL) or ethyl acetate (1 mL) as solvent. The reaction time was elongated to 48 h. **^{1}H NMR** (d_6 DMSO, 25°C): δ = -; **^{13}C NMR** (d_6 DMSO, 25°C): δ = 69.6 (educt); **IR** (ATR): $\tilde{\nu}$ = 3383 (vs), 2359 (vw), 2188 (w), 1979 (vw), 1966 (vw), 1677 (m), 1625 (vs), 1507 (m), 1434 (m), 1390 (m), 1378 (m), 1347 (m), 1287 (m), 1224 (s), 1143 (m), 1089 (s), 1014 (m), 876 (m), 850 (s).

Attempted synthesis of trichloromethyl tetrazole according to Z. P. Demko and K. B. Sharpless[85]

In a 250 mL flask was added 40 mL dry propionitrile or butanone, Cl_3CCN (2 mL, 20 mmol), NaN_3 (1.43 g, 22 mmol) and $ZnBr_2$ (4.53 g, 20 mmol). The solution was refluxed for 24 h (alternative: 2 h). After cooling to r. t. 25 mL 4 M HCl and 100 mL ethyl acetate was added and the reaction mixture stirred for further 30 min. In case of obtaining a precipitate ethyl acetate was added until the solid was solved. The solution was extracted with 3 x 100 mL ethyl acetate and the solvent of the combined organic layers was removed. 200 mL 0.25 M sodium hydroxide was added and the solution stirred for 30 min until a colorless solid of zinc hydroxide was obtained. The solid was filtered off and washed with 30 mL 4 M HCl. The solvent was removed until a colorless crystalline solid was obtained. **^{1}H NMR** (d_6 DMSO, 25°C): δ = 9.57 (altern. 2 h), 9.38; **^{13}C NMR** (d_6 DMSO, 25°C): δ = 171.0, 145.1, 77.2 (altern. 2 h).

Attempted synthesis of sodium trichloromethyl tetrazole according to H. Radies[72]

0.31 g (7.77 mmol) sodium azide, 0.48 mL (4.68 mmol) trichloro acetonitrile, and 30 mL dry THF were added into a 50 mL flask. The reaction mixture was stirred for 24 h at room temperature and afterwards the excess sodium azide was filtered off. The solvent was removed. The procedure was repeated using dry acetonitrile instead of THF. In both cases a brown oil was obtained. **^{1}H NMR** (d_6 DMSO, 25°C): δ = 9.47; **^{13}C NMR** (d_6 DMSO, 25°C): δ = 145.0, 116.2, 107.1, 69.8.

Detonation Velocity

Abstract: *The detonation velocities of several compounds with possible application as new secondary explosives were experimentally determined in a detonation chamber (KV-250) using the fiber optic technique. The investigated explosives are 1-amino-3 nitroguanidine (**1**), diaminouronium nitrate (**2**), dihydroxylammonium 5,5-bistetrazolate (**3**), hydroxylammonium 5-nitriminotetrazolate (**4**), oxalylhydrazide nitrate (**5**) and, 1,3,5- triaminoguanidinium 1-methyl-5-nitriminotetrazolate (**6**). The compounds were synthesized on a 20 g scale, loaded into a PE tube and initiated with an electrically ignited detonator. The measured detonation velocities were recorded using the EXPLOMET-FO-2000 system and compared with the calculated detonation parameters using the EXPLO5 code with the respective loading density of the compound.*

Introduction

Combustion, Deflagration and Detonation

Several major characteristics are allocated with (secondary) explosives. One important character is the detonation velocity. Some EMs burn relatively slow (few mm or cm per second) but if the burn rate of a slow burning material increases it can cause into a deflagration or detonation.

A combustion (burning) is defined as an exothermic chemical reaction which occurs between a fuel and an oxidant (air). The chemical reaction is very fast and accompanied by the release of heat (flame). The generated energy will raise the temperature of the unreacted material and increases its rate of reaction. An example of combustion is the ignition of a matchstick. Depending on the temperature combustion can occur with or without the formation of a flame. At low temperature the oxidation of the combustible material is very slow and no flame is observed. The rate of oxidation is increased by the application of heat. After the ignition temperature is reached the heat generations is greater than the heat loss and a flame is observed. As mentioned at the beginning, the combustion process of explosives (and propellants) is a self-sustaining, exothermic and fast oxidizing reaction with the generation of large amounts of gaseous products. They contain oxygen and fuel in their molecular structure and are classified as combustible materials. In general, propellants generate combustion gases by deflagration, whereas explosives generate gases by deflagration or detonation.[2,91]

Deflagration describes a (thermal) subsonic combustion process with the formation of flames, sparks or crackling noises. Deflagrating explosives ignite when a small unconfined part of it are contacted to flame, spark, heat, shock or friction. They burn faster and more violent then common combustible materials. The rate of deflagration increases with the degree of confinement. As a material undergoes deflagration the produced gases from the decomposition process of the crystals become trapped and the internal pressure and therefore the temperature rise which in turn increase the rate of deflagration. Deflagration of complete confined explosive materials can be classified into 'low' and 'high' order detonation. If the deflagration rates are between 1000–1800 m s^{-1} it is stated as low order and from 5000 m s^{-1} it becomes high order detonation. It can be said that unconfined materials undergo a deflagration process, whereas confined setting led to detonation processes.[2,91]

[91] M. Suceska, Test Methods of Explosives, Springer Verlag, **1995**.

An explosive material which generates a shock wave after initiation undergoes a detonation process. Depending on the compound (primary or secondary explosive) detonation velocities of the shock wave are between 1500–9000 m s^{-1}. The detonation process is always supersonic. In contrast to the heat transfer during deflagration, the detonation process is governed by the speed at which the material transmits the shock wave. Detonation can be initiated by shock or by burning to detonation (DDT).

Because the detonation process is a very complicated process, containing many mathematical equations only basic principles are discussed within this thesis.

Theoretical aspects

According to the ZELDOVICH VON NEUMANN-DOERING (ZND) model[91,92] of detonation the chemical reaction occurs in a thin chemical reaction zone under the action of a shock wave. A simplified diagram of the detonation process is given in Figure 49. This rapid and violent process differs from others like heat conduction in that all the important energy transfer is by mass flow caused by the action of the shock wave.

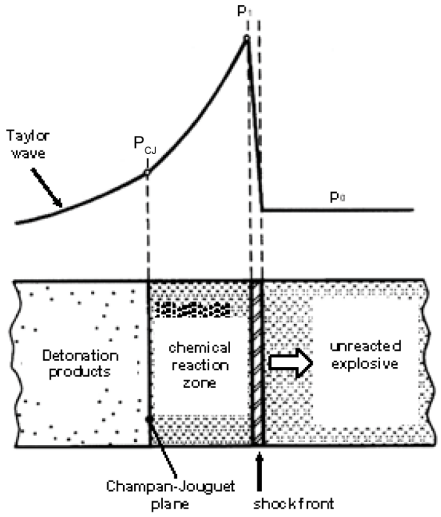

Figure 49 Schematic description of the detonation process and detonation wave structure.[4]

[92] W. Fickett, W. C. Davis, Detonation-Theory and Experiment, **1979**.

The CHAPMAN-JOUGUET postulate is based on the assumption of an ideal detonation with a complete chemical conversion of the explosive material within the shock front and a steady state of the detonation products.
The graph in Figure 50 defines the relationship between the density (volume) and the pressure during the dynamic compression of the explosive. Curve 1 represents the explosive before reaction and curve 2 the reacted explosive.

Due to the pressure of the shock wave, a thin layer of the explosive material is compressed from the initial density ρ_0 to the density ρ_1 according to curve 1 (adiabatic shock of the explosive). As a result of the dynamic compression of the explosive, an increase of the pressure p_0 to p_1 occurs. The higher pressure leads to a significant increase of the temperature in the chemical reaction zone and the chemical reaction begins. When the chemical reaction comes to an end, pressure and density reach the values p_2 and ρ_2. This state relates to the point laying on the shock adiabatic curve (2) of the detonation products. In this state, the products expand isentropically into the surrounding medium. For the steady state model of detonation the values (p_0, ρ_0), (p_1, ρ_1) and (p_2, ρ_2) lie on one line, the RAYLEIGH or MICHELSON line. The slope of the RAYLEIGH line is proportional to the detonation velocity of an explosive material. Relating to the CHAPMAN-JOUGUET postulate, the RAYLEIGH line is the tangent to the adiabatic shock curve of the detonation products. This point on curve 2, called the CJ-Point, shows the end of the chemical reaction and the steady state of the (gaseous) reaction products. The 'speed of the reaction products' corresponds to the detonation velocity.[91,92]

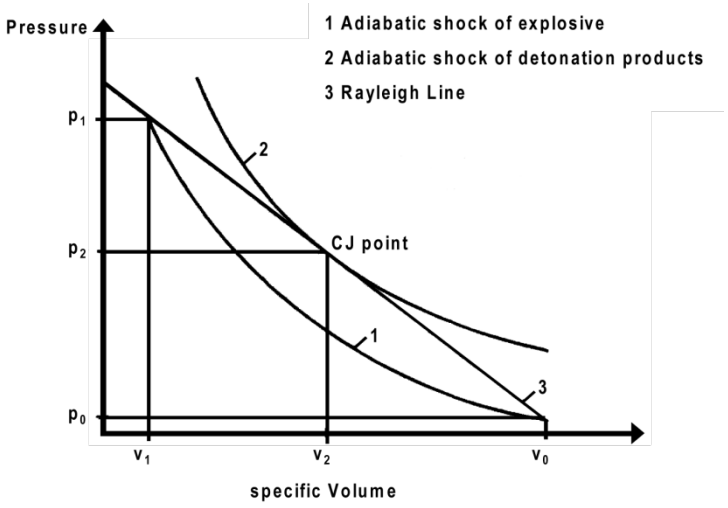

Figure 50 Steady state model of detonation.[4]

The steady state is reached as the released energy of the exothermic reaction equals the energy released to the immediate vicinity plus the energy necessary to compress and slide the crystals or particles of the explosive material.
Using thermodynamic and hydrodynamic laws, the detonation process can be described mathematically with the following equations:

$$\rho_0 D = \rho(D - W) \qquad (1)$$

$$p = \rho_0 DW \qquad (2)$$

$$e - e_0 = {}^1\!/_2\,(p + p_0)(V_0 - V) + q \qquad (3)$$

$$\gamma = -\left(\frac{\partial \ln p}{\partial \ln V}\right)_s = -\frac{V}{p}\left(\frac{\partial p}{\partial V}\right)_s = -\frac{V}{p}\left(\frac{p - p_0}{V - V_0}\right) \qquad (4)$$

Where D = detonation velocity, W = mass velocity, q = heat of detonation, e = internal energy, V = specific volume with $V = 1/\rho$ and γ = polytropic exponent, and subscript 0 indicates the unreacted explosive.
It is possible to get the relationship of the most important detonation parameters by combining equations 1 to 3, including equation 4 from the CHAPMAN-JOUGUET postulate.[91]

Experimental detonation velocity

For the experimental characterization of an explosive compound several detonation parameters, such as detonation velocity, detonation pressure, detonation product mass velocity, detonation temperature etc., must be considered. Nowadays, several dynamic methods based on different physical principles, as well as experimental test procedures, exist.[91,92] From the above mentioned properties the most important parameter for a secondary explosive is the detonation velocity, which presently can be measured quite accurately for covalent bonded compounds. Calculated VOD values can be achieved very easily with different computational methods like EXPLO5[93] or Cheetah.[94]

Every detonation process, as well as the combustion process, is accompanied by the emission of light. This makes it possible to measure the detonation velocity with different techniques. For rough estimations, simple ways like the DAUTRICHE[91] method can be applied.

[93] M. Suceska, EXPLO5.03 program **2009** and EXPLO5.04 program **2010**, Zagreb, Croatia.
[94] Lawrence Livermore National Laboratory, Cheeta 6.0 thermochemical code **2011**, Livermore, USA.

To get more accurate results, optical methods with high speed cameras or electrical methods with different types of velocity probes should be used.

The determination of the VOD is based on the measurement of the time interval needed for the detonation wave to travel through a known distance in an explosive material. The equipment should provide suitable velocity probes for the detection of the arrival of the detonation wave, and the measurement of very short time intervals (in a microsecond scale) needed for the detonation wave to travel between two or more velocity probes.

VOD experiments within this thesis were carried out with the EXPLOMENT-fo®-2000 equipment using the optical fiber technique (Figure 51 and 52). The EXPLOMENT-fo®-2000 is an electronic instrument for the precise measurement of the detonation velocity. The principle is based on measuring the time which elapses when the detonation wave passes between two probes in a selected distance. The time is then recalculated to the detonation velocity knowing the distance between two optical fibers. The EXPLOMENT has five independent timer which measures the time interval between six optical probes. Using all six fibers the instrument can provide a 'semi-continuous' VOD measurement. The optical fibers insure excellent immunity against electrical noise and there is no signal disturbance by stray currents etc.

Figure 51 EXPLOMENT-fo®-2000 measuring equipment.

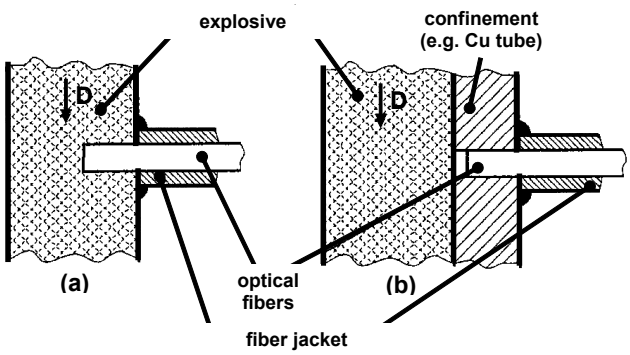

Figure 52 Possible settings for the optical fibers.[4]

The accuracy of the instrument is ± 0.1 µs for the time and better than 0.2 % for the velocity. VODs can be measured up to 10 000 m s^{-1}, what is in the range of CL-20, an explosive with one of the highest detonation velocities. The time interval is measured between 0.1 µs and 10 s.

Research objective

The final topic of this thesis includes the measurements of the detonation velocity of several new high energetic materials synthesized in our research group. Therefore several VOD tests with different densities of the material were performed. The obtained values were compared with calculated and measured detonation velocities of commonly used explosives like RDX, HMX and PETN.[95]

It was further tested whether the experimental set up established within the master thesis could be improved by variations of several parameters e. g. density of the explosive material or confinement of the explosive charge.

[95] N. Fischer, D. Fischer, T. M. Klapoetke, S. Scheutzow, J. Stierstorfer, M. Boehm, Experimentally determined detonation velocities of new secondary explosives, Proceedings of the 14th NTREM Conference, Pardubice, CZ, **2011**.

Discussion – Experimental VOD

Nitrogen rich compounds play a major role in the development of new energetic materials for the use as (gun-) propellants, explosives and pyrotechnics.[96] A main subject in our research group are secondary explosives and potential RDX replacements. The high demand of versatility is the major challenge that is faced in designing and inventing new nitrogen rich materials. Such materials should feature high thermal and mechanical stabilities and at the same time should be as high performing as possible, regarding the detonation velocity, detonation pressure and heat of explosion. Furthermore, environmental compatibility is a big issue nowadays. Unfortunately, this combination of requirements is rarely achieved.[97,98] Whereas the thermal stability as well as the sensitivity and compatibility of new potential RDX replacements can be determined comparatively easy in laboratory experiments, the only common method for obtaining the performance data are computational calculations. To compare theoretical data with real performance data, experimentally determined performance tests need to be carried out.

New secondary explosives

The detonation velocities of 1-amino-3-nitroguanidine (**1**), diaminouronium nitrate (**2**), dihydroxylammonium 5,5-bistetrazolate (**3**), hydroxylammonium 5-nitriminotetrazolate (**4**), oxalylhydrazide nitrate (**5**) and 1,3,5-triaminoguanidinium 1-methyl-5-nitriminotetrazolate (**6**), (Figure 53) were experimentally determined and afterwards compared with the calculated values using the EXPLO5 (V5.04) code.[93]

[96] L. V. De Yong, G. Campanella, A study of blast characteristics of several primary explosives and pyrotechnic compositions, Journal *of Hazardous Materials* **1989**, *21*, 125.
[97] T. M. Klapötke, J. Stierstorfer, The CN_7^- anion, *Journal of the American Chemical Society* **2009**, *131*, 1122.
[98] A. K. Sikder, N. Sikder, A review of advanced high performance, insensitive and thermally stable energetic materials emerging for military and space applications, *Journal of Hazardous Materials* **2004**, *112*, 1.

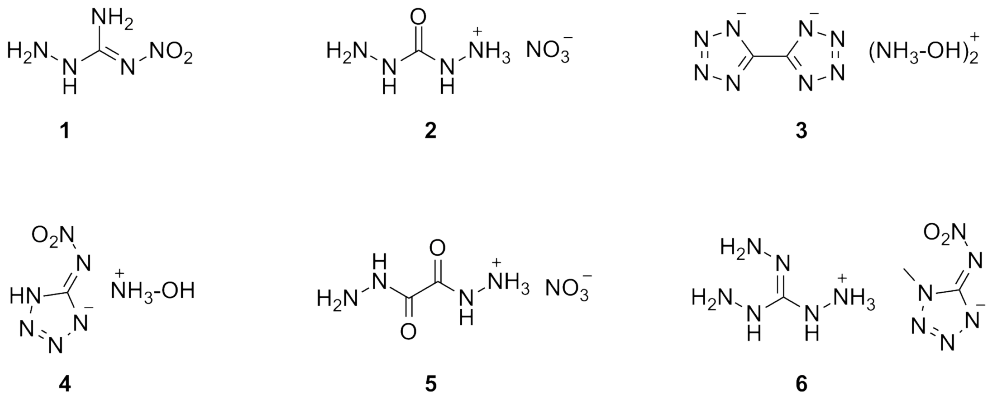

Figure 53 Overview of the investigated compounds **1**–**6**.

Mostly all the investigated compounds meet the high requirements for new secondary explosives, which means, the performance data exceed those or are at least comparable to those of commonly used RDX (Table 43). Apart from **4**, all compounds show mechanical stability towards impact, friction and electrical discharge as well as high decomposition temperatures above 180°C. The calculated performance data, in particular the detonation velocities, also reveal the potential of the compounds regarding the applicability as new secondary explosives. Compounds **1**, **2**, **3** and **6** were synthesized according to literature.[99,100,101,102] For the preparation of **4** and **5**, the following procedure was used: Oxalyldihydrazide[103] and 5-nitriminotetrazole.[104] Hydroxylammonium 5-nitriminotetrazolate (**4**) was prepared by dissolving 5-nitriminotetrazole in water followed by the addition of aqueous hydroxylamine. Oxalyldihydrazide nitrate (**5**) was prepared by simple protonation of oxalyldihydrazide with dilute nitric acid.[105]

[99] N. Fischer, T. M. Klapötke, Energetic Materials based on 1-amino-3-nitroguanidine, New Trends in Research of Energetic Materials, Proceedings of the 13th seminar, Pardubice, CZ, *1*, 113, **2010**.
[100] N. Fischer, T. M. Klapötke, Explosives based on Diaminourea, *Propellants, Explosives, Pyrotechnics* **2011**, *36*, 225.
[101] M. A. Hiskey, D. E. Chavez, High nitrogen fuels for low-smoke pyrotechnics, *Journal of Pyrotechnics* **1999**, *10*, 17.
[102] T. M. Klapötke, J. Stierstorfer, Nitrogen-Rich salts of 1-Methyl-5-nitrimino-tetrazolate: An Auspicious Class of Thermally Stable Energetic Materials, *Chemistry of Materials* **2008**, *20*, 4519.
[103] T. Curtius, K. Hochschwender, Hydrazides and azides of organic acids. XXXI. The hydrazides and azides of oxalic acid, *Journal für Praktische Chemie* **1915**, *91*, 415.
[104] T. M. Klapötke, J. Stierstorfer, Nitration Products of 5-Amino-1H-tetrazole and Methyl-5-amino-1H-tetrazole – Structures and Properties of Promising Energetic Materials, *Helvetica Chimica Acta* **2007**, *90*, 2132.
[105] D. Fischer, Master thesis, Ludwig-Maximilians-University, Munich, **2010**.

Table 43 Sensitivity, stability, and performance data of compounds **1**–**6**.

	1	**2**	**3**	**4**	**5**	**6**	**RDX**
Formula	$CH_5N_5O_2$	$CH_7N_5O_4$	$C_2H_8N_{10}O_2$	$C_2H_8N_{10}O_2$	$C_2H_8N_{10}O_2$	$C_2H_8N_{10}O_2$	$C_2H_8N_{10}O_2$
FW /g mol^{-1}	119.08	153.12	204.15	163.13	181.11	248.21	222.12
IS / J	20	9	10	2	11	8	7.5
FS / N	144	288	240	40	360	240	120
ESD / J	0.15	0.6	0.1	0.3	0.3	0.4	0.1-0.2
N / %	58.81	45.74	68.60	60.12	38.37	67.72	37.80
Ω / %	-33.6	-15.7	-47.0	-14.7	-22.1	-64.5	-21.6
T_{dec} / °C	184	242	200	180	270	210	210
ρ / g cm^{-1}	1.767	1.782	1.742	1.758	1.84	1.57	1.8
$\Delta_f H_m^\circ$ / kJ kg^{-1}	77	-180	428	291	-299	569	70
$\Delta_f U^\circ$ / kJ kg^{-1}	770	-1048	2227	1895	-1536	2419	417
EXPLO5 values							
$-\Delta_{Ex}U^\circ$/ kJ kg^{-1}	4934	5048	4841	6113	4661	4781	6125
T_{det} / K	3436	3391	3248	4219	3275	3091	4236
P_{CJ} / kbar	323	335	317	371	325	255	349
D / m s^{-1}	8977	8903	8858	9236	8655	8309	8748
V_0 / L kg^{-1}	890	910	843	853	827	847	739

Preparation of the Explosive Charges

Caution! *The preparation of the explosive charges should be done carefully and with full body protection (helmet, Kevlar® gloves, leather coat or vest, ear protection). There must be a second person present in case of emergency. No metal tubes (except detonators) should be used inside the detonation chamber! The chamber must be cleaned after each shot. If steel disks are replaced by polycarbonate (e. g. for high speed videos) the maximum charge is reduced to 100 g of TNT!*

The comparison of the old and new experimental set up for measuring the detonation velocity is shown in Figure 54 and 55. New experiments were carried out using a plastic tube of 10 cm length, 0.14 cm diameter, 0.8 cm wall thickness, and 1 cm bottom thickness. Small holes were drilled into the plastic tube to fix the optical fibers (Ø 1 mm, covered by PE jacket, overall thickness 2.2 mm from). Depending on the amount of fibers used for the test, the distances between two holes should be between 0.15 cm and 0.45 cm. Most of the experiments were done with two probes and a distance of 0.2 cm. The distance between the last probe and the bottom should be 0.5–1 cm.
About 5 mm of the PE jacket were removed carefully from one end of the fiber (complete length ~ 1 m for each fiber). Both ends were cut off with a sharp knife in order to obtain a plane end surface of the fiber. If necessary, the ends can be planed using sandpaper. The end without PE is plugged into the plastic tube to the beginning of the explosive compound. All probes must be vertical to the tube surface and with the same length inside the tube. The transmittance of the fibers should be checked with a laser pointer and the tube should be fixed in a bench vise in order to be filled with explosive.
Average amounts of the explosives for one test were 10–25 g, in order to obtain a homogenous detonation wave and a good value for the detonation velocity. The distance between the first optical fiber and the detonator and/or booster (e. g. PETN 0.2–1 g) should be 2.5 fold of the tube diameter. Before and after filling the compound inside the tube, height and diameter should be measured with a sliding caliper to calculate the density. The explosive is pressed carefully with a small round piece of wood or plastic.
For all VOD tests standard detonators DYNADET-C2-0ms (containing PETN and RDX) from ORICA Mining services were used.

a

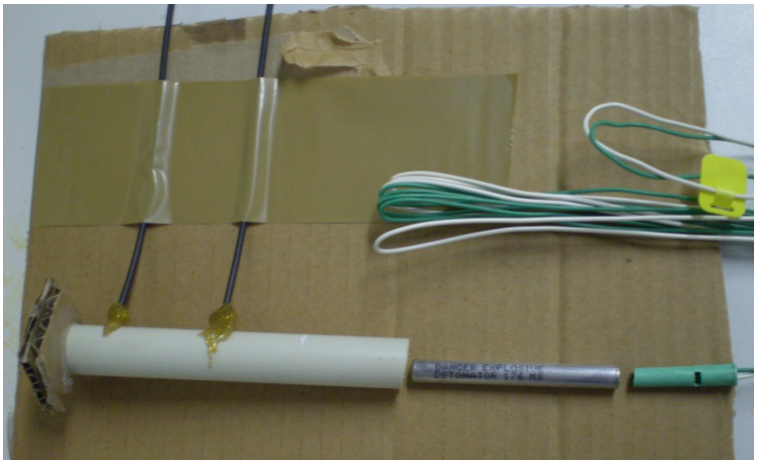

b

Figure 54 Previous (**a**) and presently (**b**) used set up for detonation velocity experiments.

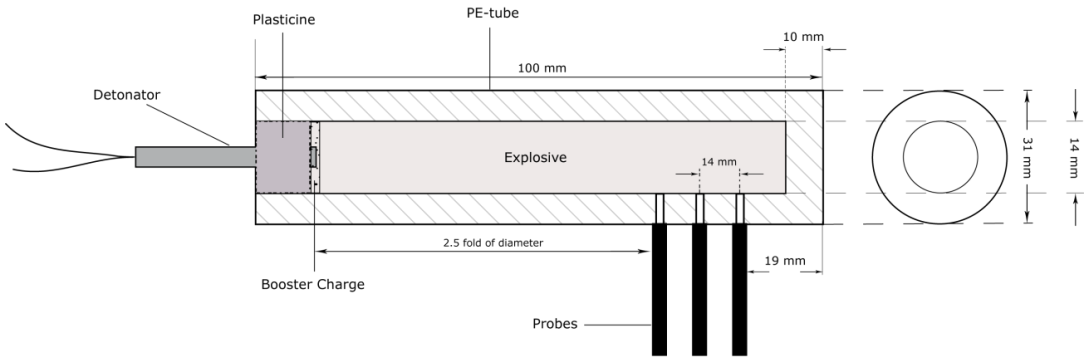

Figure 55 Presently used set up for detonation velocity experiments (schematic).

Experimentally Determined VODs

The results of the detonation velocity experiments are illustrated in Table 45–49. Obviously, single detonation velocities of the particular measurements show deviance between several hundred and thousand meters per seconds. The detonation velocities of **1**, D1,2 in VOD1 with 9650 m s^{-1} and D2,3 in VOD2 with 9493 m s^{-1} (Table 44) exceed the detonation velocities of 8977 m s^{-1} calculated for crystal density (1.77 g cm^{-3}), as well as for the respective density of 1.34 g cm^{-3}. Compound **2** was only initiated by a booster charge of 0.32 g PETN. The measured individual detonation velocities are around 6000 m s^{-1} (Table 44) for a density of 1.48 g cm^{-3}, thus around 1000 m s^{-1} lower than the calculated value of 7855 m s^{-1}. No more than 40 g of compound **1** and **2** were synthesized and therefore they were tested only twice. To compare these values with theoretical values additional measurements need to be performed. **3** could not be ignited above a density of 1.162 g cm^{-3}, which leads to a VOD of 3381 and 5572 m s^{-1}, compared to the calculated VOD of 6387 m s^{-1}. Assuming that an increased density of compound **3** causes a higher critical diameter, even increasing the standard diameter of 14 mm to 20.5 mm (VOD3) a detonation was still not observed (Table 45). The average detonation velocity of compound **4** with 6216 m s^{-1} conforms to the computational value of 6525 m s^{-1}, although the individual detonation velocities differ by around 2000 m s^{-1} (Table 46). Similar to **1** and **2** further experiments of **4** needs to be performed. Despite analogue conditions and similar densities, average values between 4000 and 5000 m s^{-1} of VOD1 and 2 (Table 47) for compound **5** disagree with the average detonation velocities of VOD3 – 5. Latter experimental values are in good agreement with the calculated values of around 7000 m s^{-1} for a density between 1.3 and 1.4 g cm^{-3}. Just as compound **3**, **6** was not ignitable above a density of 1.169 g cm^{-3}, however, at higher densities it could be ignited by using 0.2 g PETN/0.3 g RDX (Table 48). The obtained value of 3454 m s^{-1} is about 2000 m s^{-1} lower than the calculated VOD.

Due to the large deviations of VOD results it becomes apparent that experimental VODs are still influenced by several external and internal effects. One important influence on detonation velocity experiments is the density of the explosive material. The denser the sample is pressed into the tube, the higher is the detonation velocity, whereas high homogeneity throughout the whole length is aspired. However, directly pressing the loose sample into the tube causes layers of different densities and a density gradient. This may have a significant effect on the detonation velocity, since the velocity increases in more dense layers, which can be a reason for the variance of the single measured VODs. In addition, the pressure of the shock wave leads to a dynamic compression of the unreacted material, resulting in a significant temperature and pressure increase, which obviously has different effects depending on the density. Moreover, air gaps are a main issue concerning detonations and the shock front in particular. Since the shock front travels faster through air gaps than through the explosive material, this leads to an inhomogeneous and faster forwarding of the detonation front, which suggests a higher detonation velocity. To avoid these air gaps a high density is aspired.

In contrast the negative effect of too high densities can be seen in the detonation velocity tests of dihydroxylammonium 5,5-bistetrazolate (**3**), which became unreactive. Discussing VOD results for high densities, the critical diameter for the respective compound must be considered. For good detonation velocity measurements, a stable and mainly planar detonation front is also favored. In the early stages of the detonation, the shock front expands tapered and becomes planar with increasing propagation. Thus, a preferably long distance between the point of ignition and the first optical fiber is desired. A large amount of explosive is necessary or compromises between tube length and the amount of material have to be made. The tube length and the preferably long traveling distance of the detonation front to the first optical fiber also limited the distance between the points of measurement, which leads to a higher error margin. In addition, the diameter of the optical fiber itself (1 mm) and the distance of 14 mm to the second optical fiber lead to a greater range of error.

A good experimental set up considers all the above mentioned complex problems; therefore modifications of the old set up were conducted. Preferable would be a tube length (confinement) of more than 15 cm with an appropriate diameter to provide a stable and planar detonation front and to consider the critical diameter of an explosive. Most energetic materials have small critical diameter (except TNT) and a tube diameter of 2 cm should be enough for densities below crystal density. Large tube length requires large amounts of explosives. Hence, this parameter wasn't changed for the new set up to avoid the synthesis of more than 50 g of secondary explosives for one experiment. To obtain high densities and a better fixing of the optical fibers tubes used during the master thesis were replaced by

tubes with a wall thickness of 8 mm and a bottom thickness of at least 10 mm (Figure 55). Alternatively, the explosive can be pressed into pellets prior to use and loaded afterwards. However, this method can lead to extra air gaps between confinement and pellet while using tubes. Another method would be a fixing of several pellets by small amounts of glue and the exchange of the optical fibers my metal pins or plates.
It was found that covalent bonded compounds such as picric acid or HMX (Table 49) show comparable values whereas most of the salts tested within this thesis show strong deviations of the calculated values. Therefore it can be assumed that values of symmetric and/or covalent bonded molecules indicate more homogenous (more ideal) detonation behavior then ionic molecules and leading to more comparable VODs.

The experimental determination of detonation velocities is still a complex task with many parameters and effects to consider, which influence and interfere with each other. Despite the experimentally determined detonation velocities, the tested compounds, especially 1-amino-3-nitroguanidine (**1**), dihydroxylammonium 5,5´-bistetrazolate (**3**) or oxalylhydrazide nitrate (**5**) remain promising new secondary explosives since they are cheap and easy to synthesize and they show very good calculated detonation parameters.

Table 44 Experimental detonation velocities of compound **1** and **2**.

Compound 1	VOD 1	VOD 2	**Compound 2**	VOD 1	VOD 2
Ø / mm	14.1	14.1		14.1	14.1
h_{empty} / mm	100.1	100.2		100.4	100.2
h_{loaded} / mm	73.9	93.9		83.7	86.7
m / g	16.1	21.8		17.0	20.0
ρ / g cm^{-3}	1.387	1.481		1.305	1.482
$m_{booster}$ / g	0.3 (PETN)	-		-	0.32 (PETN)
$x_{1,2}$ / mm	15.4	14.7		14.6	14.2
$x_{2,3}$ / mm	14.3	14.2		14.3	14.1
$D_{1,2}$ / m s^{-1}	9650	7726		-	6780
$D_{2,3}$ / m s^{-1}	5958	9493		-	5862
D_{av} / m s^{-1}	7804	8610		-	6321
D_{cal} / m s^{-1}	7507	7846		7246	7855

Table 45 Experimental detonation velocity of compound **3**.

Compound 3	VOD 1	VOD 2	VOD 3	VOD 4	VOD 5
Ø / mm	14.1	14.0	20.5	14.0	14.0
h_{empty} / mm	100.4	99.9	100.0	99.9	99.9
h_{loaded} / mm	82.29	86.4	92.9	87.8	90.0
m / g	15.0	18.5	40.0	19.0	10.0
ρ / g cm^{-3}	1.162	1.389	1.303	1.401	0.721
$m_{booster}$ / g	-	-	1.0 (RDX)	0.3 (PETN)	-
$x_{1,2}$ / mm	14.5	14.0	14.8	14.0	14.1
$x_{2,3}$ / mm	13.9	13.9	13.9	14.0	14.0
$D_{1,2}$ / m s^{-1}	3381	-	-	-	4375
$D_{2,3}$ / m s^{-1}	5572	-	-	-	3888
D_{av} / m s^{-1}	4477	-	-	-	4132
D_{cal} / m s^{-1}	6387	-	-	-	4695

Table 46 Experimental detonation velocity of compound **4**.

Compound 4	VOD 1
Ø / mm	14.2
h_{empty} / mm	100.4
h_{loaded} / mm	85.8
m / g	15.0
ρ / g cm^{-3}	1.101
$m_{booster}$ / g	-
$x_{1,2}$ / mm	14.4
$x_{2,3}$ / mm	14.1
$D_{1,2}$ / m s^{-1}	7220
$D_{2,3}$ / m s^{-1}	5211
D_{av} / m s^{-1}	6216
D_{cal} / m s^{-1}	6525

Table 47 Experimental detonation velocity of compound **5**.

Compound 5	VOD 1	VOD 2	VOD 3	VOD 4	VOD 5
Ø / mm	14.1	14.0	14.1	20.6	14.0
h_{empty} / mm	100.2	100.0	100.1	100.1	100.1
h_{loaded} / mm	88.8	87.3	88.3	90.0	87.2
m / g	22.0	20.0	18.0	39.9	19.4
ρ / g cm^{-1}	1.577	1.486	1.309	1.331	1.443
$m_{booster}$ / g	0.3 (PETN)	-	-	-	-
$x_{1,2}$ / mm	14.0	14.0	14.0	13.8	14.1
$x_{2,3}$ / mm	14.1	14.0	14.0	14.1	14.0
$D_{1,2}$ / m s^{-1}	5048	Calc.	5600	8088	5620
$D_{2,3}$ / m s^{-1}	4689	3927	7777	6125	8763
D_{av} / m s^{-1}	4869	8975	6689	7107	7192
D_{cal} / m s^{-1}	7765	7401	6877	6949	7318

Table 48 Experimental detonation velocity of compound **6**.

Compound 6	VOD 1	VOD 2	VOD 3	VOD 4
Ø / mm	14.0	14.2	14.2	14.0
h_{empty} / mm	100.2	100.4	100.3	100.0
h_{loaded} / mm	85.8	88.8	85.7	85.5
m / g	22.0	22.0	20.0	15.4
ρ / g cm^{-1}	1.667	1.564	1.473	1.169
$m_{booster}$ / g	-	0.3 (PETN)	0.8 (PETN)	0.2 PETN / 0.3 RDX
$x_{1,2}$ / mm	14.3	14.0	14.5	14.0
$x_{2,3}$ / mm	14.1	14.1	14.0	13.9
$D_{1,2}$ / m s^{-1}	-	-	-	3671
$D_{2,3}$ / m s^{-1}	-	-	-	3236
D_{av} / m s^{-1}	-	-	-	3454
D_{cal} / m s^{-1}	8702	8290	7935	6443

Table 49 Calculated and experimental VOD for common explosives (Lit. values[106]).

Explosive	**Exper. [m s^{-1}]** (**Density [g cm^{-3}]**)	**Calc. [m s^{-1}]** (**Explo5**)[93]	**Distance** [mm]	**Literature** (**Density [g cm^{-3}]**)
Picric acid[a]	5130 (0.9)	4959	20	7400 (1.76)
	5263 (0.9)		20	
	4615 (0.9)		24	
	4181 (1.0)	5314	23	
	7000 (1.3)	6117	21	
HMX[a]	6000 (1.0)	6075	21	9100 (1.95)
	6250 (1.1)	6402	20	
	9523 (1.3)	7128	20	
RDX[a]	7600 (1.0)	6088	19	8700 (1.89)
	4617 (1.0)		20	
TNT[b]	1919 (1.0)	5154	19	6930 (1.61)
	2777 (1.0)		20	
	9130 (1.3)	7176	21	
PETN[b]	7741 (0.9)	5587	24	8260 (1.76)
	2238 (0.9)		45	
	8333 (1.2)	6585	20	
	7219 (1.3)	6896	44	
NGA1[b,c]	4181 (0.6)	4812	23	8895 (1.79)
	8333 (0.8)	5482	20	
	6250 (1.0)	6257	35	
NGA2[b,c]	5405 (1.0)	5885	20	8750 (1.79)

[a] ±4 % error
[b] ±3 % error
[c] nitro glycerin analogue[47]

[106] J. Köhler, Explosivstoffe, 10. Auflage, Wiley-VCH, **2008**.

EXPLO5 calculations

Calculations of the detonation parameters were carried out using the EXPLO5 V5.04 code.[93] The program is based on the steady-state model of equilibrium detonation, referring to the BECKER-KISTIAKOWSKY-WILSON equation of state (BKW EOS) for gaseous detonation products and the COWAN-FICKETT equation of state for solid carbon.[107] The calculation of the equilibrium composition of the detonation products is achieved by applying the modified WHITE-JOHNSON-DANTZIG free energy minimization technique. The program is designed to enable the calculation of detonation parameters at the CHAPMAN-JOUGUET (CJ) point. The BKW equation in the following form was used with the BECKER-KISTIAKOWSKY-WILSON-NEUMANN (BKWN) set of parameters $(\alpha, \beta, \kappa, \theta)$ as stated below, with X_i being the mol fraction and k_i the molar covolume of the *i*-th gaseous product (see also chapter 1, Introduction).[107,108]

$$\frac{pV}{RT} = 1 + xe^{\beta x} \qquad x = \frac{(\kappa \Sigma X_i k_i)}{[V(t + \theta)]^{\alpha}}$$

$$\alpha = 0.5, \qquad \beta = 0.176, \qquad \kappa = 14.71, \qquad \theta = 6620.$$

VOD values of compound **1** – **6** were calculated for the respective density achieved in the particular experiments and for crystal density. All important data is given in Table 44-48. Experimental densities vary from 0.7 to 1.6 g cm^{-3}, whereas crystal densities are in the range of 1.6 to 1.8 g cm^{-3}. Beside compound **4** and **5** all theoretical VODs obtained for the crystal density are higher than the VOD of RDX with 8748 m s^{-1} at a density of 1.80 g cm^{-3} (Table 43, 46, 47). Moreover, compound **4** has a detonation velocity of 9236 m s^{-1} for a density of 1.75 g cm^{-3}.

The averaged experimental values between optical fiber 1 and 2 and between 2 and 3 of several measurements of compound **1**, **3**, **4** and **5** match the computational values, although significant deviation of the single VODs in each experiment are observed. VODs measured for several common explosives, listed in Table 49, are in good agreement with their calculated values, especially for HMX, NGA1 and 2. Due to the large critical diameter of TNT experimental values are not conform to its theoretical detonation velocity.

[107] M. Suceska, Calculations of the detonation properties of C-H-N-O explosives, *Propellants, Explosives, Pyrotechnics* **1991**, *16*, 197.

[108] a) M. Suceska, Calculation of detonation parameters by EXPLO5 computer program, *Material Science Forum*, **2004**, 465 b) M. Suceska, Evaluation of detonation energy by EXPLO5 computer code results, *Propellants, Explosives, Pyrotechnics* **1999**, *24*, 280 c) M. L. Hobbs, M. R. Baer, Proceedings of the 10th Symposium (International) on Detonation, ONR 33395-12, Boston, **1993**.

Because all calculations consider the ideal behavior of a detonation and equilibrium of the detonation products it is not possible to match these values with experimental detonation velocities perfectly. The obtained deviations for several experiments are in the range of tolerance and the average values are still comparable with the theoretical detonation velocities.

Conclusion

The detonation velocity is one of the most important parameters discussing secondary explosives. Because it is relatively easy to calculate the detonation parameters for most of the new synthesized energetic materials, the experiment is still challenging.

A couple of new explosives which meet the high requirements as possible RDX replacements were synthesized within our research group. Several detonation velocity experiments were performed and the results compared with the calculated values obtained with the EXPLO5 code. It was further investigated if the old set up established during the master thesis was improved by changing the density of the compound and the confinement. As expected for experimental values the deviation of the single VODs is high and the mean values are comparable with the calculated values. Although the experiments are influenced by many parameters like density, crystal size and/or shape, air gaps, confinement, etc. the obtained results for all tested compounds are acceptable especially for oxalyldihydrazide nitrate. It was further observed that compounds with a symmetric molecular unit like RDX or HMX show better (more ideal) detonation characteristics than the tested salts.

In summary it can be stated that both set ups (old and new) are applicable. The advantage of the new set up is a better fixing of the optical fiber and the possibility of higher densities due a higher wall thickness of the confinement. Because of safety reasons the amount of new synthesized explosive compounds is limited. The advantage of the old set up is the need of less quantities of explosive material. Therefore from safety aspects and synthesis cost (each VOD should be repeated at least 3-5 times) the old set up is still useful.

Experimental Section

Equipment

Caution! *Although no problems occurred during the synthesis and handling of the materials studied in this work, some of the neutral compounds and their salts are sensitive energetic materials. Safety equipment such as Kevlar® gloves, leather coat, wrist protection, face shield, ear protection, grounded equipment, and shoes are mandatory.*

General Method. All chemicals and solvents were used as received (Sigma–Aldrich, Fluka, Acros Organics) unless stated otherwise. MELTING POINTS were measured with a Linseis PT10 DSC, calibrated with standard pure zinc and indium. Measurements were performed at a heating rate of 5°C min^{-1} in a closed aluminum sample pan with a 1 µm hole on top for gas release and under a nitrogen flow of 20 mL min^{-1} with an empty identical aluminum sample pan as reference. The values were checked by a Büchi Melting Point B-450 apparatus. The M. p. values are not corrected. MASS SPECTROMETRY was conducted on a JEOL MStation JMS 700 machine. All NMR SPECTRA were recorded with a Jeol Eclipse 270, Jeol EX 400, or a Jeol Eclipse 400 instrument. The chemical shifts are quoted in ppm relative to TMS (^{1}H, ^{13}C), and $MeNO_2$ (^{14}N, ^{15}N). For NMR signals the common abbreviations were used: s (singlet), d (duplet), t (triplet), q (quartet), and m (multiplet). INFRARED (IR) SPECTRA were recorded with a Perkin–Elmer Spektrum One *FT-IR Spectrum BXII* with *Smith ATR Dura Sample IRII* instrument. The absorption is given in wave numbers (cm^{-1}) with a range of 100 to 4000 cm^{-1}. Transmittance values are qualitatively described as very strong (vs), strong (s), medium (m), weak (w), and very weak (wv). RAMAN SPECTRA were measured with a Bruker MULTIRAM 1064 2000R NIR FT-Raman instrument equipped with a Nd:YAG laser (1064 nm). The intensities are given in percentages of the most intense peak and are given in parenthesis. ELEMENTAL ANALYSES (C, H, N) were performed with a Vario El and Netsch STA 429 Simultaneous Thermal Analyzer. SENSITIVITY DATA were determined using a BAM drop hammer, BAM Friction tester, and an OZM electrical discharge testing device.[52,53]

Synthesis

Hydroxylammonium 5-nitriminotetrazolate (4)

5-Nitriminotetrazole (1.59 g, 12.2 mmol) was dissolved in a few mL water and a solution of silver nitrate (2.07 g, 12.2 mmol) was added. Silver 5-nitriminotetrazolate precipitated instantly as a white solid. The product was filtered off and washed with water to remove excess of acid. The white solid was resuspended in 50 mL of warm water and treated with a solution of hydroxylammonium chloride (0.84 g, 13.0 mmol) in 20 mL water. The mixture was stirred at 30°C for 1 h with exclusion of light and the formed silver chloride was filtered off. The filtrate was evaporated and the residue recrystallized from ethanol/water to yield **4** as a white solid (1.70 g, 85%). **DSC** (5°C min^{-1}): T = 180°C (dec.); **IR** (KBr): $\tilde{\nu}$ = 3125 (s), 2958 (s), 2776 (m), 2711 (s), 1617 (m), 1598 (m), 1539 (s), 1431 (s), 1383 (m), 1321 (vs), 1244 (m), 1213 (m), 1188 (m), 1153 (m), 1108 (m), 1061 (m), 1039 (m), 1003 (m), 872 (w), 823 (w), 777 (w), 753 (w), 742 (w), 700 (w), 493 (w); **Raman** (300 mW): $\tilde{\nu}$ = 2715 (1), 1541 (100), 1452 (1), 1433 (1), 1381 (4), 1332 (36), 1158 (7), 1110 (4), 1070 (4), 1036 (22), 1014 (85), 875 (8), 744 (14), 695 (1), 494 (3), 427 (4), 413 (15); **^{1}H NMR** (d_6 DMSO, 25°C): δ = 10.95; **^{13}C NMR** (d_6 DMSO, 25°C): δ = 158.3; **MS** m/z (FAB^+): 34.0 [NH_3OH^+]; m/z (FAB^-): 129.1 [$HATNO_2^-$]; **EA** ($CH_5N_7O_3$, 163.10): found(calc.): C 7.38(7.36), H 3.09(3.17), N 60.12(57.40) %; **Sensitivity data**: IS 2 J, FS 40 N, ESD 0.30 J; grain size: 100 - 500 µm.

Oxalyldihydrazide nitrate (5)

1.18 g (10 mmol) Oxalyldihydrazide was added to a mixture of 5.5 mL 2 M nitric acid and 10 mL water. The suspension was heated up until all oxalyldihydrazide has dissolved and then poured to 20 mL ethanol. The suspension was cooled to 5°C, filtered off and dried at r. t. Yield: 1.68 g (93%) of colorless crystalline **5**. **DSC** (5°C min^{-1}): 273°C (dec.); **IR** (ATR): $\tilde{\nu}$ = 3307 (w), 3178 (w), 3028 (w), 2775 (w), 1674 (m), 1531 (m), 1326 (s), 1243 (s), 1152 (w), 1088 (w), 995 (m), 802 (m), 709 (m); **Raman** (300 mW): $\tilde{\nu}$ = 3224 (4), 1735 (9), 1703 (15), 1584 (12), 1553 (28), 1346 (19), 1289 (23), 1206 (9), 1094 (10), 1049 (100), 1003 (4), 938 (15), 812 (2), 719 (7), 510 (5), 400 (5); **^{1}H NMR** (d_6 DMSO, 25°C): δ = 8.28; **^{13}C{^{1}H} NMR** (d_6 DMSO, 25°C): δ = 157.8; **EA** ($C_2H_7N_5O_5$, 181.11): found(calc.): C 13.50(13.26), H 3.74(3.90), N 38.59(38.67) %; **Sensitivity data**: IS 11 J, FS 360 N, ESD 0.3 J; grain size 500-1000 µm.

SUMMARY

One area of our research group is the synthesis of new additives for mainly red and green pyrotechnics and infrared signal flares. So far, the research on pyrotechnics comprises only the synthesis of new compounds and a visible impression of the emitted color. Because one important effect of pyrotechnics is the emission of light the major concerns are now on evaluating the color purity of the light (visible pyrotechnics) or the amount of emitted radiation (infrared pyrotechnics).

Commonly used near infrared emitting pyrotechnics are so called *Black Knight* compositions. They consist of potassium or potassium and cesium nitrate, silicon powder, hexamine and a binder. In combination with night vision devices NIR pyrotechnics are used e. g. for illuminating large (battle) fields at night. Hence, the present thesis concentrates on several objectives:

- the establishment of a set up for radiometric NIR emission experiments with the new OCEAN OPTICS spectrometer and further the development of a MATLAB code for evaluating the obtained data.
- the synthesis of several potassium and cesium high nitrogen compounds, such as bistetrazolates, azotetrazolates or triazolates (Figure A)
- the preparation of new formulations based on *Black Knight* compositions
- the determination of their sensitivity data concerning impact, friction and electric discharge and decomposition behavior
- the comparison of the data obtained from the MATLAB code with standards given in literature and with 46 new prepared formulations

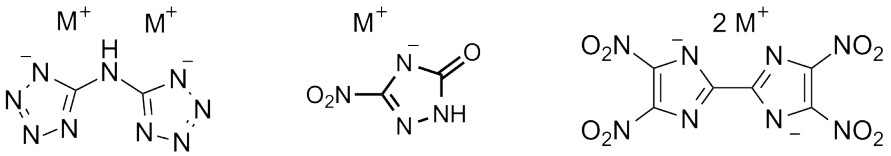

Figure A Chemical structures of BTA (**left**), NTO (**mid**), and TNBI (**right**) salts (M = K, Cs).

The most important topic which is related to the work with explosives/energetic materials is safety. Exclusively all new pyrotechnic formulations are insensitive against impact or electric discharge. Only few compositions (e. g. BK_RDX, _CsAzOT) are sensitive (25-7 J) against impact and several (e. g. NTO5, BTA2) are moderately sensitive (35-25 J). The blending of the compounds with the remaining ingredients and the preparation of pressed pellets proceeded without complications. Only several possible hexamine replacements (DETT, EDD, DETP) are incompatible with the other components.

As additives in pyrotechnic compositions it is assumed that high nitrogen compounds release large amounts of nitrogen and dissipate condensed reaction products from the hot core zone. Hence, they can improve the radiant emission.

In summary it can be stated that high nitrogen compounds did not necessarily improve the combustion behavior of *Black Knight* compositions. Several formulations comprising e. g. K and Cs 4,4´,5,5´-tetranitro-2,2´bisimidazole, 5,5´bistetrazolyl amine or 3,3´-bis(1,2,4-oxadiazol-5-one) show large flame sizes and a good burning behavior (steady combustion). In contrast formulations comprising 5-aminotetrazole, 5,5´-bistetrazolate or 5,5´-azotetrazolate produce sparks, where impossible to be lighted or burned with very small flame sizes and consequently low IR output. Although the IR output of most of the formulations is in the region of reference formulations several compounds (BOX, DNT, BTA, TNBI) are still of further interest.

Since the establishment of the new set up the work on pyrotechnics is no longer limited to the synthesis of new materials. A further important tool which might be now useful is the calculation of several pyrotechnic parameters. To understand the different combustion characteristics of similar constituted pyrotechnic flares variables like the oxygen balance, heat of formation, temperature or oxidizer to fuel ratio should be investigated. Several calculations were carried out within this thesis. Although the oxygen balance of the composition influences the burn characteristics no trend could be observed for new formulations. However, an O/F ratio of 2.33 results in good burn times and is therefore recommended for future experiments. The attention should be also focused on the heat of formation, due to a high influence on the spectral efficiency.

Experiments with different mixed grain sizes prove the importance of the homogeneity of the composition. In addition to safety reasons it might be meaningful to use ultra sonic mixing devices or industrial mixing equipments.

Future work should also comprise additives like boron or ferric oxide, due to a positive effect on the burn rate. Different binders like laminac or lupersol should be tested to further decrease the amount of visible light and therefore to increase the concealment index χ ($I_{\mathrm{NIR}}/I_{\mathrm{Vis}}$).

Improvements of the burn rate or NIR emission could be obtained by adding nitrocellulose or ammonium nitrate to some extent. However, the amount of IR emitting compounds (potassium and cesium) should be still high.

A second project which was related to the area of pyrotechnics comprises the synthesis of new additives for MTV decoy flares. These flares consist of the materials magnesium (fuel), Teflon® (oxidizer) and Viton® (binder) and are used as aerial infrared countermeasure to counter a homing missile. Hostile missiles detect the IR signature of an aircraft which is given by the α/β ratio.

Commonly used MTV decoys produce small hot core zones compared to the size of an aircraft. Therefore new additives in MTV payloads should contain a large amount of fluorine due to the oxidizing effect and a large number of N–N or C–N bonds due to the formation of nitrogen. Similar as for NIR pyrotechnics discussed above it is assumed that a high nitrogen content enlarges the surface of the hot core zone, disseminates reaction products and improves the radiant emission.

Based on the PhD thesis of H. RADIES several compounds are of interest (Figure B).

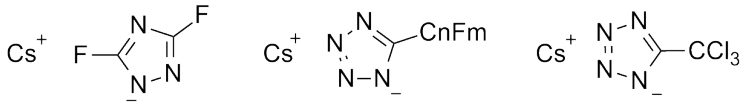

Figure B Chemical structures of cesium difluoro-1,2,4-triazolate (**left**), cesium trifluoromethyl tetrazolate (C_nF_{2n+1}) (**mid**), and the chlorine derivative (**right**) for n = 1; m = 3.

Compound **2** was synthesized *via* trifluoro acetonitrile and sodium azide and the resulting sodium salt was converted into the cesium salt. The cesium salt was fully characterized and the obtained data compared with values given in literature. 50 g of the compound were sent to the Frauenhofer Institut for several stability and decomposition experiments.

A further interesting compound is trichloromethyl tetrazole and its salts. Several attempts were carried out to synthesize **3**. Although the compound is mentioned in literature it could not be isolated. Only weak signals observed in the mass spectra indicate the existence of this salt.

The last topic of this thesis concentrates on a possible new set up for experimental detonation velocity tests. The detonation velocity (VOD) is one important parameter concerning new secondary explosives. While it is relatively easy to calculate several detonation parameters, experimental values are normally not expected to be identical with the calculated values. The old set up established within the master thesis is useful for small charges and low densities. Therefore the confinement was changed and several possible RDX replacements (Figure C) synthesized in our research group were tested with the new setting.

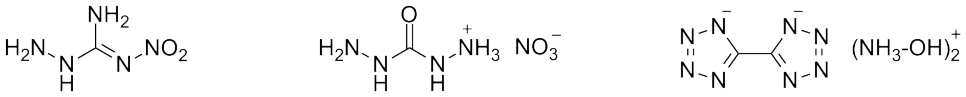

Figure C Small overview of the investigated compounds 1-amino-3-nitroguanidine (**left**), diaminouronium nitrate (**mid**), dihydroxylammonium 5,5-bistetrazolate (**right**).

The obtained values were compared with the calculated values for each compound and with both values obtained for RDX. As expected the deviations of individual VODs are large. However, the average values for several compounds e. g. 1-amino-3-nitroguanidine, hydroxylammonium 5-nitriminotetrazolate, and oxalylhydrazide nitrate are in a good range. As desired the densities of the material for each test were higher compared to the old set up. But not all compounds detonate at high densities e. g. dihydroxylammonium 5,5-bistetrazolate, and 1,3,5-triaminoguanidinium 1-methyl-5-nitriminotetrazolate.

It was found that both set ups are applicable. Depending on the sensitivity data of new synthesized compounds the old set up is preferable due to lower amounts of explosive. The new set up is useful for large charge sizes of 30–40 g and higher densities depending also on the critical diameter of the compound.

APPENDIX

Abbreviations and Conversations

ANFO	Ammonium nitrate fuel oil
BAM	Bundesanstalt für Materialforschung und –prüfung
BK	'Black Knight' (pyrotechnic composition)
br	broad
calc.	calculated
Cd	Candela
conc.	concentrated
dec.	Decomposition
δ	Chemical shift in ppm (NMR)
DSC	Differential Scanning Calorimetry
d	Duplet (NMR)
EM	Energetic material
FOV	Field of View
h	Hour(s)
HEM	High energetic material
HNC	High Nitrogen Compound
HMX	Octahydro-1,3,5,7-tetranitro-1,3,5,7-tetrazocine
HNS	Hexanitrostilben
IR	Infrared spectroscopy
IR	Infrared (spectral region)
J	Joule
Lit.	Literature
M.p.	Melting point
MTV	Magnesium Teflon® Viton® (Flare composition)
m	medium (Intensity in the IR spectra)
m	Multiplet (NMR)
M	mol L^{-1}
min	Minutes
mL	Milliliter
ms	Milliseconds
NIR	Near Infrared (spectral region)
nm	Nanometer
NMR	Nuclear Magnetic Resonance
NTO	3-Nitro-1,2,4-triazol-5-on
PETN	Pentaerythritol tetranitrate
ppm	parts per million

RDX	Hexogen
r. t.	room temperature
s	Singlet (NMR)
s	strong (Intensity in the IR spectra)
s	seconds
θ	Theta
t	Triplet (NMR)
t	Tons
TFAA	Trifluoroacetic anhydride
TCAA	Trichloroacetic anhydride
Ω	Oxygen balance
VOD	Velocity of Detonation
vs	very strong (Intensity in the IR spectra)
w	weak (Intensity in the IR spectra)
W/sr	Watt / steradian
χ	Concealment Index (I_{NIR}/I_{Vis})

User guide for the HR2000+ES Spectrometer (only Irradiance measurements)

Measurements required a dark and sample spectrum with the same integration time and calibration file. It is not necessary to store a reference spectrum. Absolute irradiance measurements are not relative to another measurement.[15]

1. Open SpectraSuite
2. Click inside the Graph (A) window to show the selected settings (Data sources)
3. Set Integration time (100 ms)
4. Select Absolute Irradiance Measurement (via File/New… or Icon Ī)
5. Wizard window opens -> Select Existing Acquisition (Aktive Erfassung)
6. Select Source (only one spectrometer is selectable)
7. Get Irradiance Calibration from File
8. Browse HR+C1888_090811_OOIIrrad.cal file (should be already selected!)
9. Select Fiber Diameter (fix: 3900 microns! of cosine corrector)
10. Switch-off the light and measure dark spectrum by click on the dark lamp button
11. Finish -> an active Absolute Intensity Graph (B) appears
12. Click inside Graph (B) window to highlight them in the Data source window
13. Select Processing -> processing mode -> Minus Dark Spectrum
14. A new Graph (B) appears with a new y-axis (Intensity in counts)
15. Select File -> Save -> Save spectrum -> Save window appears
16. Highlight Data source HR+C1888, Dark spectrum subtracted!
17. Select Save every scan and Stop after number of scans: e. g. 350
18. Data options -> select Tab separated with (or without) headlines
19. Save within your folder (browse) -> give a name -> number of character: e. g. 1
20. NOTICE: Push the 'Accept' button not until starting your measurement, means light your flare!! If you do so the measurement starts from that time on!
21. Switch-off the light and ignite sparkler
22. When the sparkler ignites the flare push the 'Accept' button
23. Wait till all data is saved
24. Run x,y-files through MATLAB codes (CD) for intensity values and plots

Matlab code for Intensity and 3D plots

```
%Eingaben-----------------------------------------------------------------
----

prompt = {'Integration time','Datapoints','Headerlines',}; %data
window opens
dlg_title = 'Konstanten'; %titel
num_lines = 1;
def = {'0.1','2030','17'}; %fixed values (integration time, data
points, headlines)

answer = inputdlg(prompt,dlg_title,num_lines,def); %output
int_zeit = str2num(answer{1}); %integration time
datapoints=str2num(answer{2}); %distance to detector
headerlines=str2num(answer{3}); %headerlines (file format ocean optics
txt file)

%push buttons
uicontrol('style','pushbutton','string','Open Files',...
                'units','normalized','position',[.0 .9 .2 .1],...
                'callback','folder = uigetdir()')

uicontrol('style','pushbutton','string','Plot',...
                'units','normalized','position',[.2 .9 .2 .1],...
                'callback','uiresume(gcbf)')


uiwait;
cd(folder);
dirListing = dir(fullfile(cd, '*.txt')); % opens data
numfiles = size(dirListing,1); % number of data

% Input-Data manipulation-------------------------------------------------

for x = 1:numfiles %For-loop changes ',' by '.'
Filex = dirListing(x).name;
 Name{x}=textscan(Filex,'%s%s','delimiter','.');
    Filex    = memmapfile(Filex,'Writable',true);
    comma    = uint8(',');
    point    = uint8('.');
    Filex.Data(( Filex.Data==comma)) = point;
    %read inkrementierungs number of files
    n(x)=sscanf(dirListing(x).name, '%*c%u.txt');
end

%new sort of files (ASCII(standard)--> numeric
[~, index] = sort(n); %position of the file
File = dirListing(index);%new sort of the files
```

```
%reading files and build matrix
for x = 1:numfiles
    [wave,int]= textread(File(x).name,'%f
%f',datapoints,'headerlines',...
    headerlines);
    [max_value,indexnumber]=max(int); %Max-Intensity of graph
    intzeit(x)=int(indexnumber); %time function
    Matrix(:,x)=int; %matrix
end

%PLOTS-------------------------------------------------------------------
----
%3D Plot
t=linspace(0,(length(dirListing))*int_zeit,(length(dirListing)));
Z=transpose(Matrix);
[X,Y]=meshgrid(wave,t);

subplot('position',[ 0.15 0.6 0.8 0.2]);
mesh(X,Y,Z);
axis tight;
set(gca,'fontsize',10,'FontName','verdana');
xlabel('Wavelength [nm]');
ylabel('Time [s]');
zlabel('Intensity [Counts]');
title('Intensity and Wavelength as a Function of Time',
'FontWeight',...
      'bold', 'fontsize',11)


%max intesity plot (timline)
 v=linspace(0,(length(dirListing))*int_zeit,(length(dirListing)));
subplot('position',[0.15 0.2 0.3 0.2]);
plot(v,intzeit);
axis tight;
set(gca,'fontsize',10,'FontName','verdana');
title('MaxInt (timeline)','FontWeight','bold', 'fontsize',11);
xlabel('Time [s]');
ylabel('Intensity [Counts]');

%max intensity plot

%Processing for max spectra
[max_value2,indexnumber2]=max(intzeit);
Filemax = File(indexnumber2).name;
[wave,MaxVektor]= textread(Filemax,'%f
%f',datapoints,'headerlines',...
    headerlines);

%Plot
subplot('position',[0.65 0.2 0.3 0.2]);
plot(wave,MaxVektor);
axis tight;
set(gca,'fontsize',10,'FontName','verdana');
```

```
title('Max Intensity Graph','FontWeight','bold','fontsize',11);
xlabel('Wavelength [nm]');
ylabel('Intensity [Counts]');

uicontrol('Style','text',...
        'Position',[350 400 50 20],...
        'String','Burntime')

uicontrol('style','edit','string','',...
                'units','normalized','position',[.6 .9 .2 .05],...
                'callback','btime=get(gcbo,''String'')')
uicontrol('style','pushbutton','string','Update',...
                'units','normalized','position',[.4 .9 .2 .1],...
                'callback','uiresume(gcbf)')

uiwait;
X=0;
Y=0;
en=str2double(btime)/int_zeit;
Matrixbt=Matrix(1:datapoints,1:en);

%3D Plot update
t=linspace(0,str2double(btime),str2double(btime)/int_zeit);
Z=transpose(Matrixbt);
[X,Y]=meshgrid(wave,t);

subplot('position',[ 0.15 0.6 0.8 0.2]);
mesh(X,Y,Z);
axis tight;
set(gca,'fontsize',10,'FontName','verdana');
xlabel('Wavelength [nm]');
ylabel('Time [s]');
zlabel('Intensity [Counts]');
title('Intensity and Wavelength as a Function of Time',
'FontWeight',...
      'bold','fontsize',11)
```

Matlab code for Radiometric Calculations

```
%Eingaben-----------------------------------------------------------
-----

prompt = {'Integration time','Datapoints','Headerlines',...
          'Detector distance','Burntime'};%prompt window
dlg_title = 'Konstanten'; %titel
num_lines = 1;
def = {'0.1','2030','17','1','35'}; %fixed values

answer = inputdlg(prompt,dlg_title,num_lines,def); %back to values
integrationtime = str2num(answer{1}); %integration time
datapoints=str2num(answer{2});  %datapoints
headerlines=str2num(answer{3}); %headlines
distance=str2num(answer{4}); %distance to detector
btime=str2num(answer{5});   %burn-time

%reading calibration file from ocean optics spectrometer!!----------
-----------------------------------
[wave2,calx]= textread('calfilex.txt','%f
%f',datapoints,'headerlines',0);

%push  buttons-----------------------------------------------------
---
uicontrol('style','pushbutton','string','Open Files',...
                'units','normalized','position',[.0 .9 .2 .1],...
                'callback','folder = uigetdir()')
uicontrol('style','pushbutton','string','Plot',...
                'units','normalized','position',[.2 .9 .2 .1],...
                'callback','uiresume(gcbf)')
uiwait;
cd(folder);
dirListing = dir('*.txt');% Files

%definitions
%creates one empty column with 2047 zeros
Vektor=zeros(datapoints,1);

%open and read files-----------------------------------------------

for x = 1:length(dirListing)
File = dirListing(x).name;

    %change ',' by '.'
    Name=textscan(File,'%s%s','delimiter','.');
    File    = memmapfile(File,'Writable',true);
    comma   = uint8(',');
    point   = uint8('.');
    File.Data(( File.Data==comma)) = point;
    %read data
    Files = [dirListing(x).name];
```

```
    [wave,int]= textread(Files,'%f %f',datapoints,'headerlines'...
    ,headerlines);
    [max_value,indexnumber]=max(int);
    intzeit(x)=int(indexnumber);

    %vector for mean spectra
    Vektor=Vektor+int;
end

%calculate mean spectra-------------------------------------

MeanVektor=Vektor./(btime./integrationtime);

%open and read data for max intensity spectra--------------------
[max_value2,indexnumber2]=max(intzeit);
Filemax = dirListing(indexnumber2).name;
[wave,MaxVektor]= textread(Filemax,'%f %f',datapoints,...
'headerlines',headerlines);

%convert   oceanoptic   calibration   data   from   [ujoule/s/nm]   ->
[watt/cm^2/nm]
%[Watt/m^2/nm] = [ujoule/s/nm]/(detector area*integrationtime)*0.01
%detector area = 3,1415926.*(0.195cm)^2 (cosine corrector)
cal=calx.*0.01.*integrationtime;


%calibration of files
MeanVektorx=MeanVektor.*cal;
MaxVektorx=MaxVektor.*cal;


%calculates baseline ([200nm-400nm])-------------------------------
 if (sum(MaxVektor(27:454))/427)<0
    mx=-(sum(MaxVektor(27:454))/427);
else
    mx=(sum(MaxVektor(27:454))/427);
end
    baseline_max = mx.*cal;


if (sum(MeanVektor(27:454))/427)<0
    mn=-(sum(MeanVektor(27:454))/427);
else
    mn=(sum(MeanVektor(27:454))/427);
end
    baseline_mean = mn.*cal;

%Baseline-noise-filter (signal to noise for the Si-detector too high
at both ends, from 400nm --> z=454
for z=454:datapoints
    h=round(baseline_max(z)*1);
 if (z+h)<datapoints & (h >0)
```

```
    MeanVektorxx(z)=(sum(MeanVektorx(z:z+h))+sum(MeanVektorx(z:z-
h)))/(2*h);
    MaxVektorxx(z)=(sum(MaxVektorx(z:z+h))+sum(MaxVektorx(z:z-
h)))/(2*h);

 elseif h==0
    MeanVektorxx(z)=MeanVektorx(z);
    MaxVektorxx(z)=MaxVektorx(z);

 end
end

%Plot graph with max intensity---------------------------------

subplot('position',[ 0.15 0.5 0.8 0.3]);
plot(wave,MaxVektorx);
axis tight;
set(gca,'fontsize',10,'FontName','verdana');
title('Max Intensity Graph','FontWeight','bold', 'fontsize',11);
xlabel('Wavelength [nm]');
ylabel('W/m^2/nm');

%Integration  procedure-----------------------------------------------
-----

%integration --> [W/m^2/nm]*nm -> [W/m^2]
%limits for all integrals

minlo = 600;    %limit for ARDEC
maxlo = 1000;
minhi = 695;    %limit for ARDEC
maxhi = 1050;
vislo = 400;    %limit for concealment index
vishi = 700;
NIRlo = 700;    %limit for concealment index
NIRhi = 1000;

%new names for columns (wavelength and intensity)
%'max' means spectra for the maximum intensity at a defined time
%'mean' means the mean spectra over the complete burning time e.g.
30sec.

lambda=wave;
I=MaxVektorxx';
Im=MeanVektorxx';


%define x-values
indlo = find(lambda > minlo & lambda < maxlo);
indhi = find(lambda > minhi & lambda < maxhi);
indvis = find(lambda > vislo & lambda < vishi);
indNIR = find(lambda > NIRlo & lambda < NIRhi);
```

```
%define y-values of the spectra (max)
I1 = I(indlo);
I2 = I(indhi);
I3 = I(indvis);
I4 = I(indNIR);

%define y-values of the spectra (mean)
Im1 = Im(indlo);
Im2 = Im(indhi);
Im3 = Im(indvis);
Im4 = Im(indNIR);


%integration of the defined limits of the spectra (max)
int1=sum(I1(1:end-1).* diff(lambda(indlo)));
int2=sum(I2(1:end-1).* diff(lambda(indhi)));
int3=sum(I3(1:end-1).* diff(lambda(indvis)));
int4=sum(I4(1:end-1).* diff(lambda(indNIR)));


%integration of the defined limits of the spectra (mean)
intm1=sum(Im1(1:end-1).* diff(lambda(indlo)));
intm2=sum(Im2(1:end-1).* diff(lambda(indhi)));
intm3=sum(Im3(1:end-1).* diff(lambda(indvis)));
intm4=sum(Im4(1:end-1).* diff(lambda(indNIR)));


%Convert [W/m^2] -> [W/sr]
I1max=int1*distance^2; Datb(2,2)=I1max;
I2max=int2*distance^2; Datb(3,2)=I2max;
Ivismax=int3*distance^2; Datb(4,2)=Ivismax;
Inirmax=int4*distance^2; Datb(5,2)=Inirmax;


%intensity for mean
I1mean=intm1*distance^2;Datb(2,1)=I1mean;
I2mean=intm2*distance^2;Datb(3,1)=I2mean;
Ivismean=intm3*distance^2;Datb(4,1)=Ivismean;
Inirmean=intm4*distance^2;Datb(5,1)=Inirmean;


%converting W/sr in candela for Ivismax
Cdmax=Ivismax.*683;Datb(6,2)=Cdmax;
Cdmean=Ivismean.*683;Datb(6,1)=Cdmean;


%concealment index for mean
mXie=Inirmean./Ivismean;Datb(1,1)=mXie;
```

```
%concealment index max
Xie=Inirmax./Ivismax; Datb(1,2)=Xie;
cnames = {'Meanspectra','Maxspectra'};
rnames = {'Xie','I1','I2','I_VIS','I_NIR','Cd'};
t = uitable('Data',Datb,'ColumnName',cnames,...
            'RowName',rnames,'Position',[70 20 215 125]);



%UPDATE-----------------------------------------------------------------

hh=1;
hs=0;

while hh==1

uicontrol('style','edit','string','',...
               'units','normalized','position',[.8 .9 .2 .05],...
               'callback','faktor=get(gcbo,''String'')')

uicontrol('Style','text',...
        'Position',[450 400 50 20],...
        'String','Faktor')
b=uicontrol('style','pushbutton','string','Stop',...
               'units','normalized','position',[.6 .9 .2
.1],'callback',...
               'hs=get(gcbo,''value'')');
uicontrol('style','pushbutton','string','Update',...
               'units','normalized','position',[.4 .9 .2 .1],...
               'callback','uiresume(gcbf)')
uiwait;
if hs==1
break
end

for z=454:datapoints
h=round(baseline_max(z)*str2double(faktor));
 if (z+h)<datapoints & (h >0)
MeanVektorxx_neu(z)=(sum(MeanVektorx(z:z+h))+sum(MeanVektorx(z:z-
h)))/(2*h);
MaxVektorxx_neu(z)=(sum(MaxVektorx(z:z+h))+sum(MaxVektorx(z:z-
h)))/(2*h);
 elseif h==0
MeanVektorxx_neu(z)=MeanVektorx(z);
MaxVektorxx_neu(z)=MaxVektorx(z);
 end
end

subplot('position',[ 0.15 0.5 0.8 0.3]);
plot(wave,MaxVektorxx,wave,MaxVektorxx_neu, 'r');
axis tight;
set(gca,'fontsize',10,'FontName','verdana');
```

```
title('Max Intensity Graph','FontWeight','bold', 'fontsize',11);
xlabel('Wavelength [nm]');
ylabel('W/m^2/nm');

I=MaxVektorxx_neu';
Im=MeanVektorxx_neu';
lambda=wave;


%define x-values
indlo = find(lambda > minlo & lambda < maxlo);
indhi = find(lambda > minhi & lambda < maxhi);
indvis = find(lambda > vislo & lambda < vishi);
indNIR = find(lambda > NIRlo & lambda < NIRhi);

%define y-values of the spectra (max)
I1 = I(indlo);
I2 = I(indhi);
I3 = I(indvis);
I4 = I(indNIR);

%define y-values of the spectra (mean)
Im1 = Im(indlo);
Im2 = Im(indhi);
Im3 = Im(indvis);
Im4 = Im(indNIR);

%integration of the defined limits of the spectra (max)
int1=sum(I1(1:end-1).* diff(lambda(indlo)));
int2=sum(I2(1:end-1).* diff(lambda(indhi)));
int3=sum(I3(1:end-1).* diff(lambda(indvis)));
int4=sum(I4(1:end-1).* diff(lambda(indNIR)));

%integration of the defined limits of the spectra (mean)
intm1=sum(Im1(1:end-1).* diff(lambda(indlo)));
intm2=sum(Im2(1:end-1).* diff(lambda(indhi)));
intm3=sum(Im3(1:end-1).* diff(lambda(indvis)));
intm4=sum(Im4(1:end-1).* diff(lambda(indNIR)));

%Convert [W/m^2] -> [W/sr]
I1max=int1*distance^2; Dat(2,2)=I1max;
I2max=int2*distance^2; Dat(3,2)=I2max;
Ivismax=int3*distance^2; Dat(4,2)=Ivismax;
Inirmax=int4*distance^2; Dat(5,2)=Inirmax;

%concealment index max
Xie=Inirmax./Ivismax; Dat(1,2)=Xie;

%intensity for mean
I1mean=intm1*distance;Dat(2,1)=I1mean;
I2mean=intm2*distance;Dat(3,1)=I2mean;
Ivismean=intm3*distance;Dat(4,1)=Ivismean;
Inirmean=intm4*distance;Dat(5,1)=Inirmean;
```

```
%concealment index for mean
mXie=Inirmean./Ivismean;Dat(1,1)=mXie;

%converting W/sr in candela for Ivismax
Cdmax=Ivismax.*683;Dat(6,2)=Cdmax;
Cdmean=Ivismean.*683;Dat(6,1)=Cdmean;

cnames = {'Meanspectra','Maxspectra'};
rnames = {'Xie','I1','I2','I_VIS','I_NIR','Cd'};
t = uitable('Data',Dat,'ColumnName',cnames,...
        'RowName',rnames,'Position',[285 20 215 125]);
end
```

X-ray Data

Table 50 X-ray data for Cs DNT and TNBI.

	CsDNT • 0.75 H_2O	Cs_2TNBI
	fx056	hx311
Formula	$C_2H_{1.5}CsN_5O_{4.75}$	$C_6Cs_2N_8O_8$
Molecular weight	304	578
T / [K]	293	293
Crystal size [mm]	0.3 x 0.1 x 0.1	0.3 x 0.15 x 0.1
Habitus	orange plates	red plates
Crystal system	orthorombic	Monoclinic
Space group	*P bca*	*C 2/m*
a [Å]	9.6332(5)	10.0357(4)
b [Å]	11.7893(5)	12.7869(4)
c [Å]	13.6302(5)	5.4750(2)
α [°]	90	90
β [°]	90	109.233(4)
γ [°]	90	90
V [Å^3]	1547.8(1)	663.37(4)
Z	8	2
ρ_{calc} [g cm^{-1}]	2.613	2.893
μ [mm^{-1}]	4.784	5.561
F(000)	1132	532
theta max [°]	26.00	25.91
Index ranges	−6≤ h ≤ 11	−12≤ h ≤ 12
	−14 ≤ k ≤ 13	−15 ≤ k ≤ 15
	−16 ≤ l ≤ 10	−6 ≤ l ≤ 6
reflns. collected	3704	3328
reflns. obsd.	1518	676
reflns. unique	1086	659
R_1, wR_2 (2σ data)	0.0345 / 0.0407	0.0140 / 0.0340
R_1, wR_2 (all data)	0.0215 / 0.0392	0.0135 / 0.0337
S on F^2	0.836	1.116
E_{max}/E_{min} [e Å^{-3}]	0.663 / −0.680	1.402 / -0.311

List of Publications

T. M. Klapötke, M. Göbel, S. Scheutzow, A. Böhm, J. Weis, *Complexindole alkaloids from Cyanobacterium*, Nachrichten aus der Chemie **2007**.

A. Böhm, M. Göbel, T. M. Klapötke, M. Krell, S. Scheutzow, J. Stohrer, J. Weis, *Danger with primary amines and methylene chloride*, Chem. Aust. **2007**.

T. M. Klapötke, A. Penger, S. Scheutzow, L. Vejs, *Synthesis, Structure, Chemical and Energetic Characterization of 1,3-Dinitramino-2-nitroxy-propane*, ZAAC **2008**, *634***,** 2994 – 3000.

N. Fischer, T. M. Klapötke, S. Scheutzow, J. Stierstorfer, *Hydrazinium 5-aminotetrazolate: An Insensitive Energetic Material Containing 83.72 % Nitrogen*, Centr. Europ. J. Energ. Mater. **2008**, *5(3-4)*, 3 – 18.

E.-C.-Koch, Susanne Scheutzow*, Review: On the Relation between Sensitivity Parameters and Molecular Structure of Energetic Materials*, NATO-MSIAC **2009**, 1-55, Brussels, Belgium.

N. Fischer, T. M. Klapötke, S. Scheutzow, J. Stierstorfer, D. Piercey, *Diaminouronium Nitriminotetrazolates – Thermally Stable Explosives*, ZAAC **2010**.

E.-C. Koch, T. M. Klapötke, A. Hahma, H. Radies, S. Scheutzow, *Combustion Properties of Blackbody Infrared Flare Compositions Based on Perfluoroalkylated Tetrazoles, Magnesium and Viton*, in: Eneregtic Materials for High Performance, Insensitive Munitions and Zero Pollution, Fraunhofer-Institut für Chemische Technologie (ICT), Pfinztal **2010**, pp 133-1 – 133-4.

A. Ilie, C. Rat, S. Scheutzow, C. Kiske, K. Lux, T. M. Klapötke, C. Silvestru, K. Karaghiosoff, *Metallophilic bonding and agostic interactions in gold(I) and silver(I) complexes bearing sulfur tetrazol unit*, Inorg. Chem. **2011**, *50*, 2675.

N. Fischer, T. Klapötke, S. Marchner, M. Rusan, S. Scheutzow, J. Stierstorfer, *A Selection of Alkali and Alkaline Earth Metal Salts of 5,5´-Bis(1-hydroxytetrazole) in Pyrotechnic Compositions*, PEP, submitted **2012**.

Poster Presentations

Synthesis and Characterization of the Oxygen-rich Energetic Material Melaminium Dinitrate (MDN), S. Scheutzow, R. Friedemann, M. Göbel, T. M. Klapötke, 10th NTREM Conference, Pardubice, CZ **2007**.

Analysis of Residues in the AESTUS Engine for the ATV Mission, S. Scheutzow, A. Nieder, T. M. Klapötke, O. deBonn, G. Obermaier, 11th NTREM Conference, Pardubice, CZ **2008**.

Investigation of Products and Velocity of Detonation of "Improvised Explosive Filler", N. Barl, T. M. Klapötke, B. Krumm, S. Scheutzow, F. X. Steemann, 12th NTREM Conference, Pardubice, CZ **2009**.

Solid Nitroglycerine Analoga With Improved Energetic Properties, A. Penger, T. Altenburg, S. Scheutzow, L. Vejs, T. M. Klapötke, 12th NTREM Conference, Pardubice, CZ **2009**.

Silver Nitriminotetrazolate: A Promising Primary Explosive, D. G. Piercey, T. M. Klapötke, N. T. Mayr, S. Scheutzow, J. Stierstorfer, USA **2009**.

Metal Salts of N,N´- Dinitroguanidine as Colorant and IR Illuminant, T. Altenburg, T. M. Klapötke, A. Penger, S. Scheutzow, 13th NTREM Conference, Pardubice, CZ **2010**.

Combustion Properties of Blackbody Infrared Flare Compositions Based on Perfluoralkylated Tetrazolates, Magnesium and Viton, E.-C. Koch, T. M. Klapötke, A. Hahma, H. Radies, S. Scheutzow, ICT **2010**.

Silver Nitriminotetrazole - A Promising Primary Explosive, D. Piercey, T. M. Klapoetke, N. Mayr, S. Scheutzow, J. Stierstorfer, 13th NTREM Conference, Pardubice, CZ **2010**.

Experimentally determined detonation velocities of new secondary explosives, M. Boehm, N. Fischer, D. Fischer, T. M. Klapoetke, S. Scheutzow, J. Stierstorfer, 14th NTREM Conference, Pardubice, CZ **2011**.

Oral presentations

Experimental and Computational Determination of Detonation Velocity, S. Scheutzow, Australian Energetic Material Symposium, Flinders University, Adelaide, Australia, December 1st **2008**.

High-Nitrogen Propellants, Pyrotechnics and Explosives – Some Aspects of Detonation Velocity, T. M. Klapötke, S. Scheutzow, J. Stierstorfer, K. R. Tarantik, University of Melbourne, Melbourne, Australia, December 9th **2008**.